

https://dspace.org/

Characterisation of inhibitor binding to the LEDGF/p75-binding domain of HIV-1 integrase

Harrison, Angela Theresa

2018
https://hdl.handle.net/10539/26980

Downloaded from a DSpace repository. https://dspace.org/

Characterisation of inhibitor binding to the LEDGF/p75-binding domain of HIV-1 integrase



By

Angela Theresa Harrison

A thesis submitted to the Faculty of Health Sciences, University of the Witwatersrand, in fulfilment of the requirements for the degree

Of

Doctor of Philosophy

Declaration

I, Angela Theresa Harrison declare that the work presented in this dissertation is my own, unaided work. It is being submitted for the degree of Doctor of Philosophy in Medicine in the University of the Witwatersrand, Johannesburg. This work has not been submitted before for any degree or examination at this or any other University.

…….

26th Day of September, 2018

Dedication

I dedicate this dissertation to my Mom and Dad for being there through all the stresses and making me food when I got home. I love you and thank you.

My dearest husband Riaan, from the day you have known me I have been studying. Thank you for the support and putting up with my grumpiness when things were not working. I love you unconditionally. A new unknown journey starts for both of us.

Publication and conference proceedings

S Mosebi, **A Harrison**, S Abrahams, Q Fish, M Coyanis, T Rashamuse. Decoding discrepancies in allosteric inhibition of HIV-1. USA-Italy commission meeting for Advanced Materials and Nanotechnologies, 11-12 May 2017, University of Rome, Italy.

A Harrison, S Mosebi, R Hewer, M Papathanasopoulos. Comparison of HIV-1 IN-LEDGF/p75 inhibitors through Hydrogen Amide Exchange. International conference of Clinical and Basic Science Research, 27-29 November 2017, Cape Town, RSA.

Abstract

Human immunodeficiency virus type 1 (HIV-1) integrase (IN) catalyses the irreversible integration of the viral genome into the host genome with the aid of the host co-factor lens epithelium derived growth factor (LEDGF/p75). LEDGF/p75 protects HIV-1 IN from proteasomal degradation, facilitates transport and directs DNA binding. Allosteric IN inhibitors (ALLINIs) were discovered in 2010 by Christ et al and then several research groups followed suite. ALLINIs were found to cause aberrant multimerisation of HIV-1 IN and have a profound effect on virion maturation. In previous studies lovastatin and cefdinir were identified to be inhibitors of the HIV-1 IN-LEDGF/p75 interaction. In this study, the aim was to characterise the interaction of both compounds in comparison with a known ALLINI, CX05168 with HIV-1 IN, and determine their modes of action. After the expression and purification of the recombinant proteins, the compounds were screened through an AlphaScreen assay to assess their ability to inhibit the HIV-1 IN-LEDGF/p75 interaction. All three of the compounds: lovastatin, cefdinir and CX05168 inhibited the interaction with IC_{50} values of 1.97 ± 0.28 µM, 4.05 ± 0.18 µM and 1.33 ± 0.5 5µM for subtype B HIV-1 IN and 1.98 ± 0.28 µM, 5.22 ± 0.92 µM and 1.79 ± 0.63 µM for subtype C HIV-1 IN, respectively. The AlphaScreen was then adjusted for the addition of donor DNA. This caused a reduction in the potency of CX05168 and cefdinir but had no effect on lovastatin. The IC_{50} values for cefdinir and CX05168 increased to 52.02 ± 1.82 µM and 20.46 ± 0.76 µM for subtype B HIV-1 IN and 41.87 ± 0.95 µM and 21.28 ± 0.52 µM for subtype C HIV-1 IN, respectively. This was the first indication that lovastatin had a different mode of action. With the findings that ALLINIs cause HIV-1 IN to aberrantly multimerise follow up tests included the compounds in two separate assays to determine if they caused multimerisation. The first assay was a cross-linking study and the second was differential light scattering assay. The only compound shown to have the ability to cause aberrant multimerisation was CX05168. Follow up tests were conducted to determine if the compounds had any stabilising effect on the HIV-1 IN enzyme. In agreement with the multimerisation assay only CX05168 showed any effect on the stability of HIV-1 IN. In this assay a difference in the potency of CX05168 on the subtype C HIV-1 IN was seen, where less stabilisation occurs. Hydrogen deuterium exchange mass spectroscopy was used to determine binding sites or allosteric changes to HIV-1 IN. Overall visual allosterism on HIV-1 IN subtype B and C was seen with CX05168. Lovastatin had clear binding areas that differed from CX05168, whereas cefdinir showed few areas of binding or similarities. This indicated that all three compounds displayed different binding models and in combination with the other assays confirmed their different modes of action. Surface plasmon resonance was used to determine the binding kinetics. The noise to signal ratio for lovastatin and cefdinir proved to be too high to obtain

usable results indicating a possible poor binding ability. CX05168 showed good binding in agreement with our previous results but once again a difference in binding the subtype B HIV-1 IN and subtype C HIV-1 IN could be seen. We finalised our tests with cellular screening. Lovastatin proved to be too toxic to the mammalian cells to test antiviral efficiency. Cefdinir and CX05168 showed viral inhibition with CX05168 being less potent against the HIV-1 subtype C as opposed to the HIV-1 subtype B viruses. In conclusion, this study found that the three compounds (lovastatin, cefdinir and CX05168) inhibit the HIV-1 IN-LEDGF/p75 interaction in different ways. Results highlight that CX05168 functions as a LEDGF/p75 IN inhibitor by causing aberrant IN multimerisation, however, it is less potent towards HIV-1 subtype C, which is the predominant subtype circulating in South Africa. Lovastatin and cefdinir inhibit the direct interaction of HIV-1 IN-LEDGF/p75 without multimerisation which decreases the antiviral potency. The compounds of most value are those causing aberrant multimerisation of HIV-1 IN as they have potent downstream effects, lovastatin and cefdinir in their current chemical structure are not promising ALLINI's, and require structural modifications to fulfil their promise.

Acknowledgments

To my supervisor Dr Salerwe Mosebi, thank you for pushing me out of my comfort zones to learn new techniques, to be a better scientist and for walking this long journey with me.

To my supervisor Prof. Maria A Papathanasopoulos, thank you for always being present when help is needed, for having faith that HIV research is reaching new heights and taking us along on the path to success. Your knowledge and commitment has helped me reach a massive milestone in my life.

To my supervisor Dr Raymond Hewer, thank you for seeing the potential in me, for moulding the scientist you knew was there. My journey to my PhD was not only this portion but the journey you have walked with me from honours. I am eternally grateful for your mentorship.

To the Centre for Metal based Drug Discovery group, thank you for the help and strategy talks we had when things weren't working. Your help and guidance never went unappreciated.

A special thanks to Shaakira Abrahams and Denise Le Noury without the friends to vent to when things were unbearable who knows if we would have made it.

To Dr Thompho Rashamuse, thank you for your help with molecular modelling.

I send my thanks to Mintek, the Department of Molecular Medicine and Haematology at the University of the Witwatersrand Medical School, and the National Research Foundation (NRF) for funding and the great opportunity.

Table of contents

Publication and conference proceedings ..... **IV**

Acknowledgments ..... **VII**

List of figures ..... **XI**

List of tables ..... **XV**

List of abbreviations ..... **XVI**

1. Introduction ..... **- 2 -**

1.1 HIV epidemiology ..... **- 2 -**

1.2 HIV virion and genomic organisation ..... **- 3 -**

1.3 HIV-1 lifecycle ..... **- 4 -**

1.4 Mechanisms of HIV-1 inhibition and current antiretroviral drug target(s) ..... **- 6 -**

1.5 Integrase structure and function ..... **- 10 -**

1.5.1 Structure of IN ..... **- 10 -**

1.5.2 Function of IN ..... **- 14 -**

1.6 Lens Epithelium Derived Growth Factor ..... **- 16 -**

1.7 HIV-1 IN- LEDGF/p75 interaction ..... **- 17 -**

1.8 HIV-1 IN as a drug target ..... **- 22 -**

1.8.1 Strand transfer inhibition ..... **- 22 -**

1.8.2 HIV-1 IN-LEDGF/p75 as a target ..... **- 25 -**

1.9 Objectives of the study ..... **- 34 -**

2. Materials and Methods ..... **- 36 -**

2.1 Reagents used in this study ..... **- 36 -**

2.2 The expression, purification and validation of recombinant proteins ..... **- 36 -**

2.2.1 The expression and purification of HIV-1 IN subtype B and C ..... **- 36 -**

2.2.2 The isolation and purification of recombinant LEDGF/p75 ..... **- 39 -**

2.2.3 Removal of the Histidine tag from HIV-1 IN subtype B and C by thrombin cleavage ..... **- 41 -**

2.3 Biochemical screening of HIV-1 IN–LEDGF inhibitors ..... **- 42 -**

2.3.1 AlphaScreen ..... **- 42 -**

2.3.2 Dimerisation assay ..... **- 44 -**

2.3.3 Stability testing ..... **- 46 -**

2.3.4 Molecular modelling ..... **- 46 -**

2.3.5 Hydrogen Exchange Mass Spectroscopy (HXMS) ..... **- 47 -**

2.3.6 Surface Plasmon Resonance (SPR) ..... **- 48 -**

2.4 Screening of compounds to determine their effects on cell based processes - 49 -

2.4.1 Cytotoxicity ..... - 49 -

2.4.2 Antiviral screening ..... - 49 -

2.4.3 Time of addition (TOA) assay to determine the time point in the viral replication process when the compounds are effective ..... - 50 -

3. Results ..... - 52 -

3.1 Recombinant protein expression, purification, and modification ..... - 52 -

3.1.1 HIV-1 IN ..... - 52 -

3.1.2 LEDGF/p75 ..... - 53 -

3.1.3 Modifications of recombinant proteins ..... - 53 -

3.1.4 Catalytic activity testing of HIV-1 IN subtype B and C ..... - 54 -

3.2 Biochemical screening of HIV-1 IN-LEDGF/p75 inhibitors ..... - 55 -

3.2.1 AlphaScreen assay ..... - 55 -

3.2.2 Dimerisation assay ..... - 59 -

3.2.3 Differential scanning fluorimetry ..... - 62 -

3.2.4 Molecular modelling ..... - 63 -

3.2.5 Hydrogen exchange mass spectroscopy ..... - 66 -

3.2.6 Surface Plasmon Resonance (SPR) ..... - 76 -

3.2.7 Cellular screening ..... - 77 -

4. Discussion ..... - 80 -

4.1 Allosteric inhibition of HIV-1 IN in the presence of DNA ..... - 81 -

4.2 The allosteric inhibition effects of CX05168, cefdinir and lovastatin on HIV-1 IN multimerisation and protein stability ..... - 83 -

4.3 Allosteric integrase inhibitors induce distinct effects on the HIV-1 IN CCD ... - 83 -

4.4 The enzyme kinetics of CX05168 ..... - 89 -

4. 5 Cytotoxic and antiviral effects of CX05168, lovastatin and cefdinir ..... - 90 -

4.6 Conclusion ..... - 92 -

5. References..... - 96 -

6. Appendix..... - 112 -

List of figures

Figure 1. 1. Genomic organization of the HIV-1 genome displaying the three main structural, catalytic and envelope genes *gag*, *pol* and *env* flanked by two identical long terminal repeats**.. ..... - 3 -**

Figure 1. 2: Representative figure of an HIV virion displaying structural and functional proteins..**..... - 4 -**

Figure 1. 3: Lifecycle of HIV-1 showing the individual steps of entry, reverse transcription, integration, transcription, translation, assembly and budding**.. ..... - 5 -**

Figure 1. 4: The basic layout of HIV-1 integrase with the ribbon structure of the Catalytic Core Domain**. ..... - 11 -**

Figure 1. 5: Sequence alignment map comparing Prototype Foamy Virus (first line) and HIV-1 integrase (second line)**..... - 13 -**

Figure 1. 6: Sequence alignment map comparing Subtype B integrase (first line) and subtype C integrase (second line)**..... - 14 -**

Figure 1. 7: Schematic representation of the HIV-1 integration reaction. In the first step (i) tetrameric IN is bound to viral cDNA and LEDGDF forming the PIC and produces CA overhangs during 3' processing**. ..... - 15 -**

Figure 1. 8: The PSIP1 gene showing the exons and introns indicated in black and white respectively**..... - 16 -**

Figure 1. 9: Protein data bank crystal structure 2J4B, https://www.rcsb.org/structure/2b4j, of the two HIV-1 IN dimers interacting with LEDGF/p75**..... - 18 -**

Figure 1. 10: The HIV-1 IN CCD dimer interaction with LEDGF/p75. **..... - 19 -**

Figure 1. 11: Diagrammatical representation of the mechanistic binding of competitive inhibition**. ..... - 20 -**

Figure 1. 12: Diagrammatical representation of the mechanistic binding of uncompetitive inhibition**.. ..... - 21 -**

Figure 1. 13: Diagrammatical representation of the mechanistic binding of non-competitive inhibition**. ..... - 21 -**

Figure 1. 14: Development of raltegravir showing the steps from 5-CITEP to L-870812 through to raltegravir**..... - 22 -**

Figure 1. 15: Mechanism of action of raltegravir showing the binding to the DDE triad and the magnesium ions to the oxygen groups of raltegravir**.. ..... - 23 -**

Figure 1. 16 The catalytic core domain of integrase, magnified to show the amino acids commonly associated with raltegravir resistance **..... - 24 -**

Figure 1. 17: Chemical structure of elvitegravir**. ..... - 24 -**

Figure 1. 18: The chemical structure of dolutegravir**..... - 25 -**

Figure 1. 19: Diagrammatical representation of a standard infectious virion and a defective immature progeny virion formed after treatment with an ALLINI**..... - 28 -**

Figure 1. 20: Diagrammatic representation of a generic Quinolone compound**.. ..... - 29 -**

Figure 1. 21 (A) Ribbon 3D structure of the CCD of HIV IN with a known quinolone compound CX05168 docked indicating interacting amino acids. (B) 2D structure of known quinolone CX05168 docked indicating interacting amino acids**. ..... - 29 -**

Figure 1. 22: The development progress of NCINI compounds from the original hit from library screening to the development of BI224436**. ..... - 31 -**

Figure 1. 23: Chemical structure of a t-butylsulfonamide discovered to have ALLINI properties**..... - 31 -**

Figure 1. 24: Scaffold hopping of a 3-hydroxypicolinamide from a di-hydroxybenzamine scaffold**. ..... - 32 -**

Figure 1. 25: Structure of lovastatin shown in A and CX05168 shown in B to display the similarities in compound structure**. ..... - 33 -**

Figure 1. 26: Structure of cefdinir**.. ..... - 33 -**

Figure 2. 1 Schematic representation of the HIV-1 IN-LEDGF/p75 interaction in an AlphaScreen assay**. ..... - 42 -**

Figure 3. 1: SDS PAGE gel and western blot indicating the expression and purification of a protein at approximately 32 kDa correlating with that of recombinant subtype B HIV-1 IN**..**
- 52 -

Figure 3. 2: SDS-PAGE gel showing the expression and purification steps of a protein correlating with that of LEDGF/p75 and western blot proving the successful expression of LEDGF/p75**..... - 53 -**

Figure 3. 3: SDS-PAGE gel of HIV-1 subtype B and C IN following thrombin cleavage of the 6XHIS tag (A) and a western blot confirming cleavage of the HIS tag (B**). ..... - 54 -**

Figure 3. 4: Bar graph depicting the strand transfer activity by ELISA of both subtype B and C IN with and without addition 50nM raltegravir. **..... - 55 -**

Figure 3. 5: Effects of lovastatin, cefdinir and CX05168 on the HIV-1IN-LEDGF/p75 interaction for HIV-1IN subtype B (A) and subtype C (B)**..... - 56 -**

Figure 3. 6: Effects of lovastatin, cefdinir and CX05168 on the DNA-HIV-IN-LEDGF/p75 interaction of HIV-1 IN subtype B (A) and subtype C (B)**..... - 58 -**

Figure 3. 7 Column graph showing the percentage fluorescence of the POGz-LEDGF/p75 interaction Alphascreen assay**.. ..... - 59 -**

Figure 3. 8: Western blot study showing the cross-linking studies with HIV-1 subtype B IN (A) and subtype C IN (B)**..... - 60 -**

Figure 3. 9: Number distribution graph of the multimerisation effects of studied compounds for subtype B HIV-1 IN and subtype C HIV-1 IN..**..... - 61 -**

Figure 3. 10: Analysis of the melting temperature of HIV-1 subtype B (A) and C (B) IN in the absence of compound (blue), in the presence of CX05168 (red), lovastatin (grey) and cefdinir (yellow).**..... - 63 -**

Figure 3. 11: Molecular model of the predicted binding of compounds to the HIV-1 IN dimer interface where LEDGF/p75 would dock.**..... - 65 -**

Figure 3. 12: Hydrogen exchange heat map of HIV-1 subtype B integrase in absence of compound with deuteration for 10s, 20s, 1min, 10min and 60 min**..... - 68 -**

Figure 3. 13: Hydrogen exchange heat map of HIV-1 subtype B integrase with deuteration for 10s treated with CX05168 (A), lovastatin (B) and cefdinir (C)**. ..... - 69 -**

Figure 3. 14: Ribbon structure of the prepared binding site on integrase where the compounds bind to elicit their effects**……..- 70 -**

Figure 3. 15: Hydrogen exchange heat map of HIV-1 subtype C integrase with deuteration for 102, 20s, 1min, 10min and 60 min**..... - 71 -**

Figure 3. 16: Hydrogen exchange heat map of HIV-1 subtype C integrase with deuteration for 10s treated with CX05168 (A), lovastatin (B) and cefdinir (C). **..... - 72 -**

Figure 3. 17: HIV IN ribbon structure displaying the binding site for compound and the respective deuterium exchange in the absence of a bound compound on different parts of the subtype C HIV-1 IN enzyme (The ribbon structure of subtype B has been used as there is no subtype C structure)**..... - 73 -**

Figure 3. 18: HIV IN ribbon structure displaying the comparison of subtype B and C with the colours related to the deuterium exchange**..... - 74 -**

Figure 3. 20: Hydrogen exchange comparison heat map showing the deuterium exchange differences between subtype B and C HIV-1 IN with CX05168 (A), lovastatin (B) and cefdinir (C) treatment**..... - 75 -**

Figure 3. 21: Surface Plasmon resonance graphs for CX05168 for concentrations 10µM, 5µM and 2µM for subtype B (A) and C (B) HIV-1 IN**..... - 76 -**

Figure 3. 22: TOA results for the antiviral effects of cefdinir and CX05168 compounds at specified time points for subtype B (A) and C (B) integrase**.. ..... - 78 -**

Figure 6. 1 Standard curve for SDS PAGE gel in Figure 3.1 A for the purification and expression of HIV-1 subtype B integrase. **..... - 113 -**

Figure 6. 2 Standard curve for SDS PAGE gel in figure 3.1 B for the purification and expression of subtype C integrase. **..... - 113 -**

Figure 6. 3 Standard curve for western blot in Figure 3.1 C confirming the expression of subtype B and C integrase**..... - 114 -**

Figure 6. 4 Standard curve for SDS PAGE gel in Figure 3.2A of the purification and expression of LEDGF/p75.**..... - 114 -**

Figure 6. 5 Standard curve for the western blot in Figure 3.2 confirming the successful expression of LEDGF/p75. **..... - 115 -**

Figure 6. 6 Standard curve for the SDS PAGE gel in Figure 3.3 A of HIV-1 subtype B and C integrase before and after thrombin cleavage of the HIS tag. **..... - 115 -**

Figure 6. 7 Standard curve of the western blot in Figure 3.3 B showing the successful cleavage of the HIS tag from HIV-1 subtype B and C integrase**. ..... - 116 -**

Figure 6. 8 Standard curve of the western blot in Figure 3.7A showing the dimerization studies of HIV-1 subtype B integrase and inhibitors. **..... - 116 -**

Figure 6. 9 Standard curve of the western blot in Figure 3.7B showing the dimerization studies of HIV-1 subtype C integrase and inhibitors**. ..... - 117 -**

Figure 6. 10: Hydrogen exchange heat map of subtype B integrase with deuteration for 10s treated with CX05168**. ..... - 118 -**

Figure 6. 11: Hydrogen exchange heat map of subtype B integrase with deuteration for 10s treated with lovastatin**. ..... - 119 -**

Figure 6. 12: Hydrogen exchange heat map of subtype B integrase with deuteration for 10s treated with cefdinir**..... - 120 -**

Figure 6. 13: Hydrogen exchange heat map of subtype c integrase with deuteration for 10s treated with CX05168**.. ..... - 121 -**

Figure 6. 14: Hydrogen exchange heat map of subtype C integrase with deuteration for 10s treated with lovastatin.**..... - 122 -**

Figure 6. 15: Hydrogen exchange heat map of subtype C integrase with deuteration for 10s treated with cefdinir**. ..... - 123 -**

Figure 6. 16: Hydrogen exchange comparison heat map showing the deuterium exchange differences between subtype B and C HIV-1 IN with CX05168 treatment**.. ..... - 124 -**

Figure 6. 17: Hydrogen exchange comparison heat map showing the deuterium exchange differences between subtype B and C HIV-1 IN with lovastatin treatment.**- 125 -**

Figure 6. 18: Hydrogen exchange comparison heat map showing the deuterium exchange differences between subtype B and C HIV-1 IN with cefdinir treatment**..... - 126 -**

List of tables

Table 1.1: FDA approved drugs for the treatment of HIV-1 infection with mode of action and approval date. **..... - 7 -**

Table 1.2: Chemical modifications from ALLINI compound 3 to CX14442 showing the improvement in efficiency**..... - 27 -**

Table 3. 1: Binding energies determined for the interaction of CX05168, lovastatin and cefdinir with the predicted amino acid interactions. **..... - 64 -**

Table 3. 2: The maximum response units (RU max), Chi square, association constant (K_a), dissociation constant (K_d) and the equilibrium constant (K_D) of CX05168 for subtype B and C IN**. ..... - 77 -**

Table 3. 3: Comparison of cytotoxicity and antiviral biological activity of CX05168, lovastatin and cefdinir in MT-4 cells infected with HIV-1 NL4-3 subtype B and HIV-1 93IN905 subtype C isolates**. ..... - 77 -**

List of abbreviations

ADME	Absorption, Distribution, Metabolism and Excretion
AIDS	Acquired Immune Deficiency Syndrome
ALLINI	Allosteric HIV-1 integrase inhibitors
Alpha	Amplified Luminescent Proximity Homogenous Assay
ARV	Antiretroviral
AZT	Zidovudine
BS3	bis(sulfosuccinimidyl)suberate
BSA	Bovine serum albumin
CA	Capsid
CC_{50}	Cytotoxicity
CCD	Catalytic core domain
CCR5	Chemokine receptor 5
CID	Collision Induced Dissociation
CTD	C terminal domain
D_2O	Deuterium
DKA	Diketoacids
DLS	Differential Light Scattering
DTG	Dolutegravir
DMSO	Dimethylsulfoxide
DNA	Deoxyribonucleic acid
DSF	Differential Scanning Fluorometry
DTT	Dithiothreitol
EC_{50}	Half maximal effective concentration
EDTA	Ethylenediaminetetraacetic acid
ELISA	Enzyme linked immunosorbent assay
ELV	Elvitegravir
FDA	US Food and Drug Administration
HAART	Highly active antiretroviral therapy
HCl	Hydrochloric acid
HIV	Human Immunodeficiency Virus
HTRF	Homogenous time resolved fluorescence
IBD	Integrase binding domain
IC_{50}	Half maximal inhibitor concentration
IN	Integrase
INSTI	Integrase strand transfer inhibitor
IPTG	Isopropyl β-D-1-thiogalactopyranoside
kb	Kilo bases
kDa	Kilo Daltons
LB	Luria Bertani
LC	Liquid chromatography
LCMS	Liquid chromatography mass spectrometer
LEDGF	Lens epithelium derived growth factor
LTR	Long terminal repeat

Met/M	Methionine
Mw	Molecular weight
MWCO	Molecular weight cut off
NCC	NIH Clinical collection
NCINI	Non-catalytic site integrase inhibitors
nef	Negative factor gene
NIH	National Institutes of Health
NLS	Nuclear localization signal
NMR	Nuclear magnetic resonance
NNRTI	Non-nucleoside reverse transcriptase inhibitor
NRTI	Nucleoside reverse transcriptase inhibitor
OD	Optical density
ORF	Open Reading Frame
PAGE	Polyacrylamide gel electrophoresis
PBS	Phosphate buffered saline
PI	Protease inhibitor
PIC	Pre integration complex
PMSF	Phenylmethanesulfonylfluoride
PogZ	Pogo transposable element with ZNF domain
pol	Polymerase gene
PR	Protease
PVDF	Polyvinylidenedifluoride
RAL	Raltegravir
rev	Regulator of expression gene
RNA	Ribonucleic acid
RT	Reverse transcriptase
SDS	Sodium dodecyl sulphate
SIV	Simian Immunodeficiency Virus
Sol	Soluble
SPR	Surface plasmon resonance
ST	Strand transfer
tat	Transactivator of transcription gene
TEM	Transmission electron microscopy
TMB	3,3',5,5'-tetramethylbenzidine
TTBS	Tris buffered saline with tween 20
UNAIDS	The Joint United Nations Programme on HIV and AIDS
UV	Ultra violet
vif	Viral infectivity factor gene
vpr	Viral protein R gene
vpu	Viral protein U gene
wt	Wild type

Please note the standard IUPAC codes for amino acids have been used throughout this thesis.

Chapter 1

1. Introduction

1.1 HIV epidemiology

Human immunodeficiency virus (HIV) infection is responsible for a worldwide pandemic, with an estimated 36.7 million people living with the virus. There has been a steady decline in deaths associated with HIV with an estimated 1 million people dying in 2016 down from 1.9 million in 2005. This steady decline is possibly due to awareness or progress in access to antiretroviral drug treatment (UNAIDS fact sheet, "Latest statistics on the status of the AIDS epidemic", July 2017). Eastern and Southern Africa are most severely affected by HIV where in 2016 it was estimated that 19.4 million people were living with HIV (UNAIDS fact sheet, "Latest statistics on the status of the AIDS epidemic", July 2017). With increased efforts to fight the pandemic new infections decreased to 790 000 in 2016, a reduction of 29% from the period 2010-2016, however this amounts to 2164 new infections every day in the region. Southern Africa makes up 64% of all new HIV infections (UNAIDS fact sheet, "Latest statistics on the status of the AIDS epidemic", July 2017).

HIV can be subdivided into two types, HIV-1 and HIV-2, where HIV-1 is the predominant type. HIV-1 has high heterogeneity that is caused by several factors including the error prone proof reading ability of reverse transcriptase (RT) (Op de Coul et al., 2001; Roberts et al., 1988), the high turnover rate of HIV *in vivo* (Ho et al., 1995), selective immune pressures in the host (Michael, 1999) and recombination during the replication cycle (Temin, 1993). Due to these influences HIV-1 is further divided into four main groups; M (Major), O (Outlier), N (Non-M and Non-O), and P (Pending the identification of further human cases) (Buonaguro et al., 2007). These four groups come from a zoonotic transmission of simian immunodeficiency virus (SIV). Of the four groups, M is the predominant group found worldwide and is responsible for the current HIV pandemic (Sharp and Hahn, 2011; Hemelaar, 2012). Group M is further subdivided into 11 subtypes from A-K. Subtype B is the predominant subtype in Europe, America, Japan and Australia whereas subtype C is predominant in Southern Africa, Eastern Africa, India, Nepal and parts of China. With these countries accounting for most of the infections, subtype C is the most widely spread subtype in the world (Buonaguro et al., 2007). Groups N, O and P are less common where group O accounts for approximately 5% of the infections in several western and central African countries and is very rare outside of these regions (Buonaguro et al., 2007). HIV infection is no longer deadly but is now considered a chronic and manageable disease thanks to the improvements in antiretroviral drug therapy. However, with an increase in drug resistant HIV strains there is a constant need for novel drugs and targets.

1.2 HIV virion and genomic organization

The HIV-1 genome contains 3 open reading frames (ORF) *gag*, *pol* and *env*, these 3 ORFs encode for 9 genes which encode for at least 16 proteins vital to the functioning and survival of the virus. Figure 1.1 shows the genomic organization and the resultant protein for each gene (Simon et al., 2006).

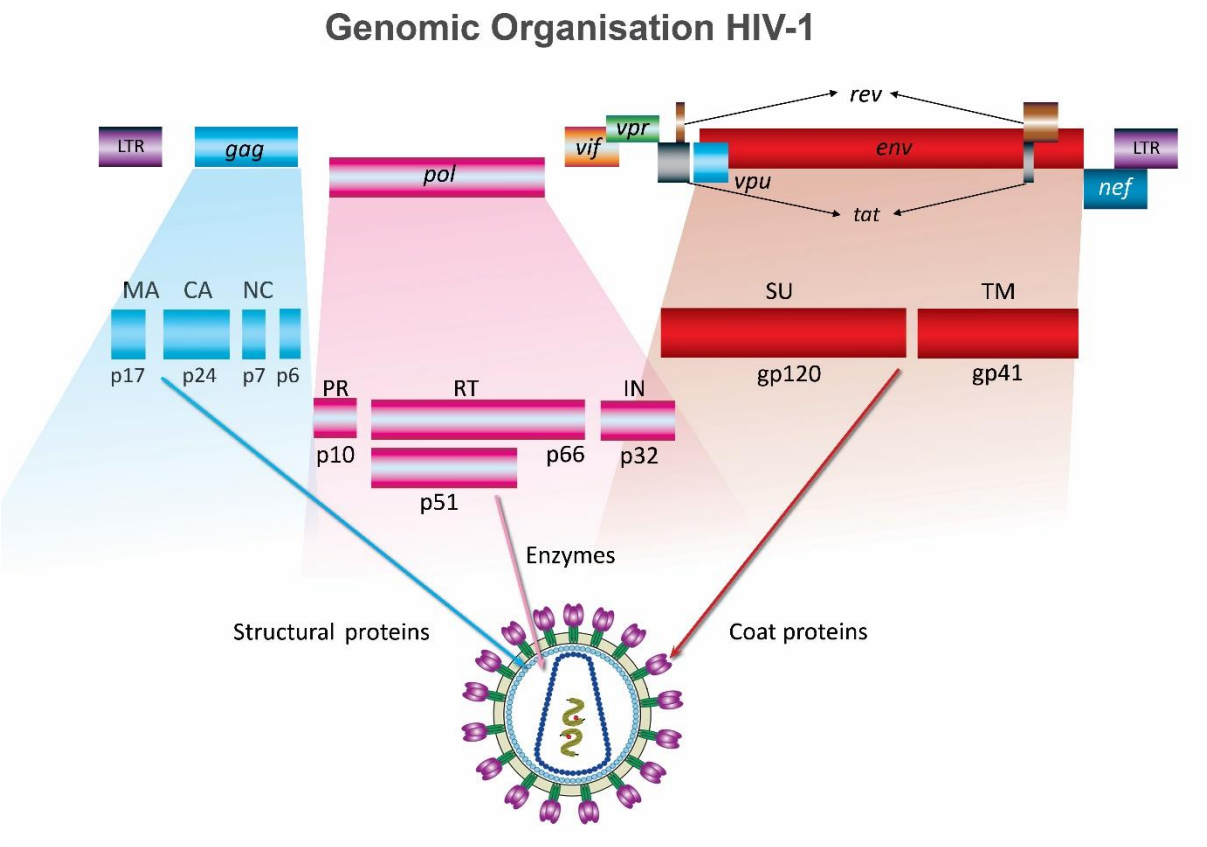


Figure 1. 1. Genomic organization of the HIV-1 genome displaying the three main structural, catalytic and envelope genes *gag*, *pol* and *env* flanked by two identical long terminal repeats. The *gag* gene codes for matrix protein, capsid proteins and nuclear cytoplasm. The *pol* gene codes for protease, reverse transcriptase and integrase proteins and the *env* gene codes for gp120 and gp41 proteins. Arrows point from the proteins towards the virion particle indicating which part of the particle they form. The figure includes regulatory genes *tat* and *rev,* and accessory genes *vif, vpr, vpu* and *nef,* needed for permanence of the virus. Picture adapted from www.stanford.edu/group/virus/retro/2005gongishmail/HIV.html.

The resultant proteins assemble to form different parts of the virion as seen in Figure 1.2. The *gag* gene translates into structural proteins, whereas the *pol* gene is responsible for

production of the enzymes vital to the replication process and the *env* gene forms the protective coat glycoproteins (Simon et al., 2006). The virion is made up of two plus strands of RNA each containing a copy of the 9 genes. The capsid, made up of p24, encloses the RNA and is surrounded by the p17 matrix. The matrix is enclosed by a host derived lipid bilayer where the glycoproteins gp120 and gp41 are embedded. The virion contains most of the components needed to replicate in a host cell with the aid of host cofactors.

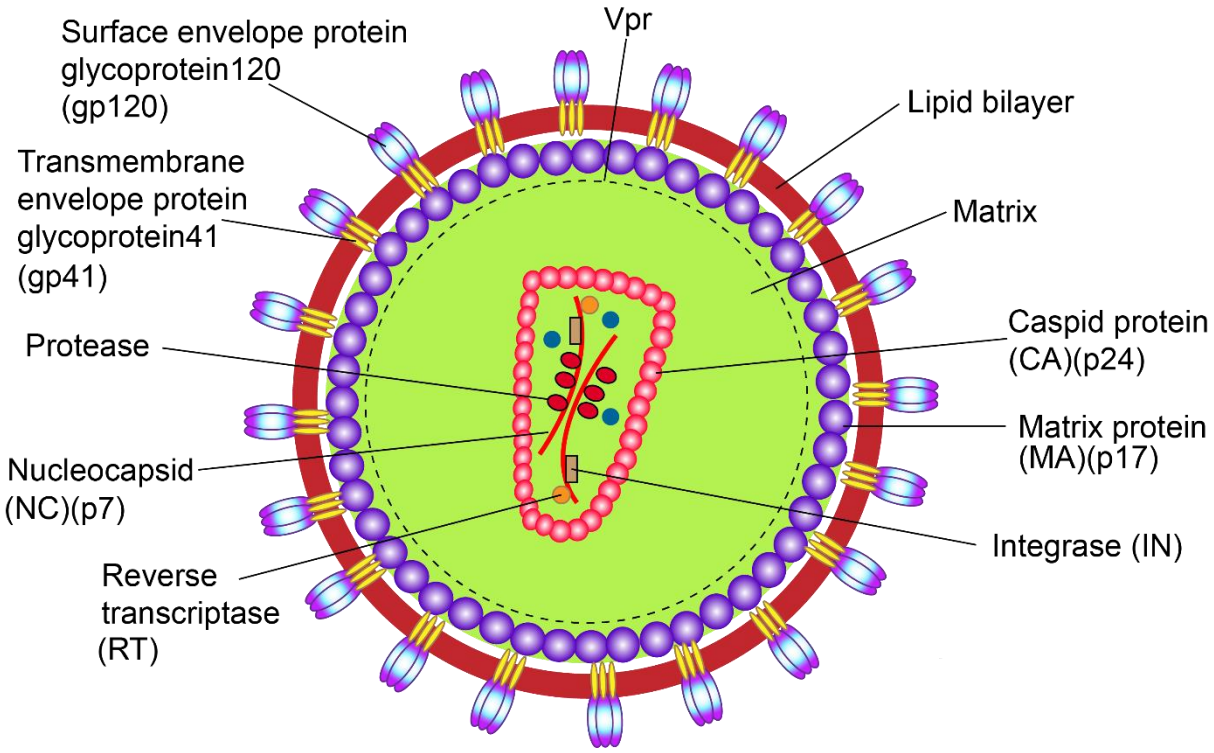


Figure 1. 2: Representative figure of an HIV virion displaying structural and functional proteins. The virion contains capsid protein (p24), matrix protein (p17), nucleocapsid (p7), reverse transcriptase, integrase and protease, as well as envelope glycoproteins, gp120 and gp41. Picture adapted Hosseini and Mac Gabhann, 2012 (Hosseini and Mac Gabhann, 2012) .

1.3 HIV-1 Lifecycle

The HIV-1 lifecycle is a multiple step process consisting of six stages: viral fusion and entry, reverse transcription, nuclear import, integration and transcription, translation and finally viral particle assembly and budding as shown in Figure 1.3.

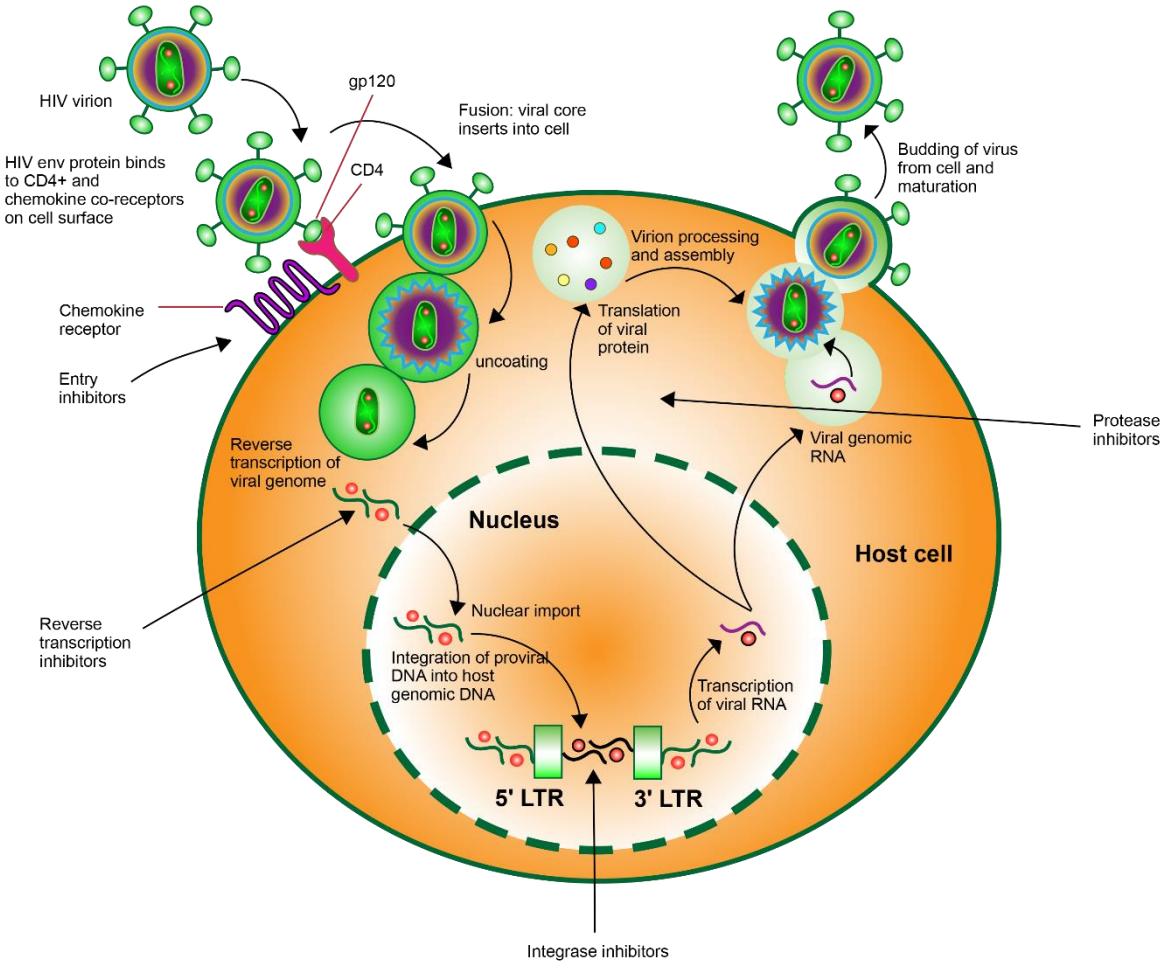


Figure 1. 3: Lifecycle of HIV-1 showing the individual steps of entry, reverse transcription, integration, transcription, translation, assembly and budding. The figure also points out the current targeted steps for antiretroviral drug intervention in the lifecycle. Figure is adapted from Rambaut *et al*, 2004 (Rambaut et al., 2004).

HIV-1 entry requires a cell that carries a CD4 receptor on the surface of the cell. The chain of events begins when the HIV-1 trimeric gp120 binds to the CD4 receptor which triggers a conformational change in the gp120 allowing for binding to the chemokine co-receptors; CXCR4 or CCR5. The co-receptor binding facilitates viral fusion and entry (Deng *et al*., 1996; Choe *et al*., 1996; Dragic *et al*., 1996; Mondor *et al*., 1998; Moulard *et al*., 2000). The viral envelope fuses with the host cell membrane allowing entry of the viral capsid into the host cell cytoplasm. The viral capsid contains the ribonuclease (RNA) genome, reverse transcriptase (RT), RNaseH and integrase (IN). The capsid is disassembled and the RNA genome is reverse transcribed into cDNA by RT. The RNaseH degrades the RNA in the RNA-DNA hybrid (Craigie, 2001; Fouchier and Malim, 1999; Gallay *et al.*, 1997; Krishnan

and Engelman, 2012). Viral IN is responsible for 3' processing of the cDNA, resulting in CA overhangs. These overhangs act as nucleophiles for the strand transfer step. The cDNA is then assembled into the pre-integration complex (PIC). The PIC consists of viral cDNA, RT, IN, Vpr, capsid, matrix and host proteins such as lens epithelial derived growth factor (LEDGF/p75) amongst other proteins. The PIC contains everything needed for nuclear transport and integration of the viral cDNA into the host DNA (Bukrinsky *et al*., 1993; Devroe, 2003). Viral cDNA is then transported into the nucleus via the PIC where integration occurs. LEDGF/p75 is a chromatin bound protein that interacts with HIV-1 IN in the cytoplasm or possibly even in the incoming viral particle and plays a role in determining the specificity of the integration site. Once the cDNA associates with the host DNA, HIV-1 IN catalyses the strand transfer reaction (Brown *et al*., 1987; Engelman *et al*., 1991; Fujiwara and Mizuuchi, 1988) (HIV-1 integration will be discussed in more detail in section 1.5). Once integration has occurred the integrated viral genome is transcribed and translated by cellular enzymes, resulting is a newly synthesized viral RNA genome and polyproteins. The Gag/GagPol and Envelope polyproteins are cleaved by viral or host proteases, respectively, to form functional proteins. All the components assemble near the cell surface and budding of an immature virion occurs from the infected cell. Viral protease completes the cleavage of the GagPol polyprotein to form a mature virion. The new viral particles are then free to infect nearby cells (Sundquist and Kräusslich, 2012). Each of these steps in the replication cycle is a potential target for drug intervention.

1.4 Mechanisms of HIV-1 inhibition and current antiretroviral drug target(s)

Highly active antiretroviral therapy (HAART) is a combination of various mechanistically different drugs targeting multiple steps in the lifecycle (Mocroft *et al.*, 2003; Laskey and Siliciano, 2014). Currently the United States Food and Drug Administration (FDA) approved drugs that target entry, reverse transcription, integration and proteolytic cleavage/maturation. Table 1.1 contains all the current United States FDA approved drugs and their mode of action.

Table 1.1: FDA approved drugs for the treatment of HIV-1 infection with mode of action and approval date.

Mechanism of Action	Brand name	Active ingredient	FDA approval date
HIV Fusion and Entry			
Fusion Inhibitors			
Binds to gp41 thereby preventing fusion of the viral envelope to the host cell membrane	Fuzeon	Enfuvirtide	13 March 2003
Entry Inhibitors			
Chemokine receptor antagonist preventing gp120 from binding CCR5	Selentry	Maraviroc	6 August 2007
Reverse Transcription			
Nucleoside Reverse Transcriptase Inhibitors (NRTIs)			
Mimics dNTPs and compete for incorporation during reverse transcription	Retrovir	Zidovudine	19 March 1987
	Videx	Didanosine	9 October 1991
	Zerit	Stavudine	24 June 1994
	Epivir	Iamivudine	17 November 1995
	Ziagen	Abacavir	17 December 1998
	Videx EC	Dideoxyinosine, Enteric-coated	31 October 2000
	Viread	Tenofovir dioproxil fumarate	26 October 2001
	Emtriva	Emtricitabine	2 July 2003
Non-Nucleoside Reverse Transcriptase Inhibitors			
Allosterically bind to reverse transcriptase thereby modifying the enzyme active site	Viramune	Nevirapine	21 June 1996
	Intelence	Etravirine	18 January 2008
	Viramune XR	Nevirapine extended release	25 March 2011
	Edurant	Rilpivirine	20 May 2011
	Sustiva	Efavirenz	17 September 1998
Integration			
Strand Transfer Inhibitors			
Binds to the active site of integrase preventing the strand transfer reaction	Isentress	Raltegravir	12 October 2007
	Tivicay	Dolutegravir	13 August 2013
	Vitekta	Elvitegravir	24 September 2014
Proteolytic Cleavage			
Protease Inhibitors			
Prevents protease activity by binding to the active site resulting in immature virions	Novir	Ritonavir	1 March 1996
	Crixivan	Indinavir	13 March 1996
	Viracept	Nelfinavir	14 March 1997
	Reyataz	Atazanavir	20 June 2003

	Lexiva	Fosamprenavir	20 October 2003
	Aptivus	Tipranavir	22 June 2005
	Prezista	Darunavir	23 June 2006
	Invirase	Saquinavir	6 December 1995
Pharmacokinetic Enhancers			
Booster	Tybost	Cobicistat	24 September 2014
Combination HIV Medication			
	Odefsey	Emtricitabine, rilpivirine & tenofovir alafenamide	1 March 2016
	Complera	Emtricitabine, rilpivirine & tenofovir disoproxil fumarate	10 August 2011
	Atripla	Efavirenz, emtricitabine & tenofovir dispproxil fumarate	12 July 2006
	Trizivir	Abacavir, lamivudine & zidovudine	14 November 2000
	Kaletra	Lopinavir & ritinavir	15 September 2000
	Epzicom	Abacavir & lamivudine	2 August 2004
	Truvada	Emtricitabine & tenofovir disoproxil fumarate	2 August 2004
	Juluca	Dolutegravir & rilpivirine	21 November 2017
	Triumeq	Abacavir, dolutegravir & lamavudine	22 August 2014
	Stribild	Elvitegravir, cobicistat, emtricitabine &tenofovir disoproxil fumarate	27 August 2012
	Combivir	Lamivudine & zidovudine	27 September 1997
	Evotaz	Atazanavir & cobicistat	29 January 2015
	Prezcobix	Darunavir & cobicistat	29 January 2015
	Descovy	Emtricitabine & tenofovir alafenamide	4 April 2004
Combination of FDA approved medications	Genovoya	Elvitegravir, cobicistat, emtricitabine & tenofovir alafenamide fumarate	5 November 2015

The first drug class as per Table 1.1, targeting entry, contains chemokine receptor antagonists and fusion inhibitors. Maraviroc is a chemokine receptor antagonist that prevents gp120 binding to the CCR5 co-receptor. Enfuvirtide is a fusion inhibitor that binds gp41 thereby preventing the fusion of the viral envelope to the host cell membrane (Henrich and Kuritzkes, 2013). The second, reverse transcription, is targeted by two classes of inhibitors, including nucleoside/tide reverse transcriptase inhibitors (NRTIs) which mimic dNTPs and compete for incorporation during reverse transcription, resulting in chain termination, and non-nucleoside reverse transcriptase inhibitors (NNRTIs) which allosterically bind to RT modifying the enzyme's conformation (Sluis-Cremer *et al.*, 2004). The third target, integration, has integrase strand transfer inhibitors (INSTIs) that bind to the IN active site preventing the strand transfer step of integration (Hazuda, 2012). This is discussed in more detail in Section 1.5. The last FDA approved target as per Table 1.1, is proteolytic cleavage/maturation with protease inhibitors (PIs) that prevent protease activity by binding to the protease active site and result in immature virions (la Porte, 2009).

Although HAART has significantly reduced the morbidity and mortality associated with HIV infection, HAART can fail due to toxicity, poor viral response or patient adherence to the regimen which can lead to the development of antiretroviral drug resistance. Drug resistance is also due to mutations caused by the high rate of viral replication, common errors of RT and high rates of recombination. With the virus's propensity to evade current treatments, constant research is therefore needed to identify novel drug targets and new drugs.

Dual mode inhibitors for reverse transcription and integration were discovered as early as 2003 (Bukrinsky *et al*., 1993). This area of research has expanded recently with more drug discovery groups focusing on finding inhibitors with dual modes of action (Gu *et al*., 2016; Meleddu *et al*., 2017; Paneth *et al.*, 2017). This is possibly due to the discovery of allosteric integrase inhibitors (ALLINIs) that have been shown to affect reverse transcription, integration as well as virion maturation (F. Christ et al., 2012; Kessl et al., 2012; Jurado et al., 2013; Kushol Gupta et al., 2014; K. Gupta et al., 2014; Deng et al., 2016; Gupta et al., 2016). Due to these findings HIV-1 IN has come to the forefront in recent times as a target for the identification of drugs with novel modes of action.

1.5 Integrase structure and function

1.5.1 Structure of HIV-1 IN

HIV-1 IN consists of three domains namely the N-terminal domain (NTD), the catalytic core domain (CCD) and the C-terminal domain (CTD). The NTD (residues 1-46) is linked to the CCD (residues 56-202) by a linker segment consisting of residues 47-55, whereas the CTD (residues 220-288) is connected to the CCD by a flexible loop made up of residues 187-194. Structural analysis indicates that each domain exists as a dimer (Cai et al., 1997; Dyda et al., 1994; Eijkelenboom et al., 1997; Goldgur et al., 1998; Lodi et al., 1995). Crystal structures have been determined for the CTD-CCD as well as CCD-NTD (Chen et al., 2000; Wang et al., 2001). However the structure differs when NTD or CTD are crystallised in isolation (Cai et al., 1997; Eijkelenboom et al., 1997). The crystal structure of CCD-CCD remains constant throughout various constructs indicating the protein-protein contacts will remain in a fully functional nucleoprotein complex (Chen et al., 2000; Dyda et al., 1994; Goldgur et al., 1998, 1998; Wang et al., 2001). Residues 1 - 46 make up the NTD, a helix bundle, which is responsible for Zn^{2+} binding through a histidine (HIS) cysteine (CYS) (HHCC) motif. This Zn^{2+} binding increases catalytic activity and also contributes to the oligomerisation of IN (Zheng et al., 1996). If mutations occur in the HHCC motif such as H12N/C or H16N/V there is a loss in 3' processing as well as strand transfer activity *in vitro* with resulting low level infection in cells (Bushman *et al*., 1993; Zheng *et al*., 1996; Cai *et al*., 1997; Goldgur *et al*., 1998; Hare *et al*., 2009a). Recent studies have shown the NTD-CCD interactions prompt HIV-1 IN tetramerisation where a mutation of K14A at the NTD-CCD interface causes a destabilisation of the tetramers and in turn compromises catalytic activities (McKee et al., 2008). Residues 56-186 make up the CCD which adopts an RNaseH-like fold and contains a catalytically active triad made up of the three amino acids D46, D116 and E152 (known as the DDE motif). The D64 and D116 co-ordinate 2 Mg^{2+} ions which are crucial for catalytic activity. The DDE motif mediates both strand transfer and 3' processing with mutations of D64N, D115N and E153Q resulting in the enzyme losing catalytic activity (Bushman *et al.*, 1993; Dyda *et al*., 1994; Jenkins *et al.*, 1996; Goldgur *et al*., 1998; Chen *et al.*, 2000). All three of the domains of HIV-1 IN contribute to the IN-DNA interaction either directly or indirectly. The same catalytic site is used for both 3'processing as well as strand transfer activity and as such the CCD is likely to be the binding site for both viral and target DNA (Beese and Steitz, 1991; Lins et al., 2000; Yang et al., 2006). Figure 1.4 shows the ribbon structure of the CCD dimer further magnified to show the area where the DDE motif occurs.

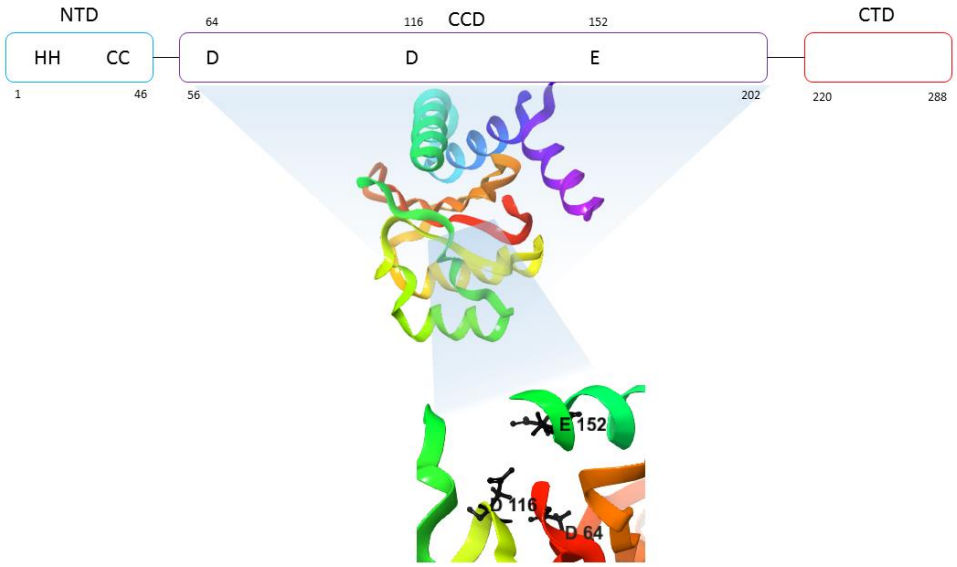


Figure 1. 4: The basic layout of HIV-1 integrase with the ribbon structure of the Catalytic Core Domain. The figure shows the formation of the DDE triad motif made up of D64, D116 and E152. Ribbon structure adapted from Protein Data bank 5KRT with use of Maestro 11.2, Schrodinger, 2017.

The final domain which consists of residues 220-288 is known as the CTD. The CTD has Src homology 2 SH3 like fold and is responsible for both host DNA and viral cDNA binding. Mutations of R262G, L234A, V260E, L241A and L242A result in the loss of DNA binding and show a reduction in *in vitro* catalytic activity (Eijkelenboom *et al*., 1995, 1997; Chen *et al.*, 2000). Mutations L241A and L242A also cause a disruption in the dimerization of IN (Lutzke and Plasterk, 1998). The correct folding of HIV-1 IN is crucial to the correct functioning of the enzyme as part of the HIV-1 replication cycle.

HIV-1 IN functions as a multimer, where in *in vitro* assays IN is found as a mix of monomer, dimer and tetramers when DNA is absent (Jenkins et al., 1996; van Gent et al., 1991; Vincent et al., 1993), however, when DNA is present the interactions of these components are stabilised (Li et al., 2006). Various experiments have been conducted to determine the exact binding points of viral DNA with IN. It has been determined via time resolved fluorescence anisotropy that two separate IN monomers bind to each viral DNA end (Delelis et al., 2008; Deprez et al., 2004). Chemical cross-linking studies showed that CCD residues K159, Q148 and Y143 tether nuclear analogues that were incorporated into the terminal section of viral DNA. K159 forms part of the helix containing E152 and potentially directly binds with viral DNA (Esposito and Craigie, 1998; Jenkins et al., 1997) whereas Q148 and Y143, found in the flexible loop, could be involved in the correct positioning of viral and target DNA (Jenkins et al., 1997). In addition to the CCD amino acids some CTD residues have been identified by cross-linking studies to interact with the LTR (Esposito and Craigie,

1998; Gao et al., 2001; Heuer and Brown, 1998, 1997). It should be noted that there is evidence to suggest that IN undergoes conformational change when DNA binds (Zhao et al., 2008). The viral cDNA forms part of the pre-integration complex (PIC). All components of the PIC are not yet known, however thus far it is known to contain cDNA, IN, matrix, nucleocapsid, RT, viral protein R, barrier to auto integration factor, high mobility group chromosomal protein A1 and lens epithelium derived growth factor (LEDGF/p75) (Bukrinsky et al., 1993; Gulizia et al., 1994; Devroe, 2003). LEDGF/p75 plays an important role in the IN-DNA interaction which is discussed in section 1.6. The viral cDNA is associated with the PIC until integration is complete (Bukrinsky et al., 1993).

The crystal structure of full length HIV-1 IN has not been resolved due to poor solubility. However, the crystal structure of the full length Prototype Foamy Virus (PFV) intasome was determined in 2010 (Hare et al., 2010a). This was considered a major breakthrough as it was the only retroviral IN to be crystalized in full length. The sequence similarity of HIV-1 IN and PFV is limited as seen in Figure 1.5. When comparing the PFV structure with the CCD of HIV-1 IN structure, the interface is the same where two dimers form a tetramer (Chen et al., 2000). The viral cDNA makes contact with the inner subunits of each dimer as well as the CTD and NTD. The CTD of PFV is a loop-helix-loop. PFV was found to interact with the strand transfer inhibitor raltegravir (RAL) indicating possible structural similarity. When looking at the structure bound with RAL, RAL has contacts with the cDNA ends making the 3’ ends unavailable for nucleophilic attack, this is synonymous with HIV-1 IN (Chen et al., 2000; Hare et al., 2010a).

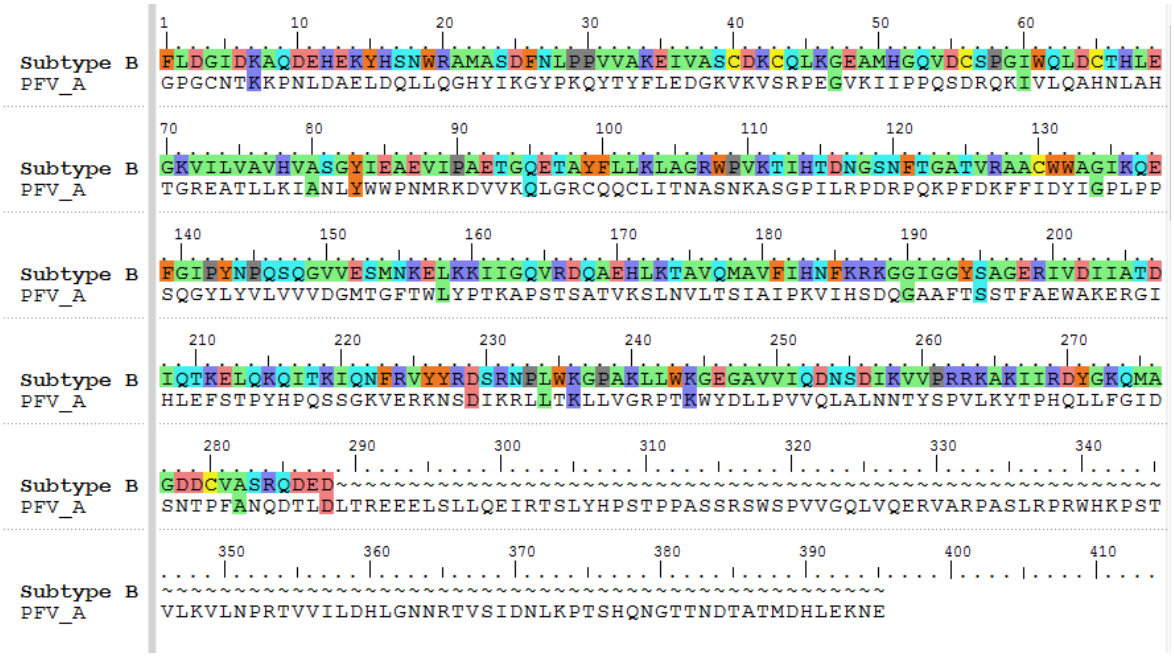


Figure 1. 5: Sequence alignment map comparing Prototype Foamy Virus (first line) and HIV-1 integrase (second line). Where the matching residues are highlighted on the second line. The sequence alignment was done using Maestro BioLuminate 11.2, Schrodinger, 2017.

As discussed in Section 1.1 dealing with HIV epidemiology it was highlighted that HIV-1 group M has many different subtypes. As Europe and America are the leaders in drug research the bulk of research is focused on subtype B. However the dominant subtype worldwide is subtype C and in South Africa this is the subtype of HIV-1 that affects most people. There are 21 amino acid difference between subtype B integrase and subtype C integrase. Figure 1.6 shows the sequence alignment map comparing both subtype to one another.

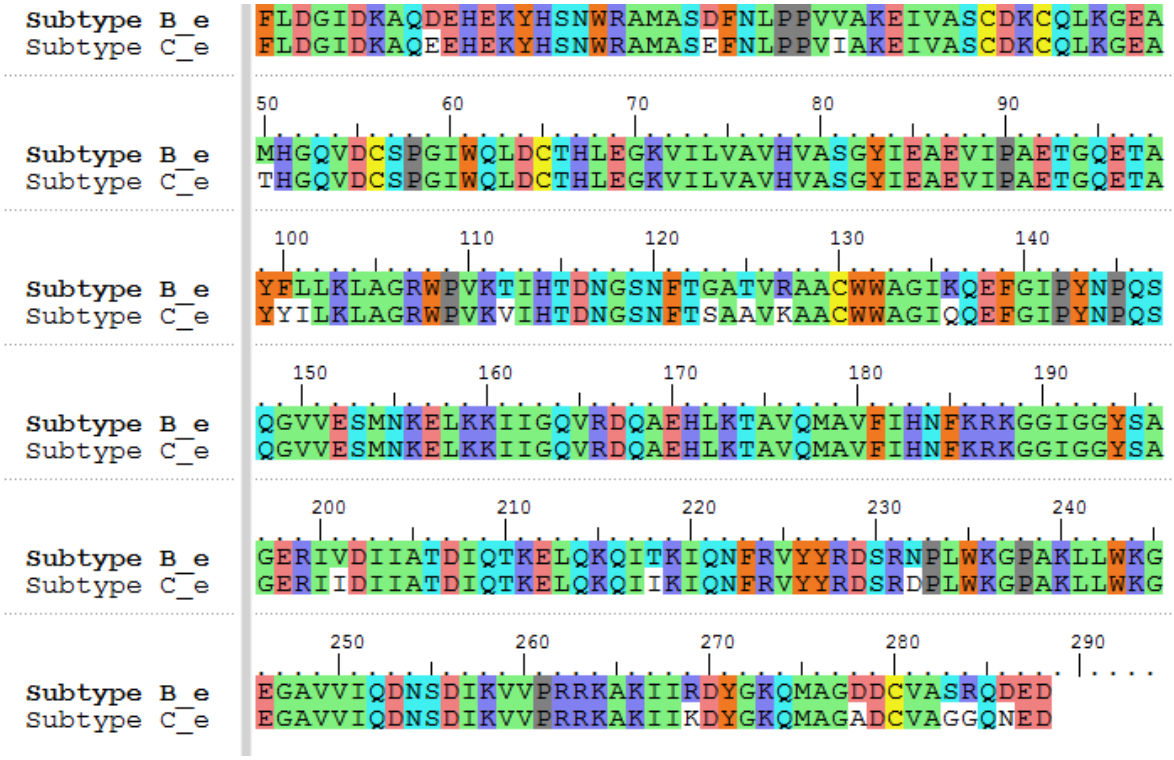


Figure 1. 6: Sequence alignment map comparing Subtype B integrase (first line) and subtype C integrase (second line). Where the difference in residues are not highlighted on the second line. The sequence alignment was done using Maestro BioLuminate 11.2, Schrodinger, 2017

1.5.2 Function of IN

The integration of the HIV-1 genome allows for permanence in the infected individual. The process of reverse transcription forms blunt ended double stranded DNA with the long terminal repeats (LTRs) at both the 3' ends (Hindmarsh and Leis, 1999). HIV-1 IN catalyses the permanent and irreversible integration of the vDNA into host DNA. The integration process involves two spatially and temporally separate reactions but both occur within the active site. In Figure 1.7 the process is displayed diagrammatically. Briefly, the initial reaction known as 3' processing where a di or trinucleotide is cleaved from each 3' end through hydrolysis occurs in the cytoplasm. This exposes the reactive hydroxyl groups that act as nucleophiles for the step known as strand transfer, which occurs in the nucleus. During strand transfer the 3' cDNA ends are used to nucleophilically attack the phosphodiester bonds of the hosts' DNA (Craigie, 2001). HIV-1 IN nicks the hosts DNA at opposite strands that are 5 base pairs apart and synchronously joins the processed ends. The single stranded gaps between the viral and host DNA are ligated by cellular enzymes, thereby completing the process of integration (Craigie, 2001). One of the cofactors that HIV-1 IN needs for full functionality is LEDGF/p75, which is detailed in Section 1.6.

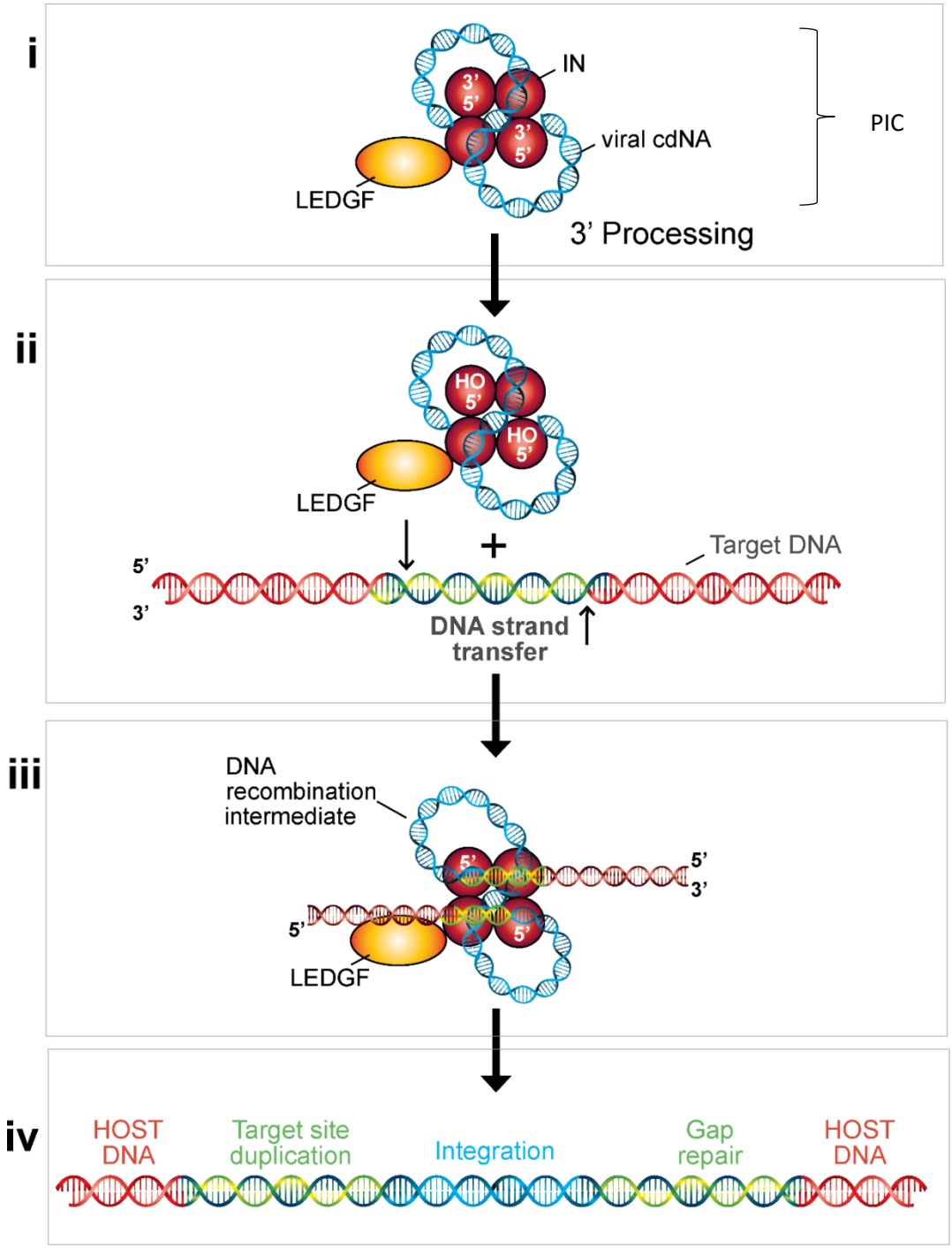


Figure 1. 7: Schematic representation of the HIV-1 integration reaction. In the first step (i) tetrameric IN is bound to viral cDNA and LEDGDF forming the PIC and produces CA overhangs during 3' processing. During step 2 (ii) the PIC is transported to the nucleus where strand transfer begins with binding to the host DNA. The penultimate phase (iii) is where binding is followed by nucleophilic attack to form phosphodiester bonds leaving a 5' DNA flap. Finally (iv) the DNA is repaired by cellular machinery resulting in integration. Diagram was drawn and altered from Bushman et al 1990 and Chen et al 2000 (Bushman *et al*., 1990; Chen *et al*., 2000).

1.6 Lens Epithelium Derived Growth Factor

LEDGF is a chromatin bound protein that is expressed ubiquitously in humans. The initial discovery of LEDGF was via micro sequencing of a co-purified transcriptional co-activator positive cofactor protein (PC4) (Hui Ge et al., 1998). Subsequently it was isolated from a mouse lens epithelium library as a cell protector from oxidative stress and was then coined LEDGF (Singh et al., 1999). The protein has 2 isoforms expressed from the PC-4 and SFR5 interacting protein gene (*PSIP1*) which is alternately spliced to form the 2 variants LEDGF/p52 and LEDGF/p75 as seen in Figure 1.8 (H. Ge et al., 1998; Singh et al., 1999). Both variants share the NTD and as such they both contain the PWWP domain, AT hook motif, nuclear localization signal (NLS) and conserved charged region. The PWWP domain is a 70 amino acid sequence that is named so due to the central core consisting of Pro-Trp-Trp-Pro, the domain is found in DNA binding proteins and functions as a transcription factor. The PWWP domain binds methylated histones as well as DNA and has been found to be associated with DNA repair, histone modification and DNA methylation. The NLS is responsible for interacting with the nuclear import function of the cell, this means that it allows PWWP proteins to access DNA (van Nuland *et al*., 2013).

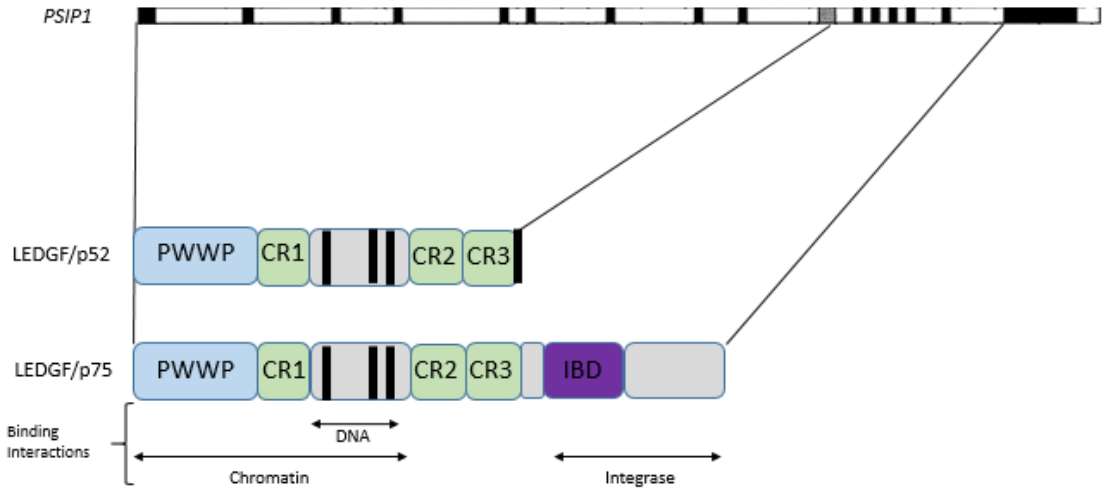


Figure 1. 8: The PSIP1 gene showing the exons and introns indicated in black and white respectively. Including the 2 splice variants LEDGF/p52 and LEDGF/p75 showing the binding interaction on the proteins where chromatin, DNA and integrase. Both proteins show the PWWP domain and LEDGF/p75 shows the integrase binding domain.

LEDGF/p75 differs from LEDGF/p52 as the CTD contains an additional 205 amino acids which contain the integrase binding domain (IBD). It was named the IBD due to the discovery of the interaction with HIV-1 IN, however it has now been found to interact with other cellular partners such as MLL1 and 2/Menin complex, JPO2, POGz, CDC7-1 activator

of S phase kinase complex and Spt6 (1WS1) (Cherepanov *et al*., 2004; Maertens *et al*., 2004; Bartholomeeusen *et al*., 2007; Yokoyama and Cleary, 2008; Bartholomeeusen *et al*., 2009; Hughes *et al*., 2010; van Nuland *et al*., 2013; Gérard *et al.*, 2015; Tesina *et al.*, 2015). JPO2 binds c-Myc via the amino acid motif 213-235 and this binding contributes to the c-Myc-mediated transformation in medulloblastoma (Huang et al., 2005). PogZ is a transposase consisting of a DDE domain at the CTD. This is common in catalytic enzymes for DNA cleavage followed by stand transfer reactions (Bartholomeeusen et al., 2009). In a similar fashion to the PIC MLL1-menin, JPO2 and PogZ are tethered to DNA via LEDGF/p75 (Bartholomeeusen et al., 2009, 2007; Maertens et al., 2006).

As more research is being done into understanding LEDGF/p75, more cellular roles are found, for example it plays a role in transcriptional regulation, cell survival, cancer pathogenesis as well as DNA repair and autoimmunity (Bowerman et al., 1989; Bukrinsky et al., 1993; Esposito and Craigie, 1998). It has also been linked to gene regulation of pathologic processes of myeloid leukaemia (Murai et al., 2014). LEDGF/p75 has been extensively studied for HIV-1 IN integration, whereby HIV-1 integrase binds at the IBD of LEDGF/p75. This domain is missing in LEDGF/p52 (Cherepanov et al., 2003).

1.7 HIV-1 IN- LEDGF/p75 interaction

LEDGF/p75 serves to protect HIV-1 IN as part of the PIC from proteasomal degradation in the cytoplasm during the process of nuclear migration. As part of the PIC, LEDGF/p75 aids in the transition from 3' processing into strand transfer as LEDGF/p75 anchors HIV-1 IN to viral cDNA. The interaction between cDNA, LEDGF/p75 and HIV-1 IN is reliant on the HIV-1 IN dimer-dimer interface, an intact IBD and the AT hook motif (Cherepanov *et al*., 2003; Busschots *et al.*, 2005).

The binding of LEDGF/p75 to HIV-1 IN is achieved by spanning the CCD-CCD interface of a single HIV-1 IN dimer and binding to the NTD of the second dimer. The binding of LEDGF/p75 to HIV-1 IN is favoured when HIV-1 IN is in tetrameric form. In this formation a V-shaped cavity is formed by the two CCDs and this cavity functions as the docking site for LEDGF/p75, as seen in Figure 1.9. The IBD of LEDGF/p75 consists of 4 α helices that form a right handed helical bundle connected by a fifth α helix (Cherepanov *et al*., 2005a; McKee *et al*., 2008; Hare *et al*., 2009a, 2009b).

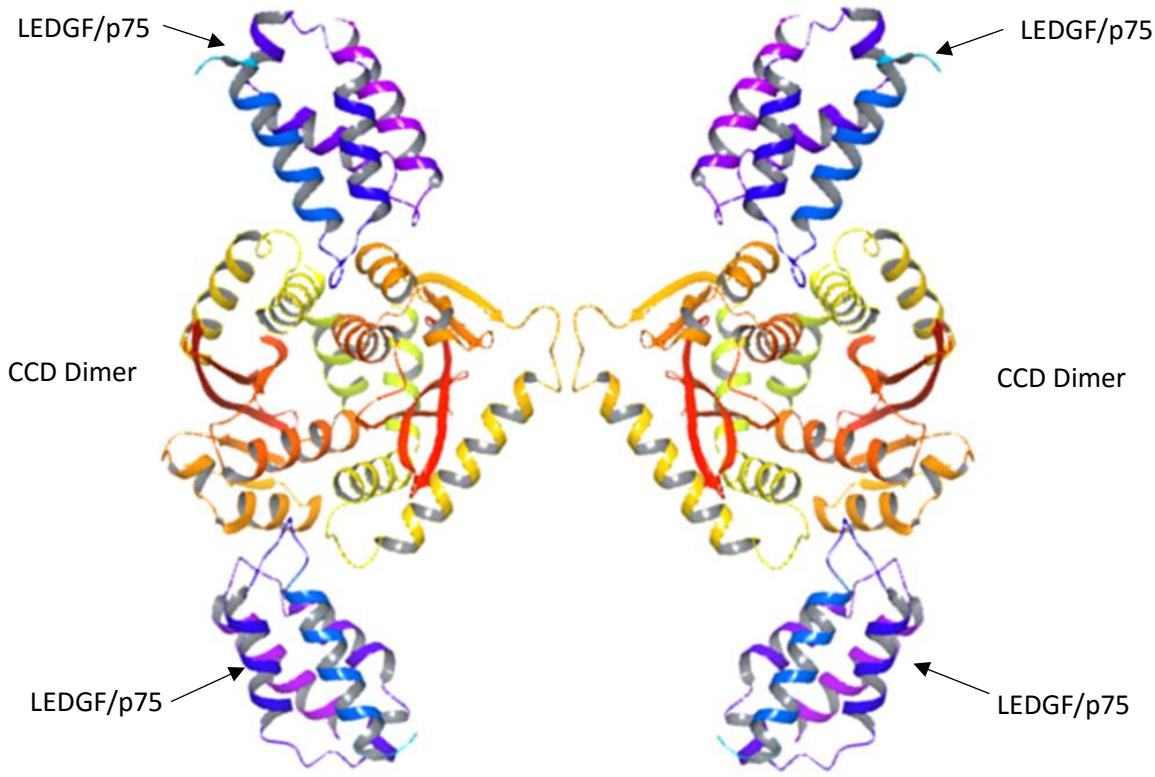


Figure 1. 9: Protein data bank crystal structure 2J4B, https://www.rcsb.org/structure/2b4j, of the two HIV-1 IN dimers interacting with LEDGF/p75. The central yellow area is that of the HIV-1 IN CCD dimer and the 4 purple and blue ribbon structures are that of LEDGF/p75 where 4 LEDGF/p75 proteins interact with an HIV-1 IN dimer. The structure was drawn using Maestro 11.2, Schrodinger, 2017.

LEDGF/p75 interacts with one dimer of HIV-1 IN via a hydrogen bond between Asp366 on LEDGF/p75 and the Glu170 and His171 of HIV-1 IN. The second dimer interacts with LEDGF/p75 through hydrophobic interactions of Ile365, Leu366, Phe406 and Val408. The interaction between LEDGF/p75 and the NTD of the second dimer is through electrostatic interactions (Busschots *et al*., 2007; Hare and Cherepanov, 2009). Figure 1.10 shows the HIV-1 CCD interaction with LEDGF/p75 with magnification to see the interacting amino acids.

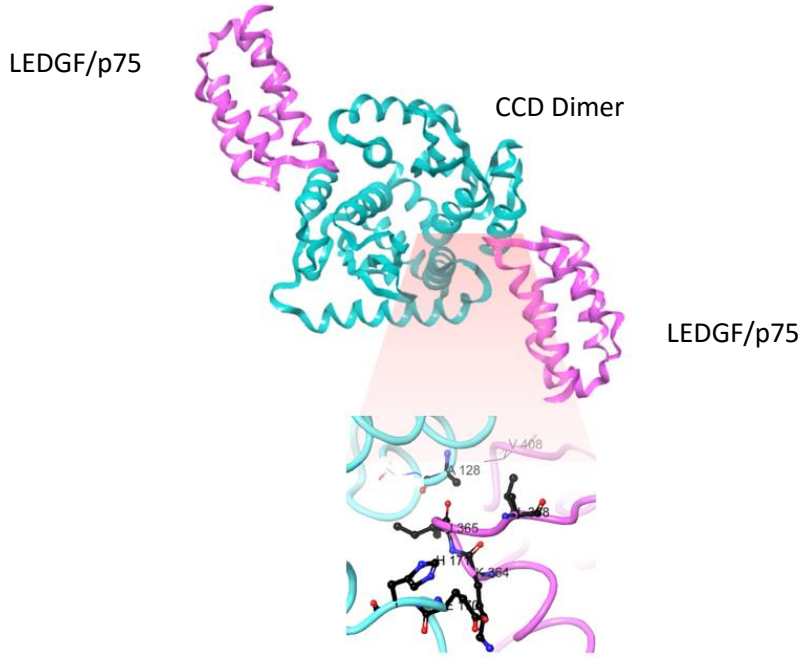


Figure 1. 10: The HIV-1 IN CCD dimer interaction with LEDGF/p75. Protein data bank crystal structure code 2B4J, https://www.rcsb.org/structure/2b4j, with expansion of the binding area showing the sites of interacting amino acids. Figure adapted from Christ *et al*., and Cherepanov *et al*., (Hare and Cherepanov, 2009; Christ *et al*., 2010).

The interaction of LEDGF/p75 and HIV-1 IN is diminished if there are mutations at Ile365, Asp366 or Phe406, with severe reduction in binding with a mutation at Val408. This indicates the V cleft's importance in the HIV-1 IN-LEDGF/p75 interaction (Cherepanov *et al.*, 2005b).

1.8 Modes of drug inhibition

1.8.1 Reversible inhibition

Drugs that fall into the class of reversible inhibitors bind to the enzyme via non-covalent interactions such as hydrogen bonds, hydrophobic interactions and ionic bonds. A combination of these interactions can result in a strong and specific bond. However, due to the weak interactions and lack of chemical bonds to the enzyme the interaction forms rapidly and dissociates rapidly. There are three types of reversible inhibition: competitive inhibition, uncompetitive inhibition and non-competitive inhibition (Berg et al., 2002).

1.8.1.1 Competitive inhibition

Competitive inhibitors compete with the substrate for enzyme binding. The inhibitor has an affinity for the active site and is often similar in structure to the real substrate. The inhibition can be overcome by increasing the concentration of the substrate so that it out competes the inhibitor (Berg et al., 2002). These types of inhibitors can only bind to the enzyme and not the enzyme- substrate complex. Due to this the enzyme kinetics are unchanged but the Michaelis constant is increased due to the interference with the binding of substrate. Competitive binding can also be allosteric provided the substrate and inhibitor cannot bind the substrate simultaneously (Berg et al., 2002). Figure 1.11 shows competitive inhibition.

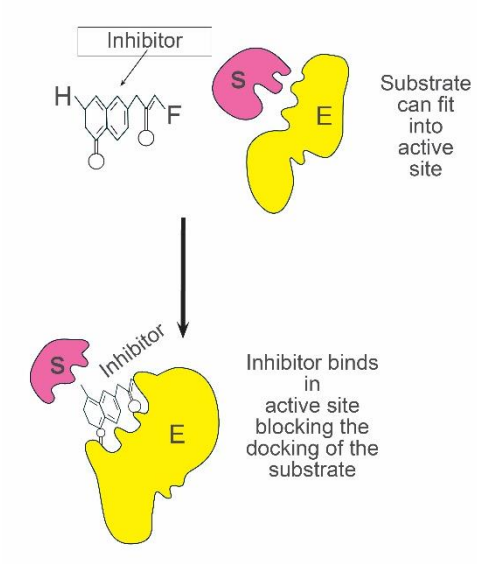


Figure 1. 11: Diagrammatical representation of the mechanistic binding of competitive inhibition. Constructed using Adobe InDesign, 2017.

1.8.1.2 Uncompetitive inhibition

An uncompetitive inhibitor binds on the enzyme-substrate complex as the binding site for the inhibitor is only formed once substrate and enzyme have interacted. This type of inhibition stops the formation of the product. The binding of the substrate structurally alters the enzyme forming a docking site for the inhibitor, both Vmax and Km are reduced in this type of inhibition (Berg et al., 2002). Figure 1.12 shows uncompetitive inhibition.

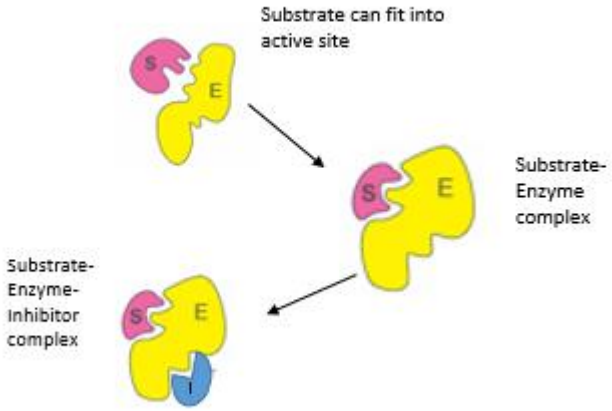


Figure 1. 12: Diagrammatical representation of the mechanistic binding of uncompetitive inhibition. Constructed using Adobe InDesign, 2017.

1.8.1.3 Non-competitive inhibition

Non-competitive inhibitors bind to the enzyme at different places simultaneously altering the enzyme's active site thereby preventing substrate binding. This in turn stops enzyme activity. No amount of increase in substrate will stop this inhibition and therefor Km is unchanged but Vmax decreases (Berg et al., 2002). Figure 1.13 shows non-competitive inhibition

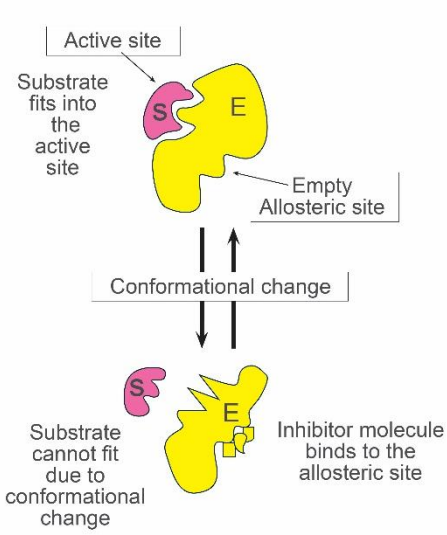


Figure 1. 13: Diagrammatical representation of the mechanistic binding of non-competitive inhibition. Constructed using Adobe InDesign, 2017

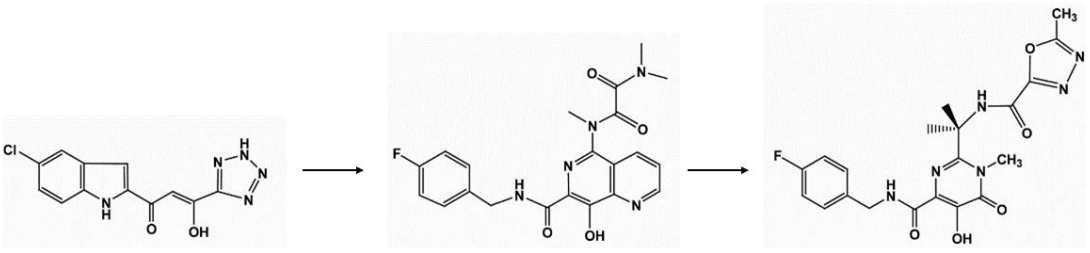
1.8.2 Irreversible inhibitors

The types of inhibitors bind to an enzyme via covalent binds that cause chemical changes to the enzymes active site which cannot be changed. The primary role of irreversible inhibitors include modification of key amino acids needed for enzymatic activity. Compounds commonly associated with irreversible inhibition contain aldehydes, alkenes and phenyl sulphonates as functional groups (Berg et al., 2002).

1.9 HIV-1 IN as a drug target

1.9.1 Strand transfer inhibition

Integrase strand transfer inhibitors (INSTIs) are the only FDA approved drugs targeting HIV-1 IN, and the first INSTIs were reported in 2000 as diketo acids (DKA) (Hazuda *et al.*, 2000). The compounds were discovered as a result of screening a large compound library for strand transfer inhibitors. 5-CITEP, a DKA was used as a template to design and develop compounds that exhibited improved inhibitory profile including bioavailability and tolerability (Lataillade and Kozal, 2006; Summa *et al*., 2008). Two variations of 5-CITEP, L-731988 and L-870812 were used to ultimately develop N-[(4-flourophenyl) methyl]-1, 6-dihydro-5-hydroxy-1-methyl-2-[1-methyl-1-[[5-methyl-3, 4-oxadiazol-2-yl) carbonyl] amino] ethyl-6-oxo-4-pyrimidine carboxamide monopotassium salt, commonly known as raltegravir (RAL). Figure 1. 14 shows the progress from 5-CITEP to RAL. RAL progressed through clinical trials to become the first FDA approved INSTI in 2007 (Cocohoba and Dong, 2008).



5-CITEP L-870812 Raltegravir

Figure 1. 14: Development of raltegravir showing the steps from 5-CITEP to L-870812 through to raltegravir. Raltegravir is a potent inhibitor of the strand transfer reaction with an IC_{50} of 2-7nM. Figure formulated with use of diagrams from Chemspider.

Due to difficulties in obtaining the crystal structure of full length HIV-1 IN, it could not be used to determine the binding and mechanism of action (MOA) of RAL. However, the PFV integrase has been crystalized, and considering that RAL is active against PFV *in vitro* it was used to give a better understanding of the MOA (Hare et al., 2010b).

Mechanistically it was found that the Mg^{2+} ions were chelated by RAL oxygen atoms that are positioned towards the DDE active site, as seen in Figure 1.15. Hydrophobic interaction between RAL and amino acids Y212 aided by interactions with P214 caused the intasome to be inactive. In addition DNA interaction was disrupted by RAL interaction with the CA nucleotide on the viral cDNA (Hare et al., 2010b).

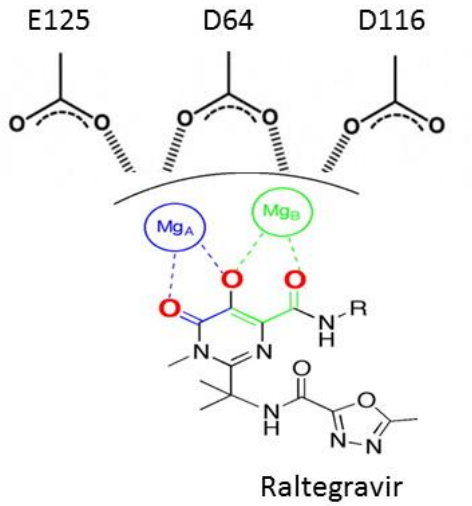


Figure 1. 15: Mechanism of action of raltegravir showing the binding to the DDE triad and the magnesium ions to the oxygen groups of raltegravir. Atoms labelled in red form part of the heteroatom donor triad which co-ordinates to the active site magnesium's chelating rings A and B where A is blue and B is green. Diagram adapted from Agrawal *et al* (Agrawal *et al.*, 2012).

Although RAL was a major breakthrough, HIV-1 drug resistance strains have since emerged. Common amino acid mutations in the HIV-1 IN that confer RAL drug resistance include N155H, Q148K/R/H, G140S and E92Q as seen in Figure 1.16 (Blanco *et al*., 2011).

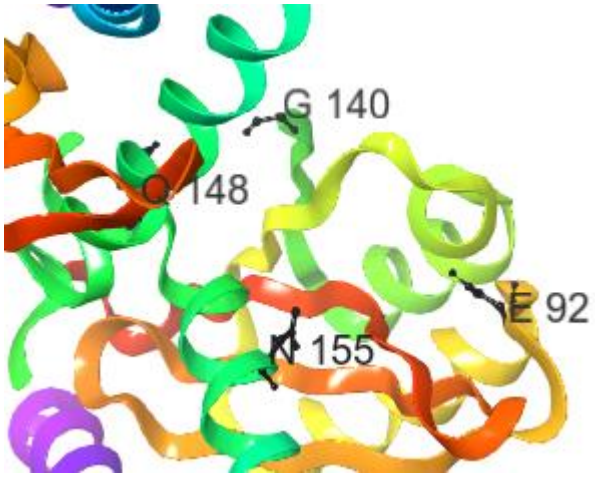


Figure 1. 16 The catalytic core domain of integrase, magnified to show the amino acids commonly associated with raltegravir resistance

DKAs were further optimized, which led to the discovery of a derivative of 4-4-quinoline-3-glyoxylic acid which displayed promising inhibition and was used as a scaffold to develop 6-[(3-chloro-2-fluorophenyl)methyl]-1-[(2S)-1-hydroxy-3-methylbutan-2-yl]-7-methoxy-4-oxoquinoline-3-carboxylic acid, commonly known as Elvitegravir (ELV, Figure 1.17) ELV was FDA approved in 2012 as part of the combination pill Stribuld, however the genetic barrier to resistance was comparable, and a high rate of dual resistance was soon seen (Sato *et al*., 2006; Al-Mawsawi *et al*., 2008). Mutations in E92Q, Q148H/K/R and N115H were all identified during clinical trials. Both RAL and ELV are first generation INSTIs.

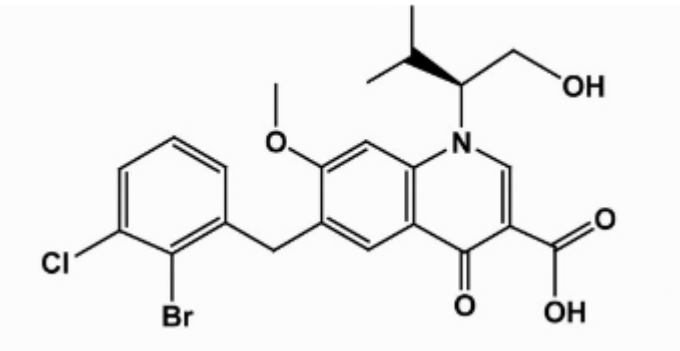


Figure 1. 17: Chemical structure of elvitegravir. Elvitegravir was co-developed by GlaxoSmithKline and Shionogi Pharmaceuticals with an IC_{50} of 16nM inhibition of strand transfer activity. Copied from Chemspider, www.chemspider.com/Chemical-Structure.4441060, date accessed 22/3/2017.

A second-generation drug known as dolutegravir (DTG) was developed by GlaxoSmithKline and Shionogi Pharmaceuticals. The development was undertaken to prevent cross resistance with RAL and ELV resistant mutations and to develop a single dose drug. DTG was FDA approved in 2013 and is active against the amino acid resistance strains N155 and Q148 (Johns *et al*., 2013). Figure 1.18 shows the chemical structure of DTG.

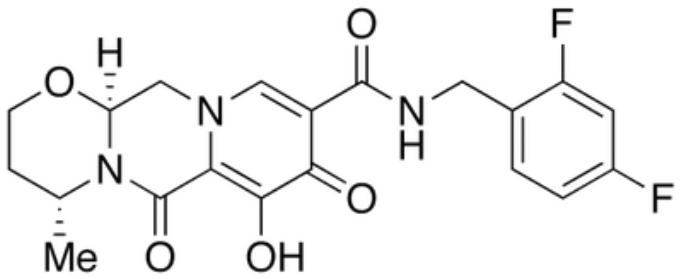


Figure 1. 18: The chemical structure of dolutegravir. DTG has strong strand transfer inhibition as well as antiviral activity with an IC_{50} of 1.07nM inhibition of strand transfer activity. Copied from Chemspider, www.chemspider.com/Chemical-Structure.25051637, accessed on 22/03/2017.

1.9.2 HIV-1 IN-LEDGF/p75 as a target

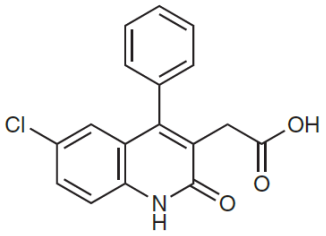
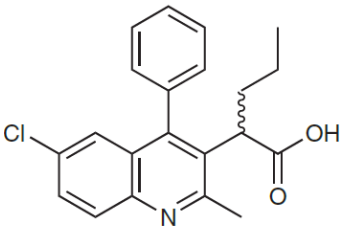
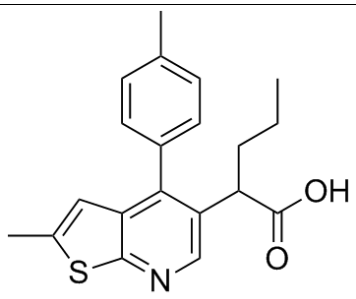
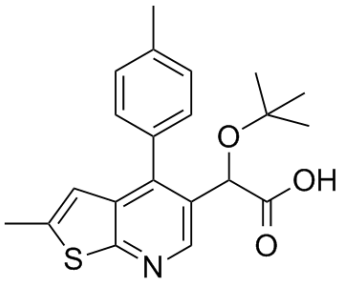
The interaction between HIV-1 IN and LEDGF/p75 has been found to be necessary for viral replication as described above. When experiments were conducted whereby LEDGF/p75 was knocked down by RNA interference, the HIV-1 IN lost its association with chromatin and was found in the cytoplasm (Vandekerckhove et al., 2006).

Due to the hydrophobic interactions between LEDGF/p75 and HIV-1 IN tetramers the interaction poses a potential target for small molecule inhibition. As previously described any alteration in amino acids Ala128, Gly170, Gln168, Tyr131 and Tyr132 has an impact on the effective binding of LEDGF/p75 to HIV-1 IN. In 2010, Christ *et al.,* published the discovery of HIV-1 IN-LEDGF/p75 inhibitors after the virtual screening of a 200 000-compound library which lead to a subset of compounds to be screened through an AlphaScreen enzyme linked immunosorbent assay (ELISA) that requires no washing between the additions of components. In the study, a compound labelled LEDGIN 3 was found to have an IC_{50} of 12.2 ± 3.4 µM for the direct protein-protein interaction of HIV-1 IN-LEDGF/p75 and had moderate EC_{50} of 41.9 ± 1.1 µM. With this compound they were able

to obtain crystallographic data for the CCD of HIV-1 IN and further synthesised 3 new analogues. The analogues showed increased activity with the best compound being LEDGIN 6 also known as CX05168 with an IC_{50} of 1.37 ± 0.36 µM and an EC_{50} of 2.35 ± 0.28 µM. This compound did not affect DNA binding and had a weak response to inhibiting the catalytic activity. This was the first report of allosteric IN activity which was then coined ALLINIs (Christ *et al*., 2010a).

Table 1.2 shows all the compounds, ranging from compound 3 to the final CX14442 compound. Modifications to CX05168 produced CX05054 with an IC_{50} of 0.58 ± 0.30 µM and an antiviral EC_{50} of 0.76 ± 0.08 µM. Further modification and improvements resulted in compound CX14442 with an IC_{50} of 0.046 ± 0.012 µM and an antiviral EC_{50} of 0.069 ± 0.003 µM. However at this point these compounds showed strand transfer inhibition with an IC_{50} of 573 nM for CX14442, and it was found that the strand transfer inhibition was incomplete maximal inhibition. CX14442 also showed 3' processing inhibition with an IC_{50} of 739 nM. Studies conducted with CX05168, CX5045 and CX14442 showed that these compounds stabilized the HIV-1 IN dimer (F. Christ et al., 2012). Differential scanning fluorometry (DSF) was used to show this stabilisation by determining at what point the protein was denatured by melting. CX14442 showed the largest increase in melting temperature of the HIV-1 IN from the untreated melting temperature of 48.1°C to 62.5°C when treated with CX14442. This stabilization was seen to be concentration dependent. The mechanism of action was still to be determined, but the crystallographic data obtained showed that CX05168 binds in the pocket formed by two monomers of HIV-1 IN. The amide chain of Glu170 and His171 of HIV-1 IN binds to the carboxylic moiety of CX05168 (Christ *et al.*, 2010a; Christ *et al*., 2012).

Table 1.2: Chemical modifications from ALLINI compound 3 to CX14442 showing the improvement in efficiency. Table formulated from Christ et al (Christ *et al*., 2010a; Christ *et al*., 2012).

Compound	Structure	[a]IC_{50} [c] (µM)	[b]IC_{50}[c] (µM)	EC_{50}[d] (µM)	CC_{50}[e] (µM)
Compound 3		12.20±3.40	ND	41.89±1.12	>150
CX05168		1.37±0.36	54.88±24.43	2.35±0.28	59.79±0.51
CX05045		0.58±0.30	5.88±0.10	0.76±0.08	72.16±5.51
CX14442		0.05±0.012	0.57±0.29	0.07±0.03	96.00±16.00

[a]HIV-1 IN-LEDGF/p75 inhibition with standard deviation (STD DEV)
[b]Strand transfer inhibition with standard deviation (STD DEV)
[c] IC_{50}, 50% inhibitory concentration. Calculated as the concentration of compound required to reduce the LEDGF/p75-IN interaction by 50%.
[d] EC_{50}, 50% effective concentration. Defined as the concentration of compound required to reduce HIV-1 replication by 50%.
[e] CC_{50}, 50% cytotoxic concentration. Calculated as the concentration of compound required to reduce cell viability by 50%.

As further research was conducted on these compounds it was discovered that the small molecule compounds were causing HIV-1 IN to aberrantly multimerise therefore preventing LEDGF/p75 from interacting with HIV-1 IN, and not directly disrupting the HIV-1 IN-LEDGF/p75 interaction (Christ *et al*., 2012; Kessl *et al*., 2012; Tsiang *et al*., 2012). Further studies conducted using a transmission electron microscopy (TEM) showed that ALLINIs

not only affect the integration step but downstream maturation was also affected (Kessl et al., 2016a; Le Rouzic et al., 2013). Progeny virus was defective showing immature non-infectious virus particles, where the genetic material was formed outside of the protective capsid (Figure 1.19).

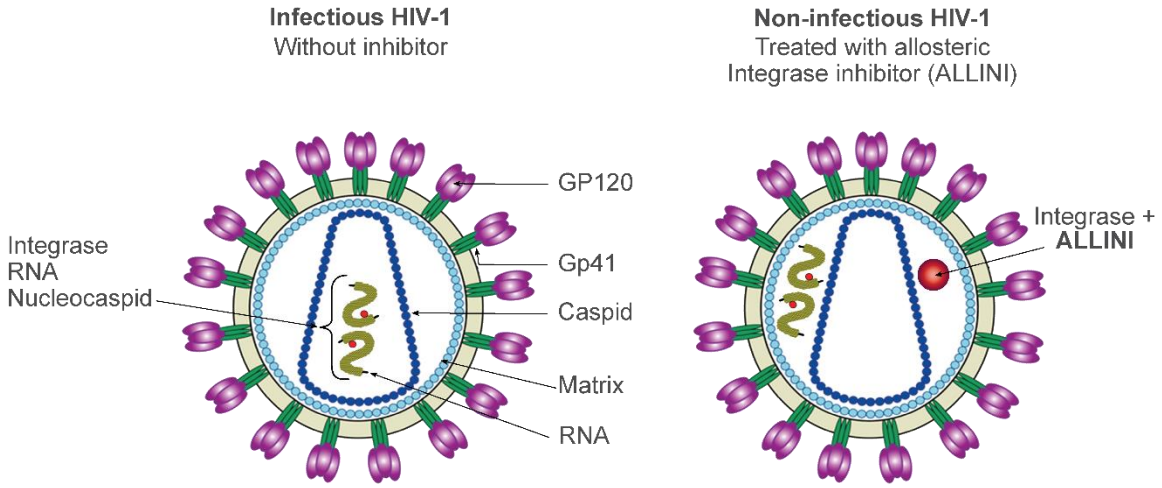


Figure 1. 19: Diagrammatical representation of a standard infectious virion and a defective immature progeny virion formed after treatment with an ALLINI. Diagram altered from Kessl *et al*., 2016 (Kessl *et al.*, 2016a)

Quinolone compounds that have been found to have HIV-1 IN-LEDGF/p75 inhibition share similarities in amino acid interactions. The compounds identified and derivatised by Christ *et al.,* are 2-(quinolin-3-yl) acetic acid derivatives. A generalised pharmacophore of a quinolone compound is shown in Figure 1.20. Derivatives of the pharmacophore bind to HIV-1 IN in a similar fashion and through crystallographic studies the amino acids interactions with these molecules were discovered (Christ *et al*., 2012; Tsiang *et al*., 2012; Jurado *et al*., 2013).

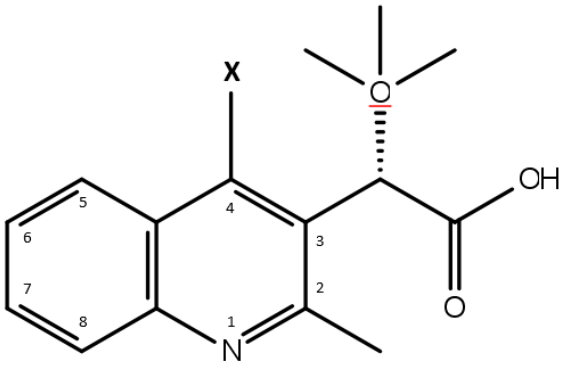


Figure 1. 20: Diagrammatic representation of a generic quinolone compound. Where X depicts an area for different functional groups. Drawn with use of Maestro 11.2, Schrodinger, 2017.

The fused ring quinolone has a carboxylic moiety extending from position 3. This carboxylic moiety forms hydrogen bonds with Gly170 and His 171. This relates to the LEDGF/p75 amino acid Asp366 interaction as seen in Figure 1.10. The carboxylic acid also forms an H-bond with Thr174. The quinolone core interacts with Ala128, Thr124 and Thr125. Position 4 on the quinolone has a functional group that sits in the cleft made between dimer A residues Thr174, Gln168, Ala169 and Met178 and residues Leu102, Ala128, Ala129 and Trp131 of chain B. This means it is in contact with both CCD molecules (Christ *et al.*, 2010a; Kessl *et al*., 2012; Tsiang *et al*., 2012; Jurado *et al*., 2013). Figure 1.21 shows the protein ribbon structure with CX05168, a quinolone compound, docked highlighting the possible amino acid interactions for quinolone compounds.

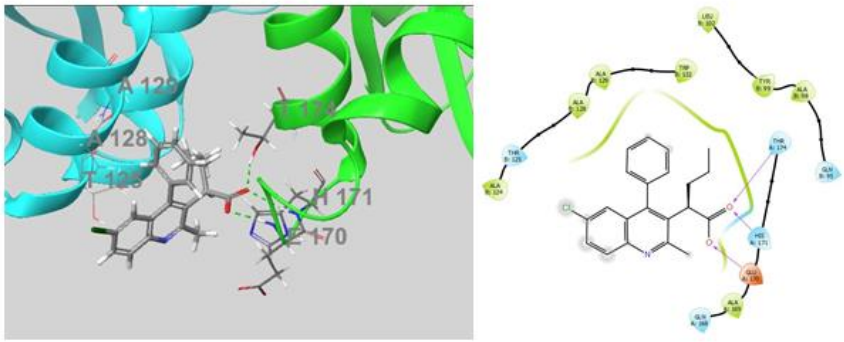


Figure 1. 21 (A) Ribbon 3D structure of the CCD of HIV IN with a known quinolone compound CX05168 docked indicating interacting amino acids. (B) 2D structure of known quinolone CX05168 docked indicating interacting amino acids.

Mutational studies have shown that HIV-1 IN mutations at Y99, L102, A128, H171 and T174 cause the enzyme to be resistant to ALLINIs. Of major importance is that when these mutations occur, they affect the LEDGF/p75 binding pocket and not the active site, and the HIV-1 strains containing these mutations remain susceptible to INSTIs. The development of new ALLINIs have shown potencies in the range of 10-90 nM EC_{50}s in an antiviral assay (Christ *et al.*, 2010a; Kessl *et al.*, 2012; Tsiang *et al*., 2012; Jurado *et al*., 2013). The antiviral potency is based on both the early and late effects, it is clear the late effects is more potent than the early effect when tested separately experimentally. However, the inhibition of a full replication round is more effective than late effects alone, clearly demonstrating the combination of both for inhibition. This effect contributes to the steep slope of inhibition.

Concurrent to the discovery of ALLINIs by Christ et al, Boehringer-Ingelheim screened a compound collection in search for HIV-1 IN 3' process inhibitors. Through screening they had various hits and narrowed it down to a single hit they refer to as HTS hit1. Through crystallographic screening it was found this molecule bound in the cleft of two CCD molecules, the cleft where LEDGF/p75 would normally bind. Due to this, they termed these molecules non-catalytic site integrase inhibitors (NCINIs). HTS hit 1 was then optimised through a sequential process forming a further 25 compounds, with each round improving or discovering the importance of a functional group to finally arrived at compound 26 now known as BI224436. This set of compounds were also quinolones similar to that discovered by Christ *et al*. After compound 13, IC_{50}s were no longer determined and the antiviral effect was rather monitored. BI224436 was found to have an EC_{50} of between 11-27 nM. *In vitro* mutational studies where virus selected for mutations of A128T, A128N and L102F when treated with BI224436 showed a drastic reduction in efficiency, however when screened with mutations that confer resistance to INSTIs BI224436 remained active against these mutations. After testing for absorption, distribution, metabolism and excretion (ADME) and animal studies, BI224436 was advanced to Phase I human clinical trials (Simoneau *et al.*, 2011; Balakrishnan *et al*., 2013; Fader *et al*., 2014b). However, BI224436 phase 1 clinical trials were abandoned presumably due to the enteropathic recirculation and no recent updates have been published. Continued efforts in improvement of the drug focused on biliary excretion. Boehringer-Ingelheim attempted scaffold hopping to improve the drug which resulted in the discovery of a pyridine series of NCINIs as opposed to the quinolone series (Figure 1.22). This pyridine series showed reduced biliary excretion and reduced enteropathic recirculation. Boehringer-Ingelheim sold the licencing agreement for NCICIs to Gilead Sciences in 2011 for further development (Fader *et al*., 2014a; Fenwick *et al*., 2014).

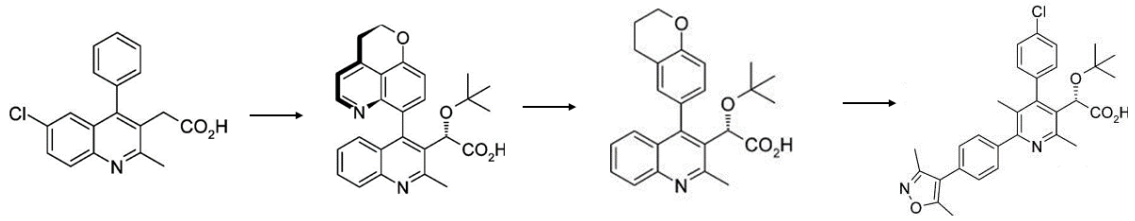


Figure 1. 22: The development progress of NCINI compounds from the original hit from library screening to the development of BI224436, through the scaffold jump to the new compound 20 with improved enteropathic recirculation. Constructed from Fenwick *et al* and Fader *et al*, (Fenwick *et al*., 2014; Fader *et al*., 2014a).

Recently Burlein *et al.,* (2017) have reported the discovery of t-butylsulfonamides as a new class of allosteric integrase inhibitors (Figure 1.23). These compounds share many characteristics with ALLINIS, however there is strong evidence to suggest that these compounds make different contact points with HIV-1 IN and interact with residues outside the LEDGF/p75 pocket of the dimer cleft (Burlein *et al*., 2017).

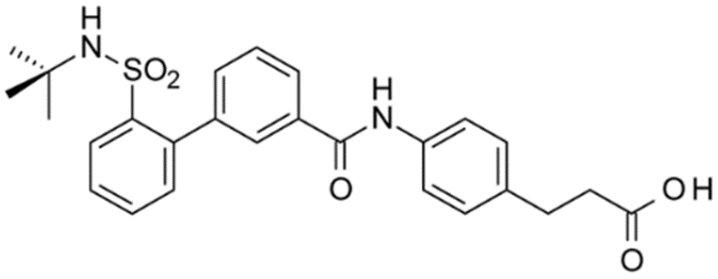


Figure 1. 23: Chemical structure of a t-butylsulfonamide discovered to have ALLINI properties. Copied from Burlein *et al* (Burlein *et al.*, 2017).

The group screened compounds through two biochemical assays to detect HIV-1 IN multimerisation and secondly to screen for strand transfer inhibition. From this screening the class of t-butylsulfonamieds were identified. With in-depth studies there were similarities between the t-butylsulfonamides and the t-butoxy acids of ALLINIs, however the way these compounds interact with HIV-1 IN appear to differ. When studying the t-butylsulfonamides it was not possible to obtain a crystal structure. Added to this, computational studies failed to find a binding model in the LEDGF/p75 pocket formed by the dimers of HIV-1 IN. They further studied how the t-butoxy resultant mutations affected the t-butylsulfonamides with

regards to viral and biological potencies. When studying A128T and T174I mutations which are known to reduce ALLINI potency by 9-fold and 500-fold respectively, it was found that the t-butylsulfonamides potency was reduced 3-fold with A128T. However in stark contrast the T174I mutation showed a 5-fold increase in susceptibility to t-butylsulfonamides. This suggests that T174 has no significant binding to the t-butylsulfonamides. With these findings the group hypothesised that compounds most likely bind with either the N- or C-terminus of HIV-1 IN (Burlein *et al*., 2017).

Zhang *et al.,* (2017) published the discovery of a di-hyroxybezamide scaffold compound inhibiting both HIV-1 IN catalytic activity as well as the HIV-1 IN-LEDGF/p75 interaction. They then used this study to develop a new novel class of 3-hydroxypicolinamide base inhibitors (Figure 1.24), via scaffold hopping which is the same strategy used by Boeringer-Ingelheim (Zhang *et al*., 2017).

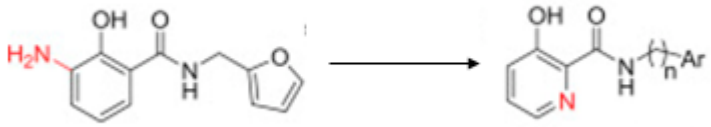


Figure 1. 24: Scaffold hopping of a 3-hydroxypicolinamide from a di-hydroxybenzamine scaffold. Copied from Zhang *et al*, 2017.

The 3-hydroxypicolinamides block HIV-1 replication via HIV-1 IN multimerisation and inhibition of the HIV-1 IN-LEDGF/p75 interaction, however they have no significant effect on the 3' processing and strand transfer activities. They found that HIV-1 replication was inhibited in T-lymphocyte C8166 cell lines via multimerisation of HIV-1 IN and the inhibition of HIV-1 IN-LEDGF/p75 interaction. Molecular modelling predicted hydrogen bonds and hydrophobic interactions with Glu170, His171, Thr174, Trp132 and Ala128 showing LEDGF/p75 disruption. These compounds showed reduced activity in comparison to ALLINIs but provide a new ally for compound development (Zhang *et al.*, 2017).

Lovastatin an FDA approved statin drug for the control of cholesterol was previously identified as an HIV-1 IN-LEDGF/p75 inhibitor within our laboratory (Harrison *et al*., 2014). Statins have been reported to have antiviral effects on HIV-1 (del Real et al., 2004; Giguère and Tremblay, 2004; Jain and Ridker, 2005; Ganesan et al., 2011) with these effects attributed to the disruption of lipid rafts (Ganesan et al., 2011), effects on protein prenylation (Iyengar et al., 1998), disruption of CCR5 and RANTES expression (Nabatov et al., 2007),

down regulation of RHO activity (del Real et al., 2004) and increased intracellular gag with decreased virus release (Amet et al., 2008). The identification was part of the screening of a compound library of previously FDA approved drugs that has been made available for repurposing. Initially the NCC-202 library was screened through homology modelling and a total of 12 compounds were identified as potential inhibitors. These compounds were subsequently screened through an *in vitro* assay where lovastatin was found to have the best inhibition. Moreover, lovastatin and CX05168 show structural similarities as seen in Figure1.25. During these studies it was seen that lovastatin appeared to function differently from CX05168 due to the lack of strand transfer activity with lovastatin.

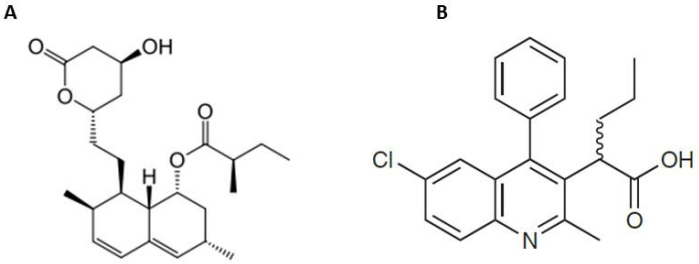


Figure 1. 25: Structure of lovastatin shown in A and CX05168 shown in B to display the similarities in compound structure. The compounds were drawn with use of Maestro 11.2, Schrodinger, 2017.

In addition to this screening, a separate study was conducted in our laboratory where the entire NCC library was screening for HIV-1 IN-LEDGF/p75 inhibition on an Alphascreen assay and from this study cefdinir, an FDA approved cephalosporin antibiotic, as seen in Figure 1.26, was identified to have a good inhibitory profile however lacked the structural similarities to the quinolone compounds such as CX05168. Cefdinir showed no strand transfer activity similar to lovastatin however the inhibitory profile of the Alphascreen assay showed similarities to the curve of CX05168. Interestingly another cephalosporin antibiotic, cefixime, has been identified as a strand transfer inhibitor (Abrahams et al., 2018).

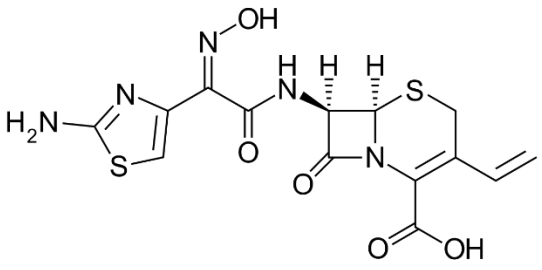


Figure 1. 26: Structure of cefdinir drawn with use of Maestro 11.2, Schrodinger, 2017.

All three compounds identified appeared to differ in mode of action. CX05168 shared a similar dose response curve profile to cefdinir but not lovastatin. Lovastatin nor cefdinir

showed any strand transfer activity unlike CX05168. With the identification of these compounds as disruptors of the HIV-1 IN-LEDGF/p75 interaction and indication of different modes of action, we proposed to elucidate their mechanism of action in comparison to the known ALLINI, CX05168. Moreover, due to the prevalence of HIV-1 subtype C in South Africa (Venner *et al*., 2016) comparisons of the compounds activities with the widely studied subtype B virus was conducted throughout the project.

1.10 Objectives of the study

The overall objective of the study focused on determining the discrepancies in the binding of a known allosteric integrase inhibitor, CX05168 and the identified HIV-1 IN-LEDGF/p75 inhibitors lovastatin and cefdinir to the binding site of LEDGF/p75 on the catalytic core domain dimer interface of HIV-1 IN. The following aims were accomplished:

1. To determine the binding sites for CX05168 in comparison to the identified HIV-1 IN-LEDGF/p75 inhibitors, lovastatin and cefdinir.
2. To evaluate the effects of inhibitor binding to the LEDGF/p75 binding pocket.
3. To determine cellular effects of CX05168 and HIV-1 IN-LEDGF/p75 inhibitors, lovastatin and cefdinir.

Chapter 2

2. Materials and Methods

2.1 Reagents used in this study

Escherichia coli (E coli) BL21 (DE3) pLysS competent cells (Promega, USA) were used in transformation reactions with recombinant plasmids encoding for HIV-1 IN subtype B (pINSD.His.Sol obtained through the NIH AIDs Reagent Program, Division of AIDS, NIAID NIH catalogue number 2958), HIV-1 IN subtype C (from isolate 05ZAFV6, designed and available within our laboratory) and pLEDGF/p75 (pFT-1 LEDGF, obtained through the NIH AIDs Reagent Program, Division of AIDS, NIAID NIH catalogue number 11396).

Test compound CX05168 was purchased from HaoYuan Chemexpress, China (catalogue number HY-10522). Lovastatin and cefdinir were purchased from Sigma Aldrich, Germany (catalogue number 1370600 and C7118, respectively).

A set of control compounds was sourced for use as positive controls in various assays and include; Raltegravir and Zidovudine (obtained through the NIH AIDs Reagent Program, Division of AIDS, NIAID NIH catalogue numbers 11680 and 3485, respectively). Auranofin was obtained from Sigma Aldrich, Germany (catalogue number A6733). All compounds were above 95% purity, as specified by suppliers.

Mammalian cell line MT-4 (obtained through the NIH AIDs Reagent Program, Division of AIDS, NIAID NIH catalogue number 120) was used in the cytotoxicity, antiviral and time of addition (TOA) assays. Expanded and titrated HIV-1 NL4-3 subtype B virus was available in the laboratory for use in antiviral and TOA assays. HIV-1 93IN905 subtype C virus (obtained through the NIH AIDs Reagent Program, Division of AIDS, NIAID NIH catalogue number 3040) was used for antiviral and TOA experiments.

2.2 The expression, purification and validation of recombinant proteins

2.2.1 The expression and purification of HIV-1 IN subtype B and C

E. coli BL21 (DE3) pLysS (Promega, USA) cells were previously transformed with HIV-1 IN subtype B and C plasmids and glycerol stocks were stored. Lysogeny Broth (LB) broth supplemented with ampicillin and chloramphenicol (100 µg/ml and 35 µg/ml, respectively) was inoculated with a glycerol stock and were grown overnight at 37°C with rapid shaking (250 rpm). The cell culture was then inoculated 1:100 into fresh LB broth containing ampicillin and chloramphenicol and incubated with shaking (250 rpm) at 37°C until the

culture reached an optical density (OD) of 0.6 at 600nm. Once the desired OD had been achieved the culture was induced to express the recombinant proteins by the addition of a final concentration of 1mM Isopropyl β-D-1-thiogalactopyranoside (IPTG) and grown for a further 3 hours. The culture was then centrifuged at 3200 *x g* for 30 minutes to harvest the cell pellets that were subsequently frozen at -80°C.

The cell pellets from the bacterial expression were then thawed on ice for 30 minutes. Cell pellets were re-suspended in IN lysis buffer (1 M NaCl, 20 mM HEPES pH 7.2, 5 mM imidazole, 10 mM $MgCl_2$, 0.25% CHAPS, 1 mM PMSF). The cell lysates were then pooled and homogenised for 1 minute. Aliquots of 1.5 ml were sonicated at 75% 0.6 cycles for a total of 3 cycles for 30 second duration, allowing for a resting period between cycles. The cell lysate was then centrifuged at 15 000 *x g* for 45 minutes to separate the cell debris and supernatant. The supernatant was then collected for affinity chromatography (Jenkins *et al*., 1996).

2.2.1.1 Purification of HIV-1 IN subtype B and C by affinity chromatography

A HiTrap™ HP (GE Healthcare, UK) affinity column was connected to an ÄKTAprime plus (GE HealthCare, UK) and equilibrated with binding buffer (1 M NaCl, 20 mM HEPES, 1mM DTT, 5 mM Imidazole). The supernatant was then loaded into the superloop and loaded onto the column at a rate of 0.5 ml/min. Binding buffer was then allowed to pass through the column for a total of 5 column volumes. The column was subsequently washed with 2 separate buffers with increasing imidazole concentrations of 60 mM and 150 mM, respectively. A 50 ml concentration gradient was set up to elute the protein into fractions. The imidazole gradient ranged from 150 mM to a final concentration of 600 mM imidazole. Fractions of 2.5 ml were collected and subsequently loaded onto a 12% stain free SDS-PAGE gel (Bio-Rad, USA) in reducing Laemmli buffer. The gel was visualized on the ChemiDoc™ MP System (Bio-Rad, USA) to determine which fractions contained a purified protein at the desired size.

The desired fractions were pooled and concentrated using an Amicon ultra filtration device with a 10 kDa cut-off size (Merck, USA). The concentrated sample was then loaded onto a PD-10 column (GE healthcare, UK) and buffer exchanged to a HIV-1 IN storage buffer (1 M NaCl, 20 mM HEPES (pH 7.5), 0.1 mM EDTA, 1 mM DTT, 10 % glycerol pH 7.4). The fractions were read on a Spectrophotometer at 280 nm and the concentration calculated using the extinction coefficient for each protein. Both recombinant subtype B and C IN were expressed and purified using the above method (Jenkins *et al*., 1996).

2.2.1.2 Confirmation of the purification of HIV-1 IN subtype B and C by western blotting

To confirm that the desired recombinant protein was purified, samples from each purification (subtype B and C) were run on a gradient SDS-PAGE reducing gel alongside a purified HIV-1 IN obtained from the NIH AIDS Reagent Program, Division of AIDS, NIAID NIH catalogue number 9420. The gel was transferred to a polyvinylidenedifluoride (PVDF) membrane utilizing an iBlot 2 gel transfer system (Life Technologies, USA). Once it was transferred the gel was visualized again with the ChemiDoc™ MP System (Bio-Rad, USA) to ensure sufficient transfer. The PVDF membrane was then placed in blocking solution (5 % bovine serum albumin (BSA) Tris buffered saline solution containing Tween 20 (TTBS) (50 mM Tris-HCl, 150 mM NaCl, 0.05 % Tween 20, pH 7.6) overnight. The PVDF membrane was subsequently washed 3 times for 5 minutes in TTBS with slight agitation. The membrane was then placed into a 2 000 x dilution of primary antiserum to HIV-1 IN (obtained through the NIH AIDs Reagent Program, Division of AIDS, NIAID NIH catalogue number 756) and incubated for 2 hours with slight agitation. The membrane was then washed again as described above and placed into a 20 000x dilution of secondary goat anti mouse antibody (Abcam, USA) and incubated for 2 hours with slight agitation. Finally, the PVDF membrane was washed as described above and placed into a chemiluminescent substrate (Bio-Rad, USA) for 5 minutes and viewed on the ChemiDoc™ MP System (Bio-Rad, USA).

2.2.1.3 Strand transfer enzyme linked immunosorbent assay (ELISA) to confirm the activity of HIV-1 IN subtype B and C

The strand transfer ELISA was utilized to test the activity of HIV-1 IN subtype B and C. Biotinylated donor DNA (sequence to that of viral DNA) was ordered from Inqaba Biotech (Biotin 5'- ACC CTT TTA GTC AGT GTG GAA AAT CTC TAG CA-3' and 5'-ACT CCT AGA GAT TTT CCA CAC TGA CTA AAA G-3'). Both DNA single strands were annealed for 1 hour at 95°C and then diluted to a working stock of 0.15 µM with 10 mM Tris-HCl, 0.1 M NaCl pH7.2. From the working stock 100 µl was added to each well of a streptavidin-coated micro ELISA plate (R & D Systems, USA) and incubated for 1 hour at room temperature with slight agitation. The contents of the wells were subsequently removed and washed three times with 0.01 M PBS solution. A final concentration of 1µM HIV-1 IN subtype B or C made up in a dilution buffer (20 mM HEPES, 75 mM NaCl, 10 mM $MgCl_2$, 2 µM $ZnCl_2$, 10 mM $MnCl_2$, 1% glycerol) was added to the plate and incubated for 1 hour at room temperature with slight agitation. The wells were subsequently washed 3 times with the dilution buffer. Raltegravir was used as a control compound and a final concentration of 10 µM RAL made up in dilution buffer was added to 2 wells of the plate and incubated for 1

hour at 37°C. Target DNA, sequence of human DNA, ordered from Inqaba Biotech Pty (Ltd) (5'-TGA CCA AGG GCT AAT TCA CT-3; fluorescein and 5'- AGT GAA TTA GCC CCT TGG TCA-3' fluorescein) was made up to a final concentration of 2.5 µM and 10 µl was added to each well and incubated at 37°C for 1 hour with slight agitation. The wells were then washed 3 times for a total of 10 minutes with a sodium citrate buffer (0.03 M sodium citrate, 0.3 M NaCl pH 7). Monoclonal anti-FITC alkaline phosphatase solution, 1:10000 (Sigma Aldrich, USA) was prepared in 50 mM Tris-HCl, 150 mM NaCl, 0.05 % Tween pH 7.4, to a working ratio of 1:10 000 and 200 µl was added to each well and incubated for 2 hours at 25°C. The wells were washed with 50 mM Tris-HCl, 150 mM NaCl pH7.4 3 times for a total of 10 minutes and finally TMB substrate was added and incubated for 30 minutes. The plate was then read on a spectrophotometer at 620 nM (xMARK™, Bio-Rad, USA).

2.2.2 The isolation and purification of recombinant LEDGF/p75

E. coli BL21 (DE3) pLysS (Promega, USA) cells containing the pLEDGF/p75 pET15b plasmid were grown overnight in fresh LB broth containing ampicillin and chloramphenicol at 37°C with rapid shaking (250 rpm). Overnight cultures were inoculated at 1:100 in fresh LB broth containing antibiotics (ampicillin, 100 µg/ml, chloramphenicol, 35 µg/ml) and incubated at 32°C with constant shaking until the OD was 0.8-0.9 at 600 nm. Once the desired OD was reached the sample was induced with a final concentration of 1mM ITPG. The temperature was then dropped to 28°C and the culture grown for a further 4 hours with rapid shaking (250rpm). The cell culture was then centrifuged at 3200 *x g* for 45 minutes and the supernatant discarded. The pellets were frozen at -80°C overnight.

Cell pellets were thawed on crushed ice for 30 minutes and then lysed in lysis buffer (1M NaCl, 25mM Tris-HCl, 0.5mM PMSF and 5mM Imidazole pH 7.4). Cell lysate was then homogenised for 1 minute and aliquoted for sonication. Samples were sonicated at 75% 0.6 cycles; each tube was sonicated for 1 minute with 3 cycles. The sonicated cell lysate was then centrifuged at 15 000 *x g* for 30 minutes at 4°C. The supernatant was pooled and the pellet discarded (Bartholomeeusen *et al*., 2007).

2.2.2.1 Purification of LEDGF/p75 from bacterial culture using affinity chromatography

A HisTrap™ HP (GE Healthcare, UK) affinity column was connected to an ÄKTAprime plus (GE HealthCare, UK) and equilibrated with 5 column volumes of binding buffer (1 M NaCl, 25 mM Tris-HCl, 1 mM DTT, 5 mM Imidazole). The supernatant was loaded onto the column and washed with wash buffer (1 M NaCl, 25 mM Tris-HCl, 1 mM DTT, 60 mM Imidazole). Once the column had been washed, a 50 ml concentration gradient from wash buffer to

elution buffer (1 M NaCl, 25 mM Tris-HCl, 1 mM DTT, 200 mM Imidazole) was set up to collect 2.5 ml fractions. The fractions were subsequently run on a stain free reducing SDS-PAGE gel (Bio-Rad, USA) to determine which fraction contained a protein at the desired size and if the protein was pure. The fractions with the protein of interest were pooled and concentrated down using an Amicon ultra-filtration device with a 10 kDa cut-off size (Merck, USA). The concentrated sample was then loaded onto a PD-10 column (GE healthcare, UK) and buffer exchanged to a sodium phosphate buffer (50mM NaH_2PO_4 pH 7.2) (Bartholomeeusen *et al*., 2007).

2.2.2.2 Ion exchange chromatography

The buffer exchanged protein was loaded onto a SP-Sepharose fast flow column (GE Healthcare, UK) that had been equilibrated with sodium phosphate buffer containing no salt. Fractions were then eluted over a 50ml gradient from Sodium phosphate buffer with no salt to elution buffer (50 mM NaH_2PO_4 and 1 M NaCl pH 7.2). The fractions were collected and run on a reducing SDS-PAGE gel to determine which fractions contained a protein at the desired size and the purity.

The fractions containing a protein at the desired size were pooled and concentrated down using an Amicon ultra-filtration device with a 10kDa cut-off size (Merck, USA). The sample was then loaded onto a PD-10 column and buffer exchanged to a size exclusion buffer (250 mM NaCl, 25 mM Tris-HCl, 2 mM DTT pH 7.4) (Bartholomeeusen *et al.*, 2007).

2.2.2.3 Size exclusion chromatography

A Superdex 200 (GE Healthcare) size exclusion column was equilibrated at 0.5ml/min overnight with buffer (250 mM NaCl, 25 mM Tris-HCl, 2mM DTT pH 7.4). The sample was loaded onto the column and allowed to elute at 0.2ml per minute with fractions of 2.5 ml collected. The fractions were run on a reducing SDS-PAGE gel to determine which fractions contained the protein at the desired size. The desired fractions were pooled and concentrated using an Amicon ultra-filtration device with a 50 kDa cut-off size (Merck, USA). The concentrate was read on a spectrophotometer at 280 nm and the concentration calculated using the extinction coefficient for the protein (Bartholomeeusen *et al*., 2007).

2.2.2.4 Confirmation of the successful expression of LEDGF/p75 through western blot

To confirm that LEDGF/p75 protein was purified, a sample from the fractions containing the protein at the desired size was run on a reducing SDS PAGE gel and the gel was transferred to a PVDF membrane utilizing an iBlot 2 gel transfer system (Life Technologies, USA).

Once it was transferred the gel was visualized again with the ChemiDoc™ MP System (Bio-Rad, USA) to ensure adequate transfer. The PVDF membrane was then placed in a blocking solution containing 5 % BSA in TTBS (50 mM Tris-HCl, 150 mM NaCl, 0.05 % Tween 20, pH 7.6) overnight. The PVDF membrane was then washed 3 times for 5 minutes in TTBS with slight agitation. The membrane was then placed into a 2000 x dilution of primary anti PSIP1 antibody (Abcam, USA) and incubated for 2 hours with slight agitation.The membrane was then washed again as described above and subsequently placed into a 20 000x dilution of secondary goat anti mouse antibody (Abcam, USA) and incubated for 2 hours with slight agitation. Finally, the PVDF membrane was washed as described above and placed into a chemiluminescent substrate (Bio-Rad, USA) for 5 minutes and viewed on the ChemiDoc™ MP System (Bio-Rad, USA).

2.2.3 Removal of the histidine tag from HIV-1 IN subtype B and C by thrombin cleavage

The HIS tags on both subtype B and C IN needed to be cleaved from the HIV-1 IN so that untagged protein could be used in certain assays, and this was achieved by the use of thrombin cleavage. A benzamidine column (GE Healthcare, UK) was charged with three bed volumes of alternating high pH buffer (0.1 M Tris-HCl, 0.5 M NaCl, pH 8.5) and a low pH buffer (0.1 M sodium acetate, 0.5 M NaCl, pH 4.5). The column was then re-equilibrated with five bed volumes of binding buffer as described above. Thrombin (Sigma Aldrich, USA) was made up in binding buffer with the addition of 25 mM $CaCl_2$ (Sigma Aldrich, USA) to a final ratio of 123 units of thrombin per mg of protein. The protein was incubated with thrombin for 4 hours with slight shaking at room temperature. The sample was subsequently loaded onto the benzamidine column and eluted using binding buffer, the thrombin binds to the column and so is removed from the solution. Collected fractions were run on a gradient stain free reducing SDS PAGE gel (Bio-Rad, USA). The fractions containing HIV-1 IN were pooled and concentrated using the Amicon ultra-filtration device with a 10 kDa cut-off size (Millipore Merck, USA). The HIV-1 IN was buffer exchanged with a PD-10 column into an HIV-1 IN storage buffer for future use. The remaining thrombin on the column was removed with 0.05 M glycine, pH 3.5. Samples of uncleaved protein and of the cleaved protein were run on a gradient stain free reducing SDS PAGE gel (Bio-Rad, USA), and transferred to a PVDF membrane for Western blotting. The membrane was then blocked overnight with blocking buffer and subsequently incubated in a 1000x dilution of primary monoclonal mouse anti-HIS antibody (Abcam, UK) then into a 5000x dilution of secondary goat anti mouse (Abcam, UK) to confirm the 6XHIS tag on the uncleaved protein and the absence of a tag on the cleaved IN proteins.

2.3 Biochemical screening of HIV-1 IN–LEDGF inhibitors

2.3.1 AlphaScreen

Alpha (amplified luminescent proximity homogenous assay) technology is an alternative to the traditional ELISA. In this assay no wash steps are needed and is a bead based assay. This type of assay can be used for an array of interactions but in our case will be used for protein-protein interactions. Two types of beads are needed for each assay. The first bead is known as a donor bead and contains phthalcyanine which is a photosensitiser that converts ambient oxygen to a reactive form of oxygen when illuminated at 620nm. The second bead is an acceptor bead and consists of a thioxene derivative that emits light. In solution, when the donor and acceptor bead are brought in close enough proximity by way of protein-protein interaction, the energy that is transferred from the singlet oxygen to the thioxene derivative results in the production of light which is measurable. Figure 2.1 shows a graphical representation of the assay principle.

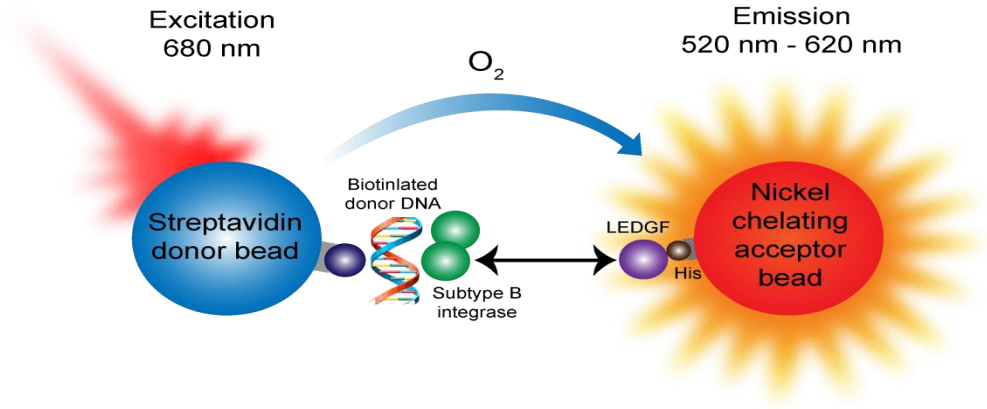


Figure 2. 1 Schematic representation of the HIV-1 IN-LEDGF/p75 interaction in an AlphaScreen assay. The streptavidin donor bead links to the biotin labelled donor DNA-IN complex which then interacts with the HIS tagged LEDGF/p75 bound to the nickel chelating acceptor bead

2.3.1.1 AlphaScreen assay without DNA

An AlphaScreen assay previously described by Christ and co-workers was used to screen the compounds (Christ *et al*., 2010). A stock solution of 1.5 µM histidine tagged HIV-1 IN subtype B or C was made up in AlphaScreen assay buffer (150 mM NaCl, 25 mM Tris, 2 mM $MgCl_2$, 1 mM DTT, and 0.01% Tween 20 and 0.02% BSA, pH 7.4). A final concentration of 300nM was added to a ½ area optiplate and incubated with each inhibitor at single doses and then later in doses ranging from 200 µM down to 0.3 µM for 30 minutes at room

temperature with gentle shaking. Subsequently 100 nM His-tagged LEDGF/p75 was added and incubated for one hour at room temperature with gentle shaking. A final concentration of 10 µg/ml nickel chelating acceptor beads (Perkin Elmer, USA) and nickel chelating donor beads (Perkin Elmer, USA) were added and incubated in the dark at 30°C with gentle shaking. The plate was subsequently read between 520-620 nm on the EnSpire® plate reader (Perkin Elmer, USA). The control ran on the plate to ensure accurate reading of the compounds effects were: beads alone, HIV-1 IN subtype B or C alone, LEDGF/p75 alone, HIV-1 IN subtype B or C and LEDGF/p75 alone, each protein in isolation with beads alone. Once single dose inhibition by the inhibitor was determined, a dose response curve was determined to obtain a half maximal inhibitor concentration (IC_{50}) for all inhibitors under investigation. The percentage inhibition for each dose was determined with use of the controls and plotted against the log of the concentration. The data obtained was plotted on a sigmoidal curve using Origin 8.1 (Origin Lab Corporation, UK) and an IC_{50} and hills coefficient was determined. Statistics were calculated using the SISA t-test found at, http://www.quantitativeskills.com/sisa/.

The original AlphaScreen was followed up by a second AlphaScreen containing donor DNA to see if the presence of viral DNA prior to inhibitor addition had any effect on the inhibitory profile of the inhibitor as was seen in studies (Frauke Christ et al., 2012).

2.3.1.2 AlphaScreen with DNA

Briefly, a stock concentration of 1.5 µM HIV-1 IN subtype B or C was incubated with 0.3 µM biotinylated donor DNA for 45 minutes at room temperature with gentle shaking. For the plate assay a final concertation of 300 nM biotinylated HIV-1 IN subtype B or C-DNA was incubated with 100 nM HIS-tagged LEDGF/p75 for 60 minutes in AlphaScreen assay buffer at room temperature with gentle shaking. For this assay the nickel chelating acceptor beads (Perkin Elmer, USA) and streptavidin donor beads (Perkin Elmer, USA) were added to a final concentration of 10 µg/ml and incubated at 30°C in the dark with gentle shaking. The plate was subsequently read between 520-620 nm on the EnSpire® plate reader (Perkin Elmer, USA). To once again ensure the response was due to inhibitor the following controls were included; beads alone, HIV-1 IN subtype B or C-DNA alone, LEDGF/p75 alone, HIV-1 IN subtype B or C-DNA and LEDGF/p75 alone, each protein in isolation with beads alone. Both single doses and a dose response curve were constructed as described above. Statistics were calculated using the SISA t-test found at, http://www.quantitativeskills.com/sisa/.

As indicated in the introductory section, PogZ is a HIV-1 IN analogue because it binds to LEDGF/p75 protein in the same spots HIV-1 IN does. This assay was then designed to determine if the inhibitors of choice were binding to HIV-1 IN or LEDGF/p75.

2.3.1.3 PogZ- LEDGF/p75 binding AlphaScreen assay

Biotinylated POGz was available within the laboratory from previous studies and used as a positive control as POGz binds to LEDGF/p75 in the same way HIV-1 IN does. The stock solutions of 1.5µM LEDGF/p75 and 500nM POGz for the assay were made up in assay buffer as described above. A final concentration of 300 nM LEDGF/p75 was incubated with each 100 µM of each inhibitor incubated at room temperature for 30 minutes and subsequently 100 nM POGz was added and incubated for 60 minutes at room temperature. Nickel chelating acceptor beads and streptavidin donor beads were added to a final concentration of 10 µg/ml. The plate was then incubated at 30°C in the dark with slight agitation and subsequently read between 520-620 nm on the EnSpire® plate reader (Perkin Elmer, USA). To ensure the effects were being caused by the inhibitors the following controls were used; beads alone, POGz alone, LEDGF/p75 alone, POGz and LEDGF/p75 alone and beads alone.

2.3.1.4 Strand transfer ELISA to determine the catalytic inhibition of HIV-1 IN subtype B and C by the compounds

The strand transfer ELISA method described in section 2.2.1.3 was utilised to determine if CX05168, lovastatin or cefdinir had any inhibitory effect on the catalytic activity of HIV-1 IN subtype B and C. A final concentration of 100 µM of each inhibitor was added at the same stage as RAL, a known strand transfer inhibitor, is added. The results were then analysed and percentage inhibition was calculated.

2.3.2 Dimerisation assay

The published HIV-1 IN-LEDGF/p75 inhibitors known as ALLINIs show drastic effects on the dimerization of HIV-1 IN. As such we ran two dimerization experiments to determine if the inhibitors had an effect on the dimerization of HIV-1 IN.

2.3.2.1 Cross-linking studies

A final concentration of 1 µM HIV-1 IN subtype B and C with histidine tags and 100 µM inhibitor were dissolved in assay buffer (50 mM HEPES pH7.1, 300 mM NaCl, 2.5 mM MgCl, 1 mM DTT). The compound and HIV-1 IN subtype B or C were incubated at a 1:1 ratio at room temperature for 1 hour. Once incubation was complete a final concentration of 25 µM of bis(sulfosuccinimidyl)suberate (BS3) was added to the mixture and incubated at room temperature for 15 minutes. The cross-linking reagent BS3 is an amine-to-amine cross-linker, and reacts with lysines on the amine groups helping to stabilise the HIV-1 IN-IN subunit interactions. To stop the cross-linking reaction, 1µl of 1M Tris base was added.

A reducing SDS-PAGE gel was run for each sample to determine the extent of multimerisation the compounds caused. The gel was subsequently transferred to a PVDF membrane and a western blot was then conducted with anti-HIS antibody as previously described to better show the extent of multimerisation or lack thereof (Li *et al*., 2006; Henriquez *et al*., 2013).

2.3.2.2 Dynamic light scattering (DLS) assay to show the multimerisation effects of inhibitors

DLS is a techniques used to study particles in solution. The diffusion coefficient is said to calculate the hydrodynamic radii and this is dependent on the shape and size of the molecule in solution. A monochromatic beam is passed through a solution containing macromolecules or in our case protein and inhibitors. As the light encounters the macromolecules the light is scattered based on shape and size of the molecules. DLS primarily measure the Brownian motion of macromolecules (Stetefeld et al., 2016). When using this method to analyse protein and small molecule interactions it is imperative that the small molecule is run in isolation first. Certain molecules can scatter light and this will show up as a peak indicating a large molecule size, which is seen as a false positive. Protein is also run in isolation and the peak should read around or below 1 as the size of the proteins monomer, dimers or tetramers should not be seen by the technique. Once protein and inhibitors have been added together and measured, if a sizable peak is determined then this is due to aberrant multimerisation of the protein forming large particles.

On the day of testing, buffer (1 M NaCl, 2 mM $MgCl_2$, 2 mM DTT and 50 mM HEPES 7.4) was prepared and filtered twice and stored on ice. Each compound was initially run with buffer alone on the Malvern Zetasizer Nano Series S90. A final concentration of 5 µM of each compound was tested under size determination mode. Once the compound showed no peaks past the one range it was tested with purified HIV-1 IN subtype B or C recombinant protein. A concentration of 200 nM HIV-1 IN subtype B or C was prepared in 1 ml buffer and allowed to equilibrate at room temperature for 30 minutes after which 5 µM compound was added and placed in the Malvern Zetasizer Nano Series S90 on size determination mode for 10 readings for a total of 30 minutes. The graphs were set to number distribution and recorded (Kessl *et al*., 2016b). The concentration of compound was subsequently increased for lovastatin and cefdinir to 100 µM.

2.3.3 Stability testing

2.3.3.1 Differential Scanning Fluorometry (DSF) to determine the stabilising effect of the compounds on HIV-1 IN subtype B and C

DSF also known as a thermal shift assay, is a rapid technique used to identify ligands that bind and stabilise a protein. A fluorescent dye such as SYPRORED which has an affinity for hydrophobic regions, is incubated with protein and ligand. As a protein unfolds more hydrophobic regions are exposed allowing the dye to bind and increase fluorescence. The melting temperature/ transition point can be calculated using a fitting procedure and this then shows the degree of stabilisation a ligand has on a protein. The higher the stabilisation the higher the melting temperature (Niesen et al., 2007).

Components for the following assay were diluted in assay buffer (10 mM HEPES [pH7.5], 500 mM NaCl, 1 mM $MgCl_2$ and 1 mM DTT). A final concentration of 1 µM HIV-1 IN subtype B and C were separately mixed with 1x SYPRO red dye (Life Technologies, USA) and 3 µM of CX05168, cefdinir and lovastatin or the equal volume of DMSO for the control. Each mixture was incubated for 5 minutes at ambient temperature and 25 µl was subsequently added to 3 wells of a 48 well PCR plate. The plate was sealed and placed in an Illumina Eco real time PCR machine.

DSF melting curves were obtained by increasing the temperature from 23°C to 95°C in steps of $1°C.min^{-1}$ and the fluorescence emission recorded (excitation @575nm, emission @625nm) at each step. The raw photon counts were analysed (Christ *et al*., 2012).

2.3.4 Molecular modelling

Molecular modelling was conducted to determine a theoretical fit of each inhibitor and predict the quality of this fit. Indication of types of bonds can add value to see how strong the compound will bind or alternately how easy the bonds will be broken.

All studied inhibitors were prepared using the CHARMM based force field function in the BIOVIA Discovery Studio software package version 4. All possible stereoisomers and conformations were generated. The CCD dimer interacting with LEDGF/p75 identified by the PDB code 2B4J was prepared by removing LEDGF/p75 from the complex and the model then prepared by the addition of missing loops, adding hydrogens, optimization of the bond lengths and angles and bond order assignment. Previously identified LEDGF/p75-HIV-1 IN inhibitors were used to train the model to ensure that the predictions are accurate. Molecular docking was performed in the allosteric site prepared. LibDock protocol generated many poses for each compound and Jain, PLP2 and LibDock were used to analyse these poses. Further optimization was then conducted, and the best poses binding energies were calculated.

2.3.5 Hydrogen Exchange Mass Spectroscopy (HXMS)

Hydrogen/deuterium exchange mass spectrometry is a techniques used to determine structural and dynamic aspects of a protein. The exposure of a protein tor peptides to deuterium causes rapid exchanged between hydrogens and deuteriums. Areas that are folded or protected by tight hydrogen bonds exchange slower than unfolded exposed regions. Initially a peptide map is constructed using a pepsin column in the absence of deuterium. This is done to obtain as many overlapping peptides as possible to increase the coverage of the protein. Subsequently the process is repeated in the presence of deuterium. The protein or peptides are run in isolation to determine the proteins structural state without inhibitor. It is then run in combination with inhibitors to determine how these inhibitors structurally effect the protein as well as determining the binding areas of these inhibitors to the amino acids, this is possible as the area will be unavailable for deuterium exchange (Konermann et al., 2011). The hydrogen exchange experiments were conducted at the Council for Scientific and Industrial Research (CSIR), Pretoria, South Africa.

2.3.5.1 Peptide map construction

A total of 150 µM of HIV-1 IN subtype B or C was diluted in labelling buffer (50 mM HEPES, 5 mM DTT, 1M NaCl) at a pH of 7.5 made with ultra-pure mass spec grade water and subsequently quenched with quenching buffer (5 M urea, 50 mM TCEP and 1% TFA). The protein was then passed through an immobilised pepsin column to digest the protein into peptides at specific cleavage points. The peptides were then injected onto an Aeris PEPTIDE 3.6 µm XB-C18 reversed phased column (Phenomenex) at 0°C coupled to an AB SCIEX QSTAR ® Elite Mass spectrometer via a 6 port switching valve. Peptides were eluted at a rate of 300 µl/min from the reverse phase column with a 5%-95% B gradient (A: 0.1% formic acid, B: acetonitrile, 0.1% formic acid). The initial peptide identification was carried out using Collision Induced Dissociation (CID) in information dependent acquisition mode. All subsequent samples were analysed in MS mode (Fitzkee *et al*., 2011).

The undeuterated controls were analysed using PEAKS 6 (Bioinformatics solutions, USA) to determine peptide coverage and peptide pool for HXD analysis. From the above method a peptide map specific to the HIV-1 IN subtype was formed.

2.3.5.2 Hydrogen Deuterium exchange

150 µM HIV-1 subtype B or C was diluted in labelling buffer as described above however, all components were made up in 100% D_2O at 20°C. At the appropriate time intervals (10 s, 20 s, 1 min, 10 min, 60 min for protein without compound and 10 s for compound containing samples) hydrogen deuterium exchange was minimalised with a 1:1 dilution with

quenching buffer and incubated at 0°C for 30 seconds. The HIV-1 IN subtype B or C with and without compounds was digested by passage through a column with immobilized pepsin (1 µg/µl). Following the digestion, 50 µl of sample was loaded on the Aeris PEPTIDE 3.6 µm XB-C18 column as described above, followed by elution of peptides and analysis as described above (Fitzkee *et al*., 2011).

The percentage back exchange that occurs once the hydrogen exchange (HDX) reaction is quenched was determined using the fully deuterated control. HDX analysis was performed using HDExaminer 1.2 (Sierra Analysis Inc, USA). Manual quality control was performed on analysed peptides (high and medium confidence peptides only) to ensure that theoretical and experimental profile matched.

2.3.6 Surface Plasmon Resonance (SPR)

All SPR experiments were carried out using the ProteOn ™ XPR 36- protein interaction array system (Bio-Rad, USA) at 25°C. The GLH sensor chip was preconditioned using 50 mM NaOH, 100 mM HCl and 0.5% SDS. The system was then equilibrated with SPR buffer (50 mM HEPES, 500 mM NaCl, 10 mM $MgCl_2$, 5 mM DTT, 0.05% Tween 20 and 0.0175% DMSO). The chip was then activated with a 1:1 ratio of 1-ethyl-3-(3-dimethylaminopropyl) carbodiimide hydrochloride (0.2 M) and sulfo-*N*-hydroxysuccinimide (0.05 M). After activation, 200 µg of both subtype B and C HIV-1 IN was immobilized on 2 flow channels per subtype on the chip made up in SPR buffer until maximum response units (RU) units were reached.

High concentration stock solutions of inhibitors were made up in 100% DMSO so that the final concentration of DMSO in the serial dilutions were below 0.1%. Serial dilutions of inhibitors were made up in SPR buffer containing no DMSO. CX05168 was serially diluted at concentrations of 10 µM, 5 µM, 2.5 µM, 1.25 µM, 0.625 µM and 0 µM. Lovastatin and cefdinir were serially diluted at concentrations of 100 µM, 50 µM, 25 µM, 12.5 µM, 6.25 µM and 0 µM. The compounds were allowed to flow over all 6 flow channels. The chip was regenerated with 10 mM glycine pH 3 in 1% phosphoric acid between compounds runs to remove the analyte (Vaisocherová *et al*., 2009). Ritonavir, a protease inhibitor, was used as a control compound as this should not bind to integrase.

Data was analysed using the ProteOn manager software 3 (Bio-Rad, USA). The response of buffer injections and response from the reference cell was subtracted to account for nonspecific reactions. Experimental data was fitted using the Langmuir model (Bio-Rad,USA).

2.4 Screening of compounds to determine their effects on cell based processes

2.4.1 Cytotoxicity

MT-4 cells were grown to high viability in 10 % RPMI media (Gibco, USA) (10% Foetal calf serum, 100 µM Penicillin/ streptomycin, 100 µM Gentomycin , and cells were seeded at 1 x 10^6 cells per ml in a final volume of 100 µl to each well of a 96 well round bottom cell culture plate. The plate was equilibrated for an hour at 37°C and 5 % CO_2. During the equilibration phase test compounds were made up in 10% RPMI solution in a serial dilution from 200 µM to 0.39 µM. A final volume of 100 µl compound made up in 10% RPMI media, as described above, was added to wells containing cells ensuring the solution was homogeneous with cells. The plate was incubated at 37°C for 5 days with 5 % CO_2. On the final day, 10 µl of MTS solution was added and mixed to ensure homogeneity of the solution with cells. The cells were incubated for a total of 4 hours taking a reading, 490nm, at 2 hours and 4hours, (xMARK^{TM}, Bio-Rad, USA.) The data was analysed and dose response curves were constructed using Origin 8.1 with the log value of the concentration plotted against the absorbance level to determine the maximal cytotoxicity CC_{50} for compounds (CC_{50}). Auranofin, a gold complex antirheumatic agent, was used as a control due to this inhibitor being very toxic to the cells with a well-known dose curve for toxicity.

2.4.2 Antiviral screening

The day prior to the antiviral screening MT-4 cells were seeded at 2 x 10^5 cells per ml. Subsequently the viability was checked and 2 x 10^5 cells per ml were incubated with HIV-1_{NL4-3} stock or HIV 93IN905 subtype C expanded virus for 90 minutes. The MT-4 cells were pelleted and virus removed and subsequently washed 4 x with 0.1 M PBS. A control set of cells were incubated without virus and washed four times with 0.01 M PBS. A final volume of 100 µl of cells were added to each well of a 96-Well U bottom cell culture plate. The plate was placed into the 37°C, 5 % CO_2 incubator to equilibrate for one hour. During the incubation, compounds were made up in RPMI media containing 10 % heat inactivated foetal calf serum (FCS). The compounds were serially diluted from 200 µM to 0.3 µM. A total of 100 µl of RPMI containing compound was added to the wells containing cells and mixed to ensure homogeneity. The plate was placed into a 37°C, 5 % CO_2 incubator for five days. Raltegravir, a known integrase inhibitor with low toxicity, was used as a control compound to ensure the assay was functioning correctly.

A Bioelisa HIV-1+2 Ag/Ab kit (BIOKIT, Spain) was used to determine the level of HIV-1 present in the samples. Briefly 100 µl of diluent buffer was added to wells of the supplied

Bioelisa plate and 100 µl of test sample or control was added. The plate was incubated for 60 minutes. Subsequently the plate was washed 5 times with wash buffer and 200µl of conjugate 1 added to the wells. The plate was incubated for 30 minutes and subsequently washed 3 times. Conjugate 2 was prepared according to manufacturer's specifications and 200 µl added to each well with 30 minute incubation. Once incubation was complete the wells were washed 5 times and 150 µl of TMB substrate was added to the wells. The reaction was followed up to 30 minutes until sufficient blue colour had developed on controls and 50 µl of stop solution was added to stop the reaction. The plate was then read at 450nm and percentage inhibition was calculated.

2.4.3 Time of addition (TOA) assay to determine the time point in the viral replication process when the compounds are effective

MT-4 cells were seeded at 2 x 10^5 cells/ml and HIV-1 $_{NL4-3}$ or HIV 93IN905 subtype C expanded virus was added to the cells and incubated for 2 hours in the incubator at 37°C and 5% CO_2. The cells were then washed 4 times with 0.1 M PBS to remove any unbound virus. Cells were then seeded into the 96 well plate. Known antiviral inhibitors, RAL and AZT, were used as controls to ensure the assay was working correctly. CX05168 was added at 30µM and cefdinir at 100µM at the following time point's representative of hours: T0, T2, T4, T5, T6, T7, T8, T9, T10, T11 and T24. T0 indicates the addition of compound at the incubation phase of assay. The p24 values were then calculated using the Bioelisa HIV-1+2 Ag/Ab kit (BIOKIT, Spain) as described above.

Chapter 3

3. Results

3.1 Recombinant protein expression, purification, and modification

3.1.1 HIV-1 IN

Following large scale protein expression in *E. coli,* and nickel affinity purification, SDS-PAGE gel analyses confirmed the successful purification and over-expression of a recombinant protein correlating in size (approximately 32 kDa) with that of soluble subtype B HIV-1 IN (Figure 3.1A) and subtype C HIV-1 IN (Figure 3.1B). The western blot analysis for both subtype B and C (C) shows the successful expression of HIV-1 IN.

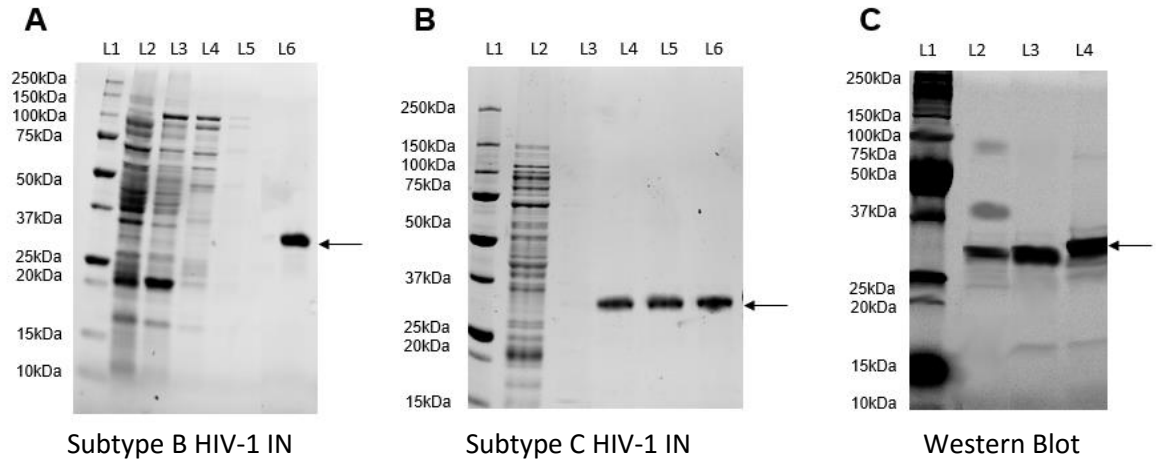


Figure 3. 1: SDS PAGE gel and western blot indicating the expression and purification of a protein at approximately 32 kDa correlating with that of recombinant subtype B HIV-1 IN. (**A**) SDS-PAGE indicating the expression and purification of HIV-1 IN subtype B, Lane 1, precision plus protein molecular weight marker (Bio-Rad, USA); Lane 2, flow through from the nickel affinity column; Lane 3, wash 1 from the nickel affinity column; Lane 4 wash 2 from the nickel affinity column; Lane 5, wash 3 from the nickel affinity column after which the protein was eluted via an imidazole gradient; Lane 6 lane containing concentrated fractions of a protein at approximately 32 kDa; (**B**) SDS-PAGE gel indicating the expression of a protein correlating with that of the recombinant subtype C HIV-1 IN. Lane 1, precision plus protein molecular weight marker (Bio-Rad, USA); Lane 2, flow-through from the nickel affinity column; Lane 3, wash 1 from the nickel affinity column; Lane 4, 5 and 6 containing at protein at 32kDa; (**C**) Western blot analysis confirming expression of recombinant HIV-1 IN subtype B and subtype C. Lane 1, precision plus protein molecular weight marker (Bio-Rad, USA); Lane 2, positive control recombinant HIV-1 IN obtained from the NIH AIDS Research and Reference Reagent Program; Lane 3, subtype B protein from gel A; Lane 4 concentrated nickel affinity chromatography purified subtype C HIV-1 IN from gel B. Figures 6.1,6.2 and 6.3 (found in the appendix) are the standard curves used to determine protein size marked with an X. for A, B and C respectively.

3.1.2 LEDGF/p75

The successful purification of LEDGF/p75 following nickel affinity chromatography, cation exchange and size exclusion chromatography is shown in Figure 3.2A, with the protein migrating at a size corresponding to LEDGF/p75, approximately 75 kDa. Identity of the LEDGF/p75 protein was confirmed through western blot analysis (Figure 3.2B).

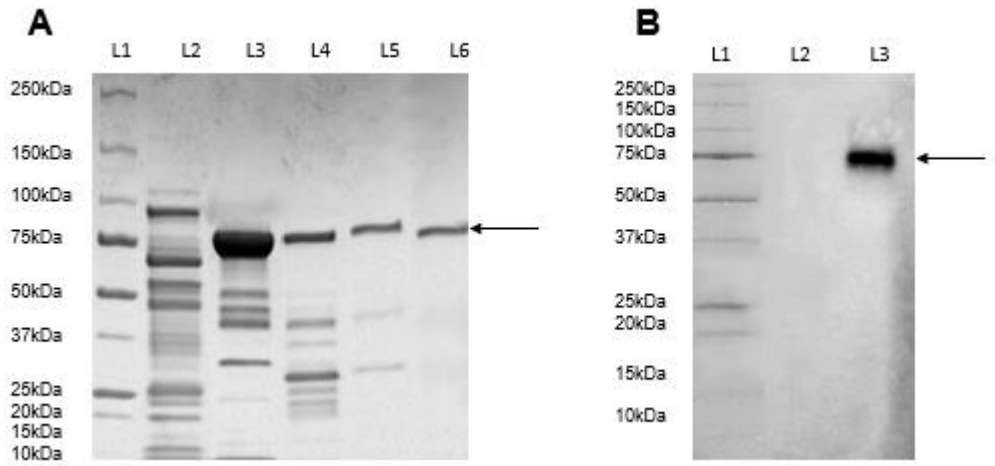


Figure 3. 2: SDS-PAGE gel showing the expression and purification steps of a protein correlating with that of LEDGF/p75 and western blot proving the successful expression of LEDGF/p75. (**A**) Lane 1, precision plus protein molecular weight marker (Bio-Rad, USA); Lane 2, flow-through from the nickel afinity exchange column; Lane 3, concentrated protein from the nickel infinity column; Lane 4, concentrated protein from the gradient fractions cation exchange column; Lane 5, concentrated protein from the size exclusion column; Lane 6, concentrated protein form the Amicon 50kDa cut-off; (**B**) Western blot analysis confirming the expression of LEDGF/p75 with primary antibody anti-PSIP1. Lane 1, precision plus protein molecular weight marker (Bio-Rad, USA); Lane 2, negative control fraction from size exclusion chromatography; Lane 3, concentrated Amicon sample after size exclusion chromatography purified LEDGF/p75. Figures 6.4 and 6.5 are the standard curves used to determine protein size marked with an X for A and B respectively.

3.1.3 Modifications of recombinant proteins

3.1.3.1 Cleavage of 6X HIS TAG

The 6X His tag attached to both the HIV-1 IN subtype B and C was successfully cleaved by thrombin for use in the AlphaScreen assay containing DNA. SDS-PAGE analysis showing the size shift in protein before and after HIS tag cleavage for both subtype B and C (Figure 3.3A) and cleavage of the 6XHIS tag was confirmed by the absence of bands in the cleaved samples by western blot analysis using Anti HIS antibody (Figure 3.3B).

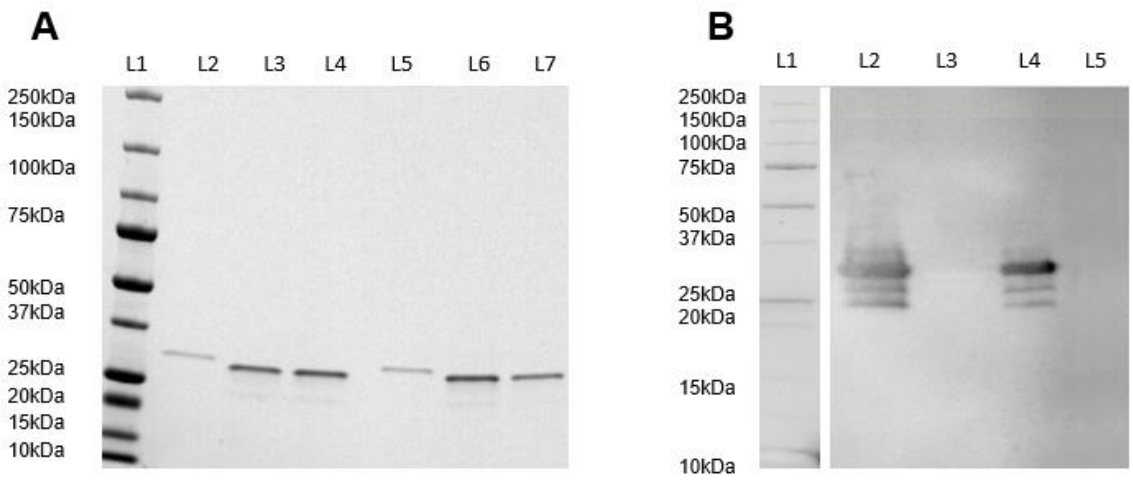


Figure 3. 3: SDS-PAGE gel of HIV-1 subtype B and C IN following thrombin cleavage of the 6XHIS tag (**A**) and a western blot confirming cleavage of the HIS tag (**B**). (**A**) Shows the SDS PAGE gel with cleaved and uncleaved HIV-1 IN subtype B and C, Lane 1, precision plus protein molecular weight marker (Bio-Rad, USA); Lane 2, HIV-1 subtype B IN 6xHIS tagged protein; Lane 3, fraction 1 of cleaved HIV-1 subtype B IN; Lane 4, fraction 2 of cleaved HIV-1 subtype B IN Lane 5; HIV-1 subtype C IN 6XHIS tagged protein; Lane 6, fraction 1 cleaved HIV-1 subtype C IN Lane 7, fraction 2 of the cleaved HIV-1 subtype C. (**B**) Shows a western blot analysis of HIV-1 subtype B and C IN following thrombin cleavage of the 6XHIS tag. Lane 1, precision plus protein molecular weight marker (Bio-Rad, USA); Lane 2, HIV-1 subtype B IN 6xHIS tagged protein; Lane 3, cleaved HIV-1 subtype B IN; Lane 4, HIV-1 subtype C IN 6XHIS tagged protein; Lane 5, cleaved HIV-1 subtype C IN. Please note that image B has been split to remove a lane that was not needed on the blot. Figures 6.6 and 6.7 are the standard curves used to determine protein size marked with an X for A and B respectively.

3.1.4 Catalytic activity testing of HIV-1 IN subtype B and C

The activity of the two HIV-1 IN subtypes (B and C) was confirmed on an ELISA based assay as described in section 2.3.1.4. As shown in Fig 3.4, the two INs were shown to be active with high absorbance values once TMB was added (1.2 at 620 nm for both subtypes) as opposed to the six-fold decrease in the RAL treated samples (0.2 at 620 nm).

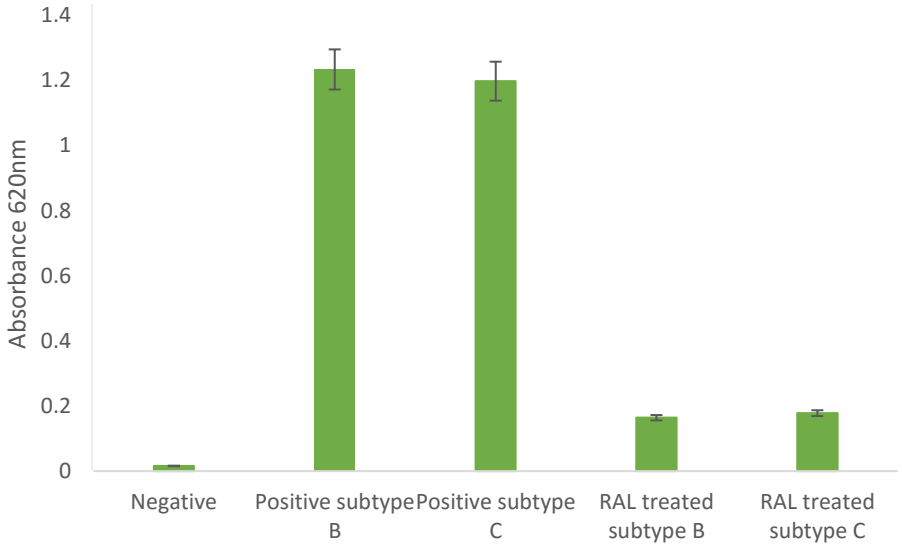


Figure 3. 4: Bar graph depicting the strand transfer activity by ELISA of both subtype B and C IN with and without addition 50nM raltegravir. The ELISA was run 3 times with duplicate samples in each run. The error bars are shown for the difference in the experimental results from each experiment. The positive samples are protein with no compound added and the negative is the absence of protein from the well.

3.2 Biochemical screening of HIV-1 IN-LEDGF/p75 inhibitors

All assays and experiments were performed for both subtype B and C HIV-1 IN to show relevance to the South African predominant subtype.

3.2.1 AlphaScreen assay

3.2.1.1 HIV-1 IN-LEDGF/p75 AlphaScreen disruption assay

A previously described LEDGF/p75 -HIV-1 IN AlphaScreen assay was performed to determine the disruption of the interaction between LEDGF/p75 (Christ *et al.,* 2010) and HIV-1 IN in the presence of the three inhibitors. Firstly, dose response curves were determined for CX05168, lovastatin and cefdinir. The dose response curves and the IC_{50} values are shown in Figure 3.5A and Figure 3.5B for subtype B and C HIV-1 IN, respectively.

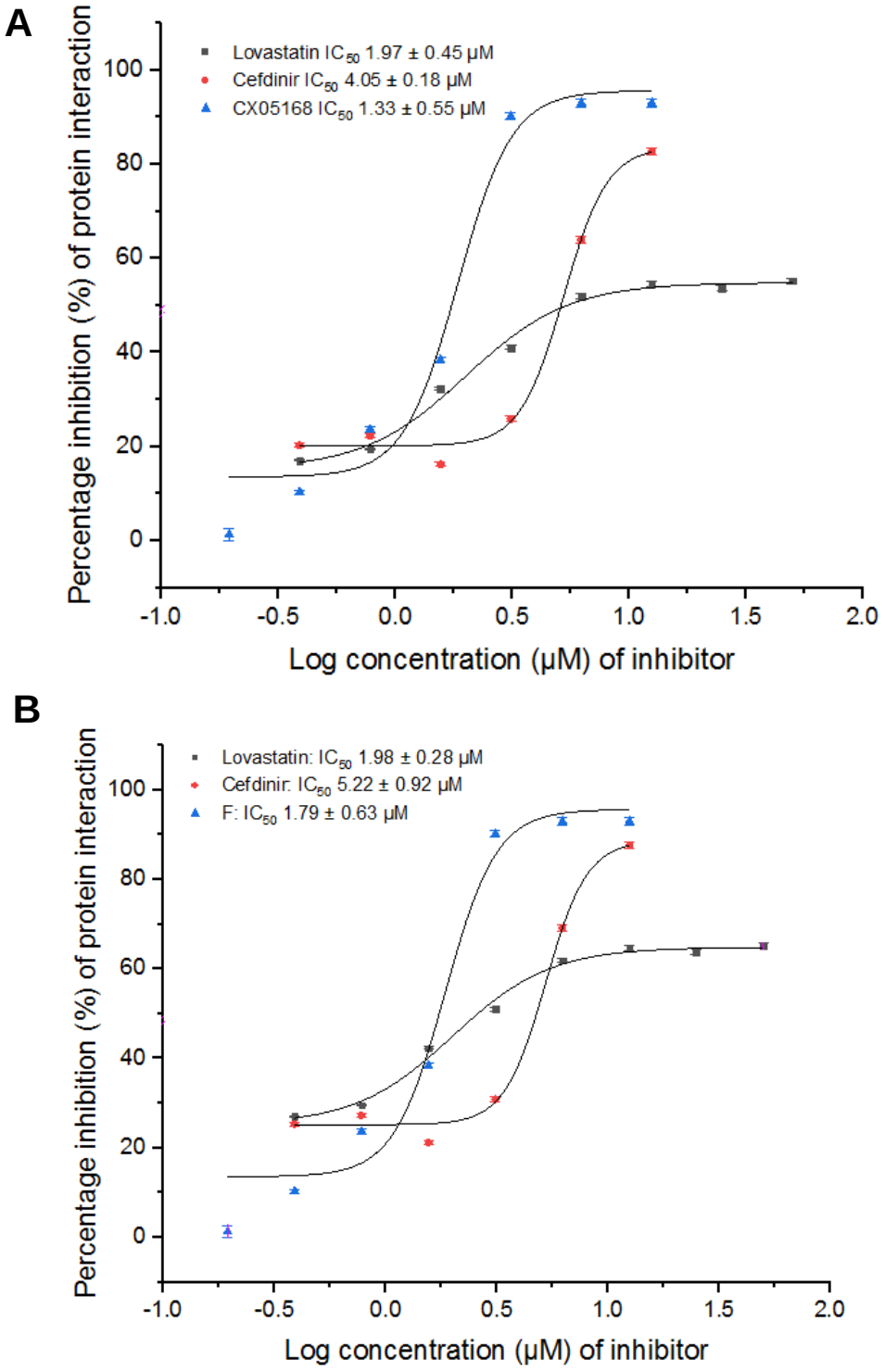


Figure 3. 5: Effects of lovastatin, cefdinir and CX05168 on the HIV-1IN-LEDGF/p75 interaction for HIV-1IN subtype B (**A**) and subtype C (**B**). The representative data of the dose response of lovastatin (square), cefdinir (circle) and CX05168 (triangle) on the HIV-1 IN-LEDGF/p75 AlphaScreen assay. The average values from 3 independent experiments are shown. The curves for each compound were plotted on the same graph for comparative purposes showing standard error bars.

The dose response curvature for CX05168 and cefdinir are similar in slope and steepness, however cefdinir does not reach 100% inhibition. The dose response curve for lovastatin does not reach 100% inhibition nor reduces to 0% inhibition in contrast to that of CX05168 and cefdinir. Additionally, only slight differences in the IC_{50} was observed between the two IN subtypes.

For CX05168 and lovastatin, the differences in IC_{50} values for subtype B and C IN was not statistically significant, with p-values of 0.20 and 1, respectively. By contrast, the difference in IC_{50} values for cefdinir was statistically significant with a p-value of 0.018.

3.2.1.2 HIV-1 IN-LEDGF/p75 AlphaScreen disruption assay containing DNA

Lovastatin, cefdinir and CX05168 were then tested in a second AlphaScreen assay where donor DNA was incorporated to see if the donor DNA has any effect on the inhibitory profile of the compounds. When lovastatin was tested in the presence of DNA no difference in inhibitory profile was seen, indicating that DNA has no effect on inhibition. When CX05168 and cefdinir are run on the assay containing DNA a vast difference in IC_{50} values was observed compared to the absence of DNA. The dose response curves and IC_{50} values are shown in Figure 3.6A and 3.6B for subtype B and C IN, respectively.

When testing CX05168 in the presence of donor DNA, the increase in IC_{50} was statistically significant where the p-value was found to be 0 for subtype B and 0 for subtype C (Figures 3.6A and 3.6B). There was however no statistically significant difference between subtype B and C IN activity when treated in the presence of donor DNA (p=0.79). In stark contrast to CX05268 when lovastatin was tested with DNA, no statistical significance was seen with the addition of DNA, clearly indicating that there is a mechanistic difference in the way CX05168 and lovastatin inhibit the LEDGF/p75-HIV-1 IN interaction. Cefdinir showed a profile similar to that of CX05168. The change in potency from the absence of DNA to the presence of DNA was statistically significant with a p-value of 0 for both subtype B and C IN. Once again in correlation to the non DNA assay, there was a statistically significant difference between the subtype B and C IN responses with a p-value of 0.

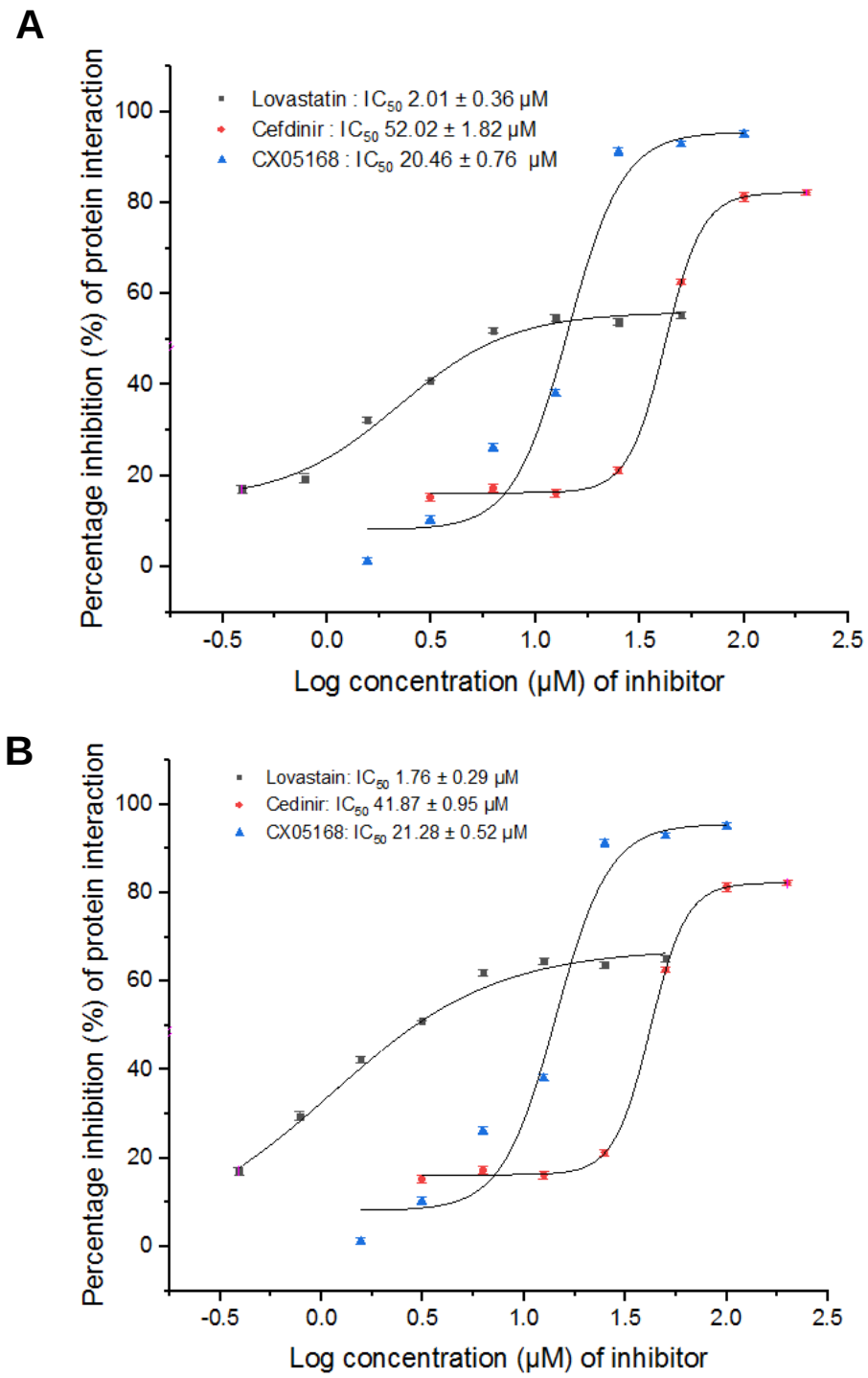


Figure 3. 6: Effects of lovastatin, cefdinir and CX05168 on the DNA-HIV-IN-LEDGF/p75 interaction of HIV-1 IN subtype B (**A**) and subtype C (**B**). Representative data of the dose response on the DNA-HIV-1IN-LEDGF/p75 interaction AlphaScreen assay. The average values for 3 independent experiments are shown. The percentage inhibition was calculated for the experiment and was plotted against the log of the concentration.

It must be noted that all compounds were cross tested with the HIV-1 IN analogue POGz to ensure the compounds were interacting with HIV-1 IN and not LEDGF/p75. None of the compounds inhibited the interaction between LEDGF/p75 and POGz as seen in Figure 3.7 thus confirming their interaction with HIV-1 IN.

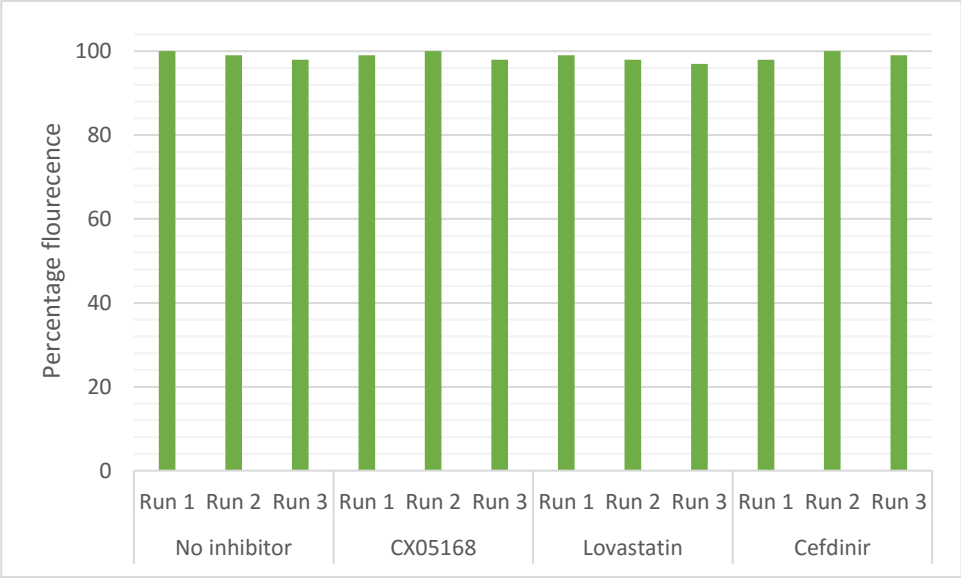


Figure 3. 7 Column graph showing the percentage fluorescence of the POGz-LEDGF/p75 interaction Alphascreen assay. Each inhibitor was run in triplicate. Full fluorescence shows a strong interaction between POGz and LEGDF/p75.

A strand transfer inhibition ELISA was performed for both subtype B and C HIV-1 IN to determine if the studied compounds has any effect on the catalytic activity of HIV-1 IN. Compounds were tested at 100 µM as described in Section 2.3.1.4 to obtain a single dose percentage inhibition. Lovastatin showed strand transfer inhibition of 6.23 ± 4.18 % and 5.69 ± 2.96 % for subtype B and C HIV-1 IN respectively and cefdinir showed strand transfer inhibition of 12.6 ± 2.18 % and 11.29 ± 1.22 % for subtype B and C HIV-1 IN respectively, however CX05168 showed a moderately higher inhibition of 34.29 ± 3.12 % inhibition at a single dose of 100 µM for subtype B IN and 32.96 ± 1.29% for subtype C HIV-1 IN.

3.2.2 Dimerization assay

3.2.2.1 Cross-linking studies

Cross-linking studies were performed with BS3 to determine if there is any increase in the formation of dimers or tetramers when treated with each of the compounds. HIV-1 IN subtype B and C was incubated with BS3 and then incubated with DMSO or compounds, respectively. Figure 3.8A and 3.8B show the results for subtype B and subtype C. In both cases treatment with DMSO, cefdinir and lovastatin show no change in monomer to dimer

or tetramer whereas a decrease in concentration of HIV-1 IN monomers is seen in addition to the formation of two higher order bands when treated with CX05168.

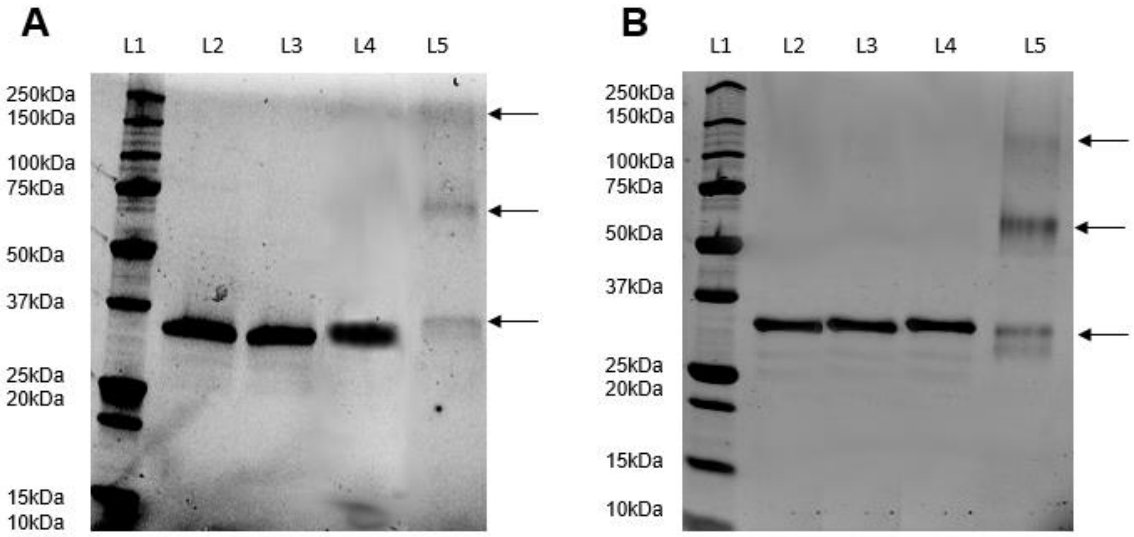


Figure 3. 8: Western blot study showing the cross-linking studies with HIV-1 subtype B IN (**A**) and subtype C IN (**B**). (**A**) Show the western blot of subtype B HIV-1 IN where Lane 1, precision plus protein molecular weight marker (Bio-Rad, USA); Lane 2, HIV-1 subtype B IN 6xHIS tagged protein with no compound; Lane 3, HIV-1 subtype B IN 6xHIS tagged protein with Cefdinir Lane 4, HIV-1 subtype B IN 6xHIS tagged protein with lovastatin and Lane5, HIV-1 subtype B IN 6xHIS tagged protein with CX05168. (**B**) Shows the western blot study showing the cross-linking studies with HIV-1 subtype C IN where Lane 1, precision plus protein molecular weight marker (Bio-Rad, USA); Lane 2, HIV-1 subtype C IN 6XHIS tagged protein with no compound; Lane 3, HIV-1 subtype C IN 6xHIS tagged protein with Cefdinir Lane 4, HIV-1 subtype C IN 6xHIS tagged protein with lovastatin and Lane5, HIV-1 subtype C IN 6xHIS tagged protein with CX05168. Figures 6.8 and 6.0 are the standard curves used to determine protein size marked with an X, circle or triangle for A and B respectively.

3.2.2.2 Differential light scattering studies

DLS studies were conducted as per method of Kessl et al (Kessl et al., 2016b) to confirm the multimerisation effects of each compound on 200 nM HIV-1 IN subtype B and C. A total of 10 measurements were taken in a 30 minute period to see if the compound had any effect on multimerisation. After 30 minutes, the only compound showing multimerisation, determined by the protein peaks at varying size estimates, measured as the diameter Z average (d.nm), was CX05168 corroborating the cross-linking studies, the number percentage is number distribution and is a measure derived from the mie theory, the optical

properties of the particles are needed to determine this figure and number distribution is used to report relative amounts of each peak. When setting the machine up number distribution is chosen, this is due to each particle size differing due to monomer, dimer and multimer. There is no homogeneity in the particle size Figures 3.9A and 3.9B show the effect of the compounds on protein size for the HIV-1 subtype B and C IN, respectively.

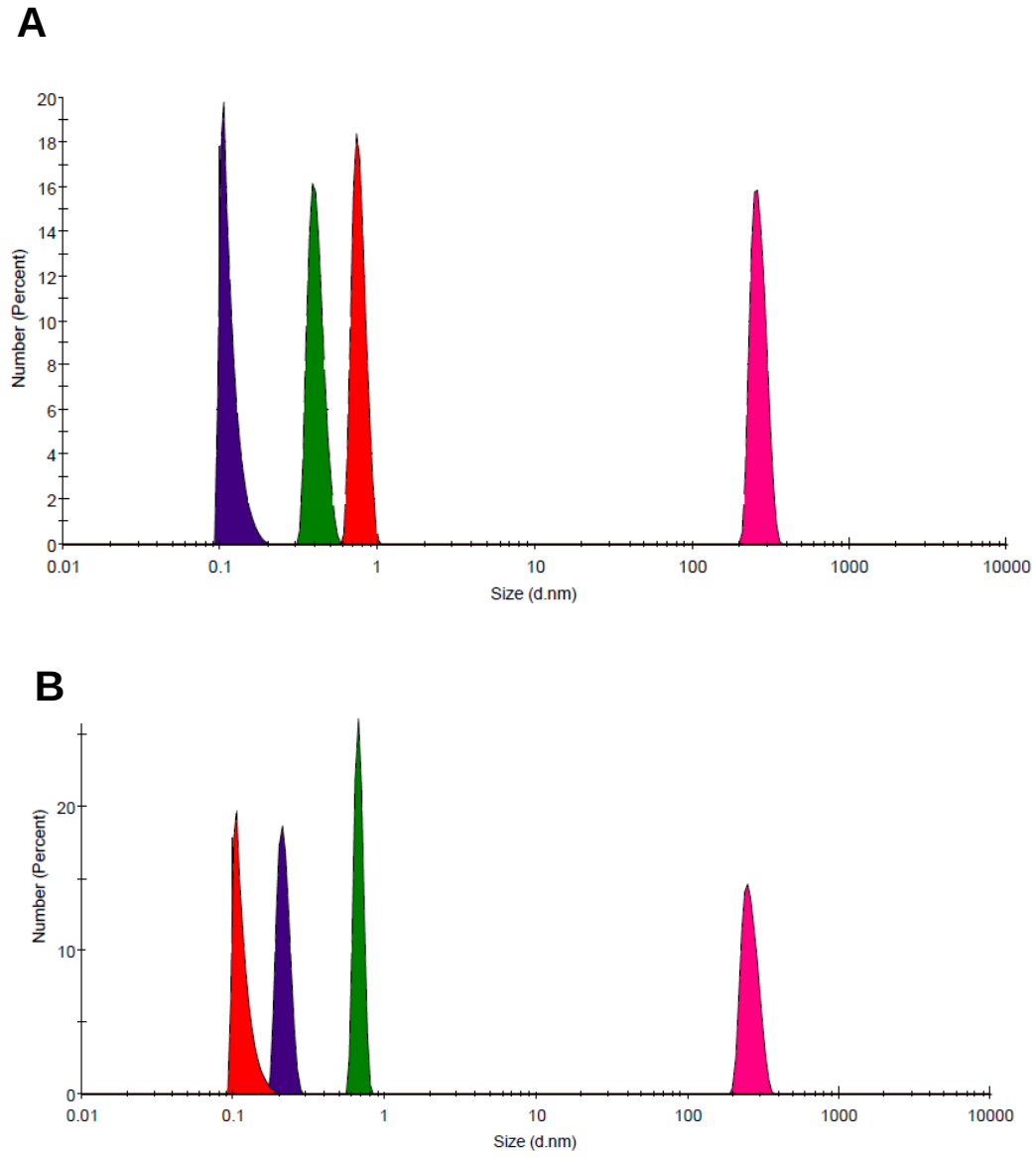


Figure 3. 9: Number distribution graph of the multimerisation effects of studied compounds for subtype B HIV-1 IN and subtype C HIV-1 IN. Differential light scattering assay was utilised to determine the number distribution of each protein treated with compound. (**A**) and (**B**) show the number distribution graph for subtype B HIV-1 IN and subtype C HIV-1 IN respectively where the red peak is HIV-1 IN incubated with DMSO, the purple peak is HIV-1 IN incubated with lovastatin, the green peak is HIV-1 IN incubated with cefdinir and the pink peak is HIV-1 IN incubated with CX05168.

Figure 3.9A and Figure 3.9B show the results for subtype B and C respectively. Any readings below 1 are considered background noise, the protein in normal state of monomer, dimer and tetramer under high ionic strength buffer is not large enough to be detected by the Zetasizer. Poly dispersity index (Pdi) for protein with no compound was 0.287 and 0.298 for subtype B and C HIV-1 IN respectively. CX05168 had a Pdi of 0.215 and 0.312 for subtype B and C respectively. The Pdi for lovastatin was determined to be 0.216 and 0.312 for subtype B and C respectively and lastly was 0.298 and 0.219 for cefdinir with subtype B and C respectively. A control HIV-1 IN was incubated with DMSO and can be seen on both graphs indicated by the red peaks and both fall below the 1 mark. Lovastatin was incubated at 1 µM initially and no increase in multimers could be seen after a 30 minute incubation for either subtype B or C, indicated by the purple peak. The concentration of lovastatin was subsequently increased to 10 µM and 100 µM and still no higher order particles could be seen. Cefdinir was initially tested at 1 µM and can be seen indicated by the green peak. No multimerisation was seen for either subtype. The concentration was subsequently increased to 10 µM and 100 µM with no effect. Once again in stark contrast CX05168 showed an increase in particle size when incubated at a concentration of 1 µM with HIV-1 IN and read over the 30 minute period. Over the course of the 30 minute period a gradual increase in size can be seen until at the 30 minute mark, indicated by the pink peak, HIV-1 IN with CX05168 can be seen between 100 -1000 $d.nm^{-1}$ for both subtype B and C.

3.2.3 Differential scanning fluorometry

The stabilizing effects of CX05168, lovastatin and cefdinir on the protein was tested by DSF using RT-PCR to show real time melt curves (Figure 3.10A and 3.10B show the melt curves for the subtype B and C IN, respectively) and samples were subsequently checked on a spectrophotometer to ensure no aggregation was occurring. The melting temperature of HIV-1 IN subtype B treated with DMSO, lovastatin and cefdinir is 45°C and with HIV-1 IN subtype C treated with DMSO, lovastatin and cefdinir is 42°C. When incubated with CX05168 the melt curve shift and the melt temperature is 54.9°C and 50.1°C for subtype B and C HIV-1 IN, respectively.

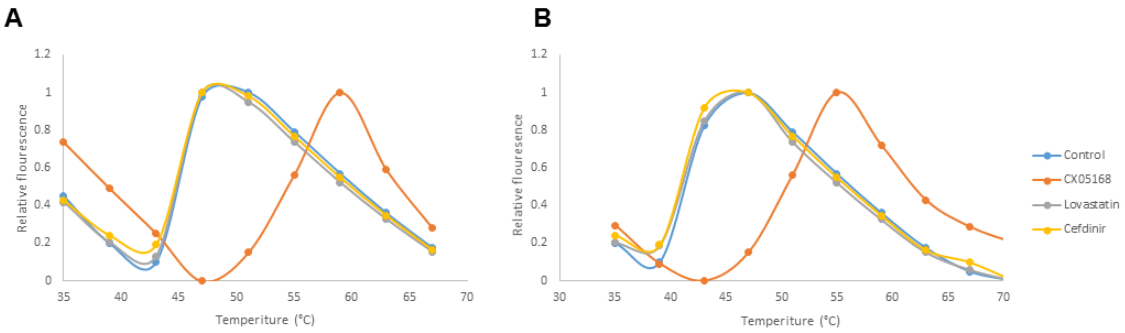


Figure 3. 10: Analysis of the melting temperature of HIV-1 subtype B (**A**) and C (**B**) IN in the absence of compound (blue), in the presence of CX05168 (red), lovastatin (grey) and cefdinir (yellow). The dotted black line represents the melting temperature for the control, lovastatin and cefdinir and the green dotted line represents the melting temperature for CX05168.

3.2.4 Molecular modelling

The binding model of CX05168, lovastatin and cefdinir to the CCD-CCD dimer was predicted by molecular modelling where the compounds were docked into the allosteric HIV-1 IN site at the LEDGF/p75 binding area. The protein databank crystal structure 2B4J was used with the removal of LEDGF/p75 from the CCD dimer interface. The docking area had coordinates of 5.123,-14.656, -16.456 and a radius of 7.9Å. Table 3.1 shows a list of the in silico reaction of CX05168, lovastatin and cefdinir and the predicted binding site amino acids. Amino acids highlighted in yellow depict corresponding amino acid bonds for all inhibitors tested. The model was trained with known LEDGF/p75 integrase inhibitors to ensure the model was accurate.

Table 3. 1: Binding energies determined for the interaction of CX05168, lovastatin and cefdinir with the predicted amino acid interactions.

Compound	Binding energy △ G kcal/mol	Amino acid interactions	CDOCKER energy kcal/mol	Jain scoring function	LibDock scoring function
CX05168	-5.441	Gln95, Ala128, Ala129, Trp131, Trp132, His171, Thr174	-18.55	3.33	82.242
Lovastatin	-24.0263	Ala98, Ala128, Ala129, Ala169, Thr174, His171	4.1587	1.01	65.108
Cefdinir	-11.2891	Gln95, Tyr99, Ala128, Ala129, His171, Thr174	-8.905	1.93	87.016

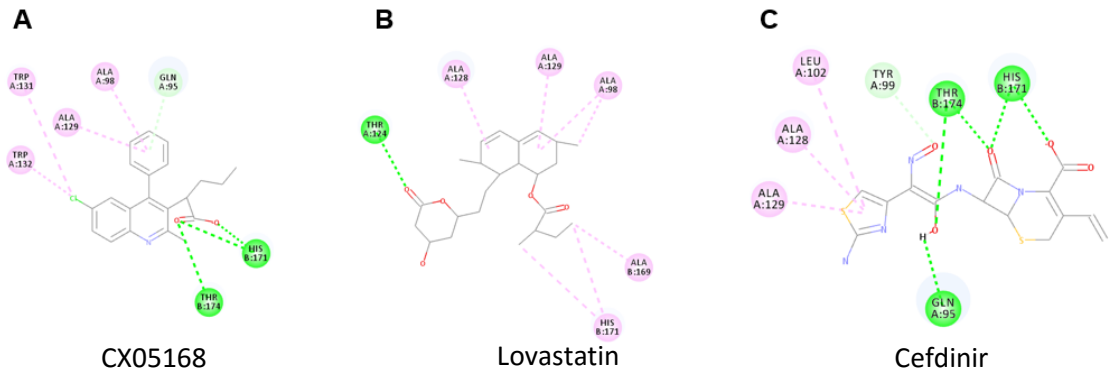


Figure 3. 11: Molecular model of the predicted binding of compounds to the HIV-1 IN dimer interface where LEDGF/p75 would dock. (**A**) Shows the hydrogen bond interactions between CX05168 and the LEDGF/p75 binding site were predicted to be at a relative distance less than 3Å. (**B**) The hydrogen bond interaction of lovastatin in the LEDGF/p75 binding site was projected to be at a relative distance of 2.88Å. (**C**) Shows the hydrogen bond interaction of cefdinir in the LEDGF/p75 binding site was projected to be at a relative distance of 3Å. These figures were generated using Maestro 11.2, Schrodinger, 2017.

The predicted model of CX05168 shows that the carboxylic acid group forms 4 hydrogen bonds with His171 and Thr174 (seen with dark green and light green dashed lines in Figure 3.10A. The phenyl ring showed hydrophobic bonds and pi donor hydrogen contact with Gln9+5, Ala98 and Ala129 (seen with pink dashed lines and light green, respectively). In addition, the chlorine was predicted to occupy the hydrophobic pocket formed by Trp131 and Trp132 indicated by dashed pink lines. The predicted model for lovastatin showed the carboxylic acid group of the tetrahydro-4-hydroxypyran-2-one moiety formed a hydrogen bond with Thr124 of CCD chain A (indicated by green dashed line in Figure 3.10B). The methyl butanoate moiety was projected towards the hydrophobic pocket of Ala169 and His 171 residue of CCD chain B (indicated by the pink dashed line). The hexahydronaphthalen-1-yl ring has hydrophobic interactions with Ala98, Ala128 and Ala129 of CCD dimer chain A (indicated with pink dashed lines)The molecular modelling for cefdinir predicted the carboxylic acid group and the carbonyl group of the 2-thia-6-azabicycloct-4-ene showed 4 hydrogen bonds to Thr174 and His171 (showed by green dashed lines in Figure 3.10C). The hydroxyl group next to the oxime moiety shows 2 hydrogen bonds to Thr174 and Gln95 (showed by pink dashed lines). The thiazole ring shown to occupy the hydrophobic pocket of amino acids Leu102, Ala128 and Ala129 of CCD chain A (shown in pink dashed lines). Finally, the carbonyl group of the oxime moiety formed hydrogen bonds to the Try99 of CCD chain A (shown in green dashed lines).

3.2.5 Hydrogen exchange mass spectroscopy

Hydrogen amide exchange experiments were conducted with full length HIV-1 subtype B and C IN. HIV-1 IN subtype B and C were initially digested on a pepsin column and passed through a C18 column to form peptide maps for each of the IN subtypes (referred to as Apo enzyme). Once the peptide maps had been constructed, HIV-1 IN was subjected to deuterium amide exchange at duration times of 10 seconds, 20 seconds, 1 minute, 10 minutes and 60 minutes – thus allowing a full spectrum of exchange (Figures 3.12 and 3.15). For all heat maps, the red areas indicate high deuterium exchange, i.e. accessibility, whereas the blue areas indicate that the site is restricted. No shading indicates areas with no peptide coverage. Based on the heat map, the peptide coverage of the Apo enzyme of subtype C IN was better than the subtype B. However, sufficient coverage was seen with both proteins for appropriate analysis (Figs 3.12 and 3.15) and for comparison to compound treated IN. It should be noted that although A128 and A129 were not covered by the subtype B Apo protein, once treated with CX05168 or lovastatin the area was available for deuterium exchange. All experiments were conducted in triplicate and the maps showing the best coverage were used for analysis.

The subtype B HIV-1 IN Apo enzyme heat map showed some areas were restricted from hydrogen exchange (Figure 3.12). The amino acids that are important with regards to LEDGF/p75 interaction are Leu 102, Ala 128, Ala 129, Trp 131, Gln 168, Glu 170, His 171, Thr 174 and Met 178 (Cherepanov et al., 2005b). The amino acid Leu 102 is restricted for hydrogen exchange in the Apo protein as well as Ala 128, Ala 129 and Trp 131 had no peptide coverage. Glu 170 and His 171 showed exchange between 60-70%, while Thr 174 showed high exchange of more than 90%. Met 178 showed exchange between 40-50%.

Subsequently, 10 second pulses were chosen as appropriate for the compound testing with CX05168, lovastatin and cefdinir, and the generated heat maps were compared to those of the two Apo enzymes. Overall, there were obvious visual differences between the Apo and IN- CX05168 and IN-lovastatin heat maps, for both subtype B and C IN as seen in Figures 3.13 and 3.16. Comparison of the accessible/inaccessible sites between the Apo protein and compound treated protein allowed for the identification of binding or structural changes attributed to the presence of the compound. The heat map for subtype B IN incubated with CX05168 showed there is restriction of exchange across a large portion of the protein. Amino acids 95, 98, 170 and 171 showed little to no exchange occurring, and amino acids 128, 129, 173 and 174 showed minimal exchange. When subtype C IN was incubated with CX05168, amino acids 95,128, 129, 170, 171, 173 and 174 showed little to no exchange whereas amino acid 98 had high exchange occurring. When subtype B HIV- IN was treated

with lovastatin, an increase in exchange was seen across the protein. Amino acid A128 and A129 showed little to no exchange and E170 and H171 showed 50% exchange. Similarly, when subtype C IN was treated with lovastatin, amino acids E170 and H171 also showed 50% exchange. Lastly, when HIV-1 IN subtype B and C was treated with cefdinir, as seen in Figure 3.13C and 3.16C respectively, very little reduction in exchange was seen. No reduction in exchange was seen with any of the key amino acids listed above. The corresponding molecular modelling figures are shown in Figures 3.14 and 3.17, confirming the accessible vs inaccessible sites.

For the IN used in this study, there are a total of 21 amino acid differences between subtype B and C IN, namely Asp 10 Glu, Asp 25 Glu, Val 32 Ile, Met 50 Thr, Leu 100 Tyr, Leu 101 Ile, Thr 112 Val, Gly 123 Ser, Thr 125 Ala, Arg 127 Phe, Lys 136 Gly, Lys 156 Phe (this is the solubilisation mutation), Val 201 Ile, Thr 219 Ile, Asn 233 Asp, Arg 270 Lys, Asp 279 Ala, Ser 281 Cys, Ser 284 Gly, Arg 285 Gly and Asp 287 Asn. Heat maps showing an overlay of common peptides for deuterium exchange between subtype B and C IN with different compounds were constructed; areas where an increase in exchange was seen in subtypes C relative to subtype B are shown in red, areas where a decrease in exchange in subtypes C relative to subtype B are shown in blue, and areas where little to no exchange between subtypes B and C are shown in grey. Results clearly highlight the subtype differences, generally attributed to an amino acid sequence difference between subtypes. For example, in Figure 3.18 A where amino acid 120 is Thr in B and Val in C.

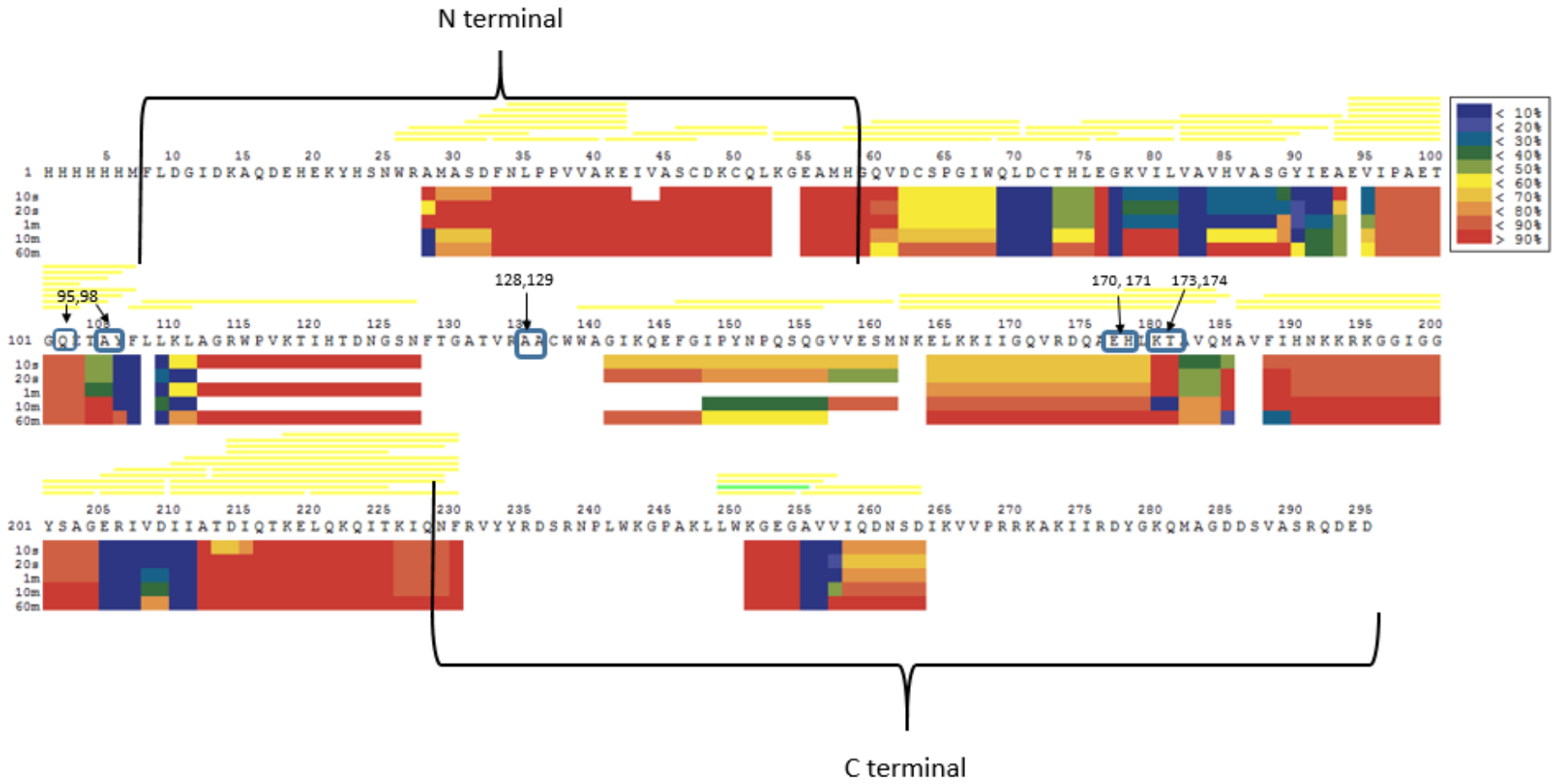


Figure 3. 12: Hydrogen exchange heat map of HIV-1 subtype B integrase in absence of compound with deuteration for 10s, 20s, 1min, 10min and 60 min. The N terminal domain and C terminal domain are labelled with the important amino acids of 128, 129, 170, 171, 173 and 174 highlighted for ease of analysis. Red areas indicate high deuterium exchange, i.e. accessibility, whereas the blue areas indicate that the site is restricted. No shading indicates areas with no peptide coverage. The yellow lines indicate overlapping peptides.

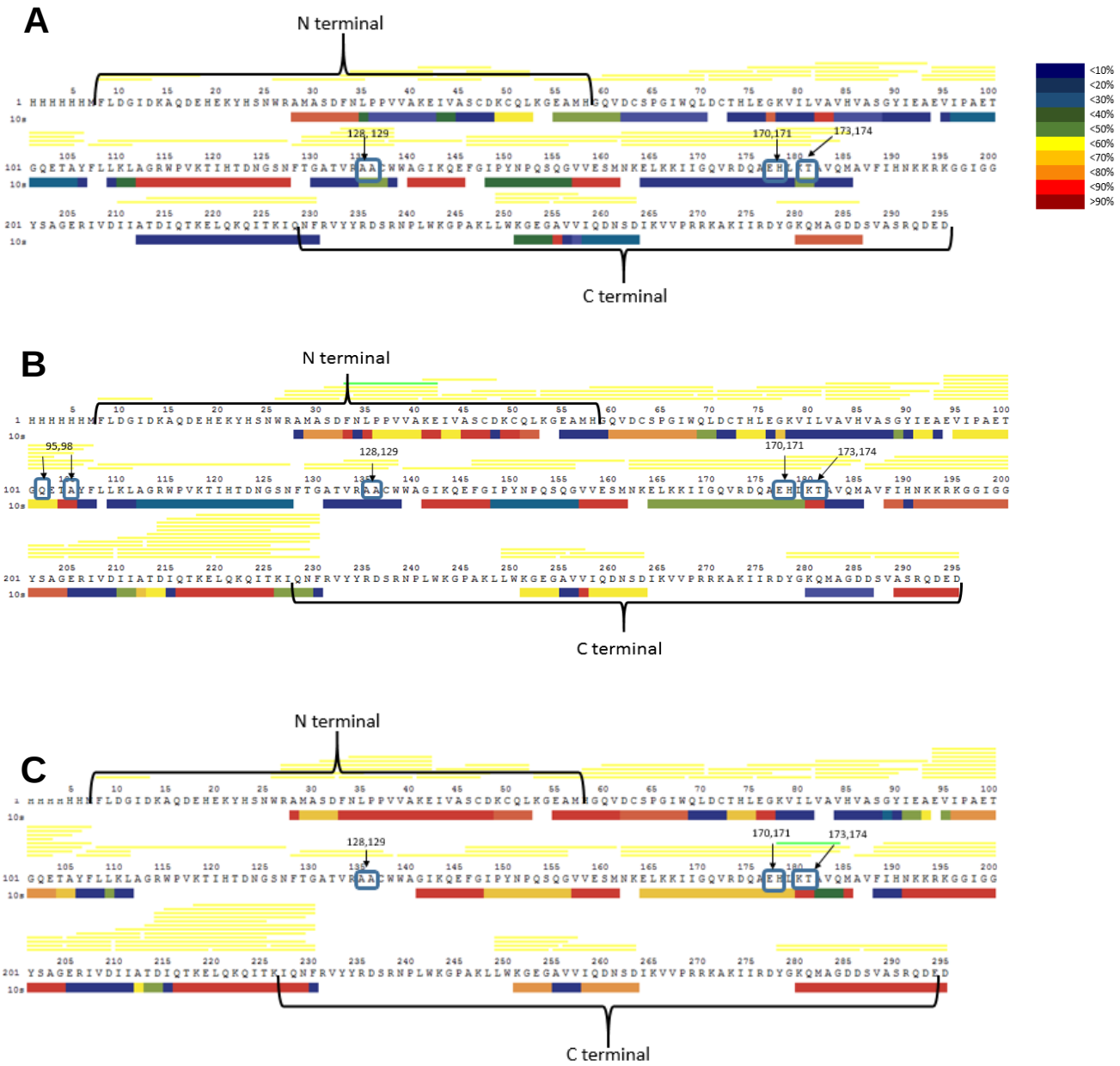


Figure 3. 13: Hydrogen exchange heat map of HIV-1 subtype B integrase with deuteration for 10s treated with CX05168 (**A**), lovastatin (**B**) and cefdinir (**C**). The N terminal domain and C terminal domain are labelled with important amino acids of 128, 129, 170, 171, 173 and 174 highlighted for ease of analysis. Red areas indicate areas of high exchange whereas blue areas indicate restricted hydrogen exchange. The colour key can be found on the right hand top corner.

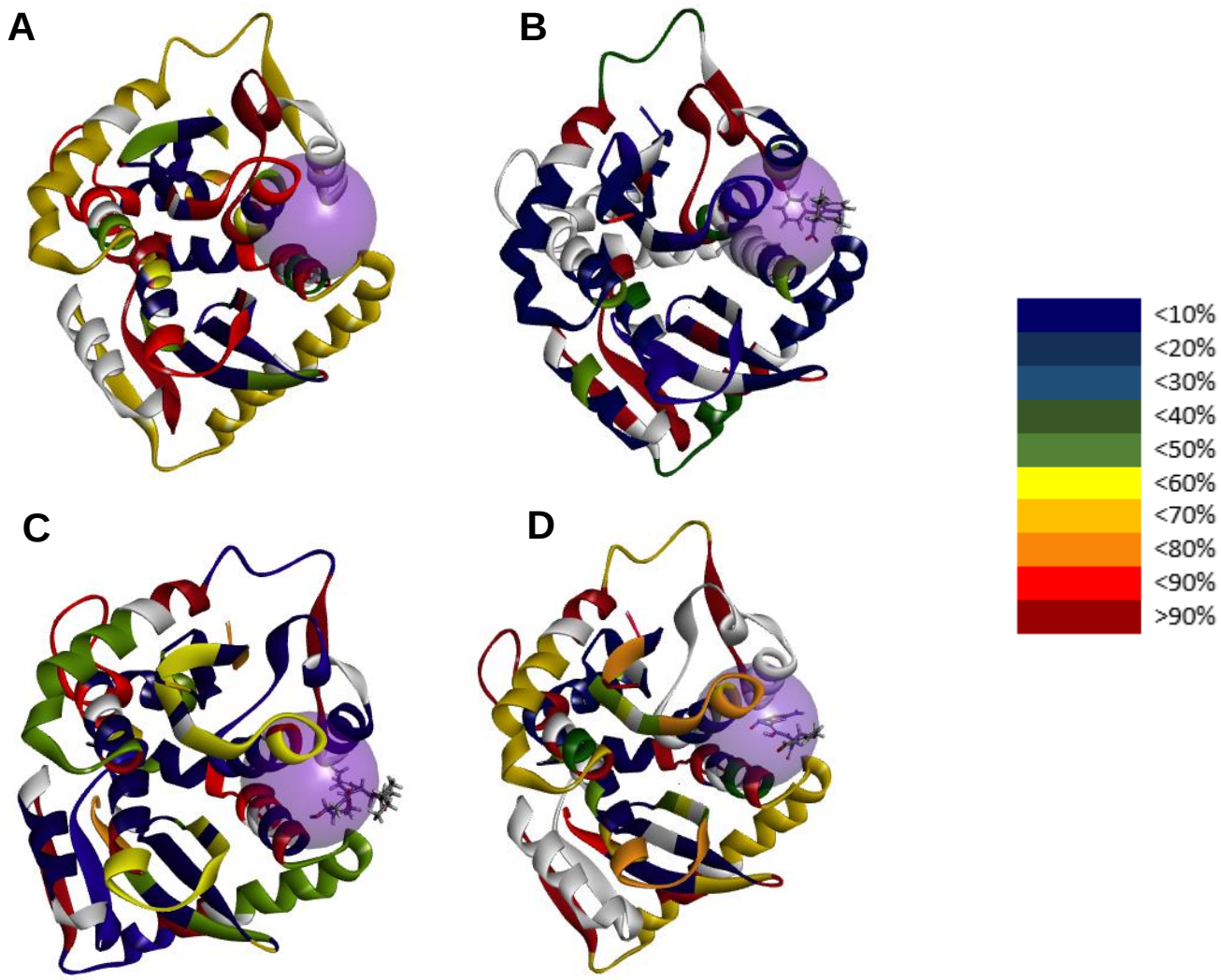


Figure 3. 14: Ribbon structure of the prepared binding site on integrase where the compounds bind to elicit their effects. The purple globe highlights the binding site. The deuterium exchange enzyme has been indicated with colour change depending on the rate of exchange for each part of the enzyme in correlation to the hydrogen exchange maps. The ribbon structure was compiled with the use of Maestro 11.2, Schrodinger, 2017. Figure A is subtype B HIV-1 IN with no compound bound. Figure B is subtype B HIV-1 IN treated with CX05168. Figure C is subtype B HIV-1 IN treated with lovastatin and Figure D is subtype B HIV-1 IN treated with cefdinir.

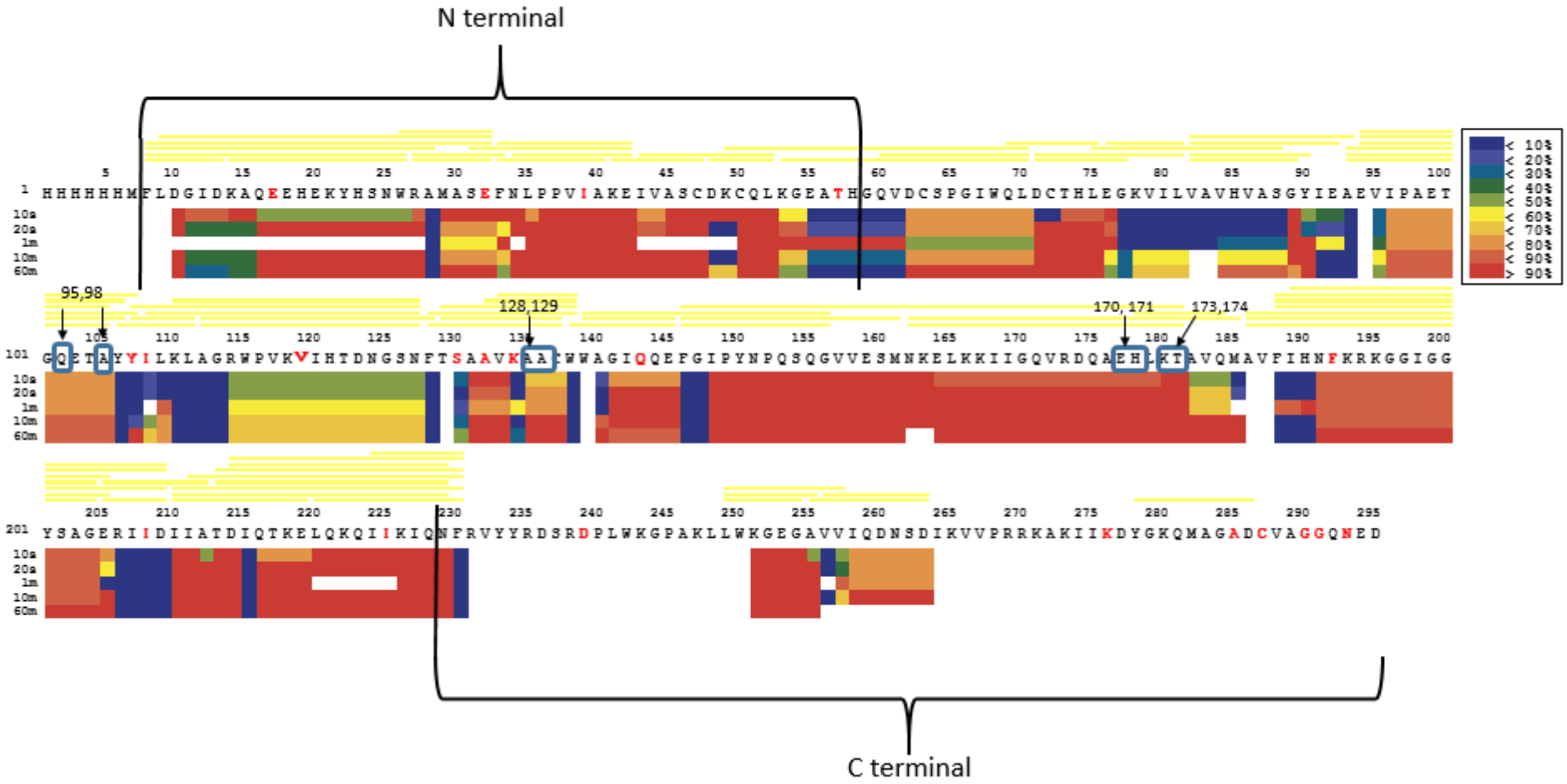


Figure 3. 15: Hydrogen exchange heat map of HIV-1 subtype C integrase with deuteration for 102, 20s, 1min, 10min and 60 min**.** The N terminal domain and C terminal domain are labelled with important amino acids of 128, 129, 170, 171, 173 and 174 highlighted for ease of analysis**.** Amino acids that differ from subtype B are in red. Areas in red are areas of high deuterium exchange whereas areas in blue are restricted from deuterium exchange

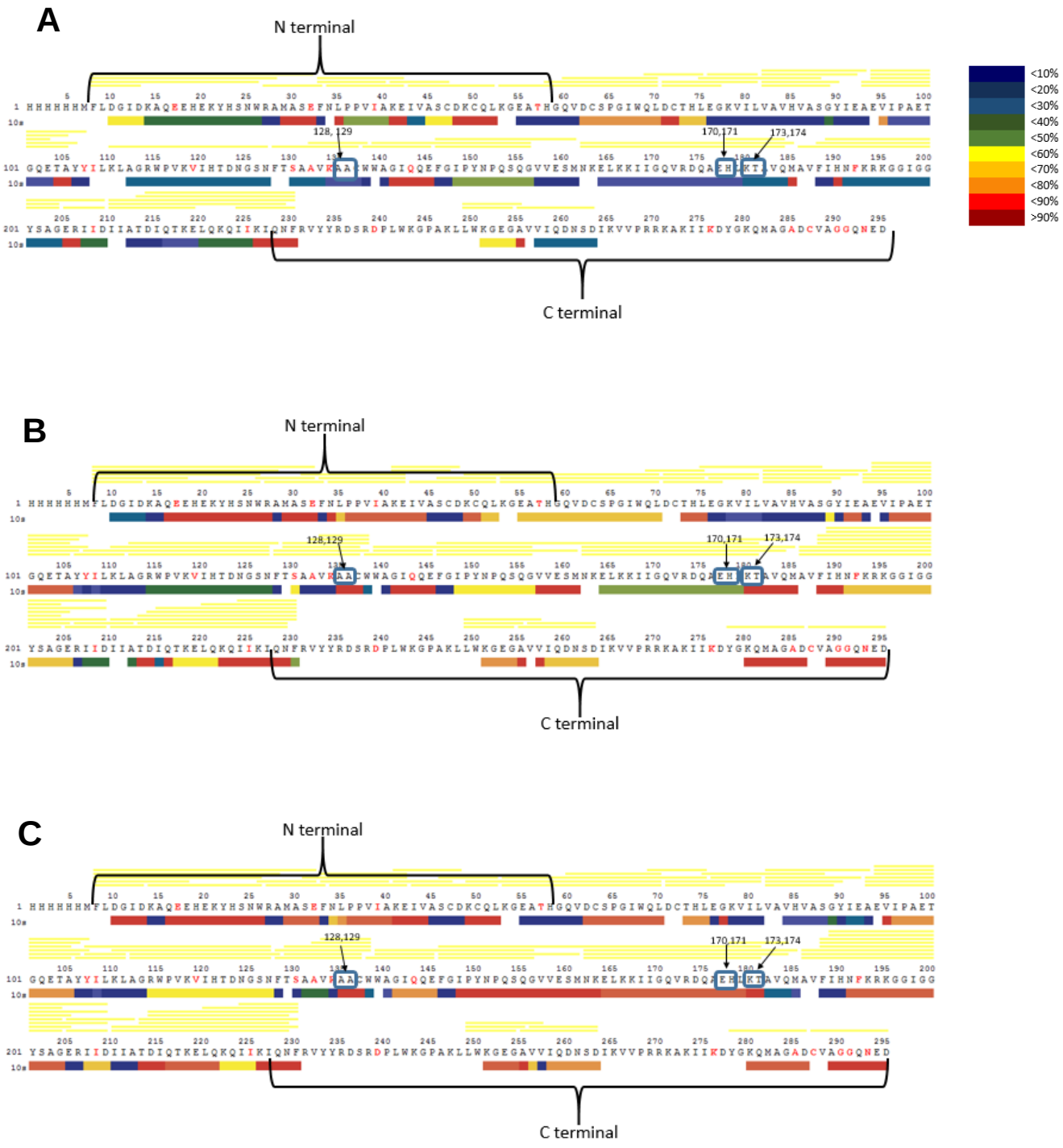


Figure 3. 16: Hydrogen exchange heat map of HIV-1 subtype C integrase with deuteration for 10s treated with CX05168 (**A**), lovastatin (**B**) and cefdinir (**C**). The N terminal domain and C terminal domain are labelled with important amino acids of 128, 129, 170, 171, 173 and 174 highlighted for ease of analysis. Red areas indicate areas of high exchange whereas blue areas indicate restricted hydrogen exchange. The colour key can be found on the right hand top corner.

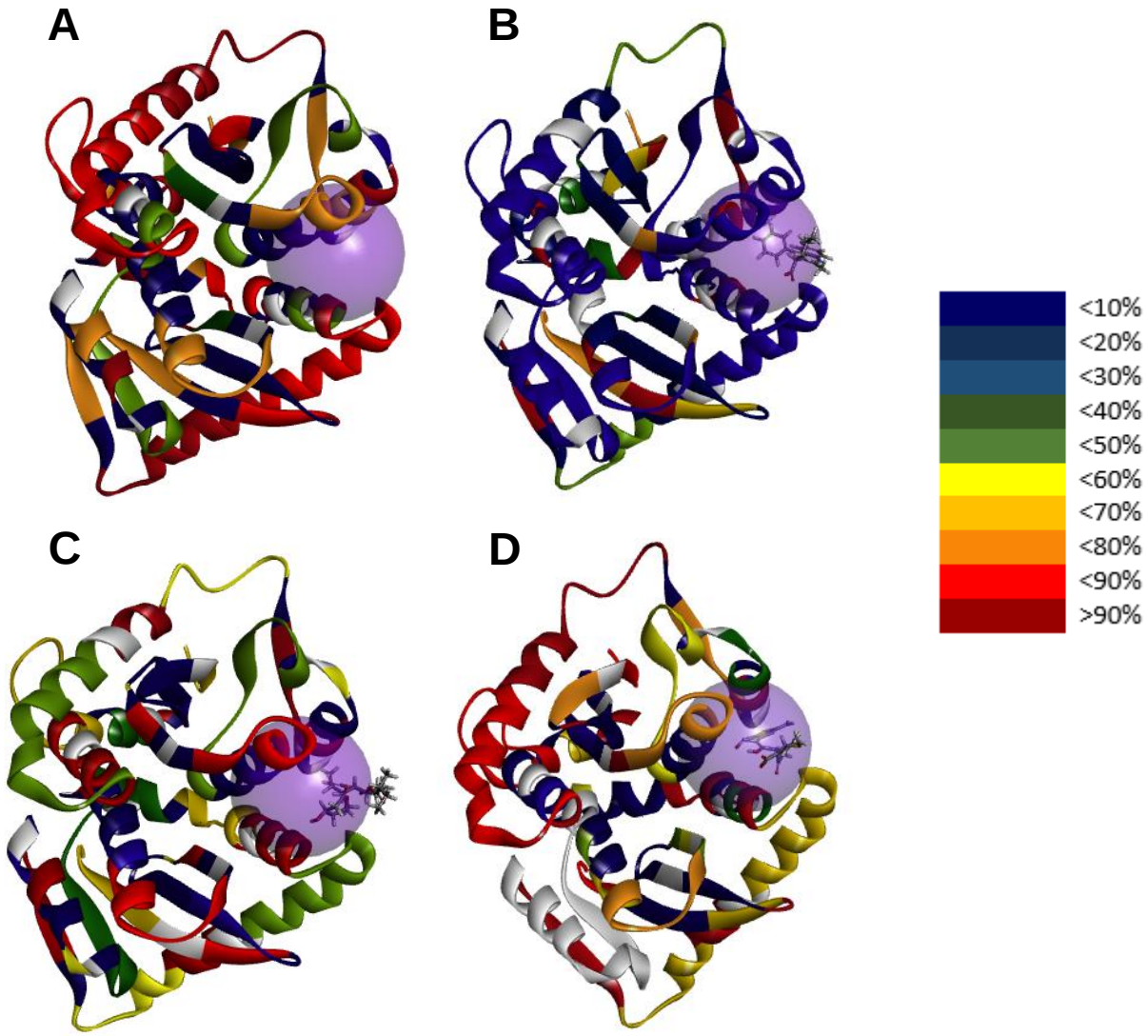


Figure 3. 17: HIV IN ribbon structure displaying the binding site for compound and the respective deuterium exchange in the absence of a bound compound on different parts of the subtype C HIV-1 IN enzyme (The ribbon structure of subtype B has been used as there is no subtype C structure). The purple globe highlights the binding site. The deuterium exchange has been indicated with colour change depending on the rate of exchange for each part of the enzyme in correlation to the hydrogen deuterium exchange heat maps. The ribbon structure was compiled with the use of Maestro 11.2, Schrodinger, 2017. (**A**) Subtype C HIV-1 IN with no compound bound. (**B**) Subtype C HIV-1 IN treated with CX05168. (**C**) Subtype C HIV-1 IN treated with lovastatin and Figure D is subtype C HIV-1 IN treated with cefdinir.

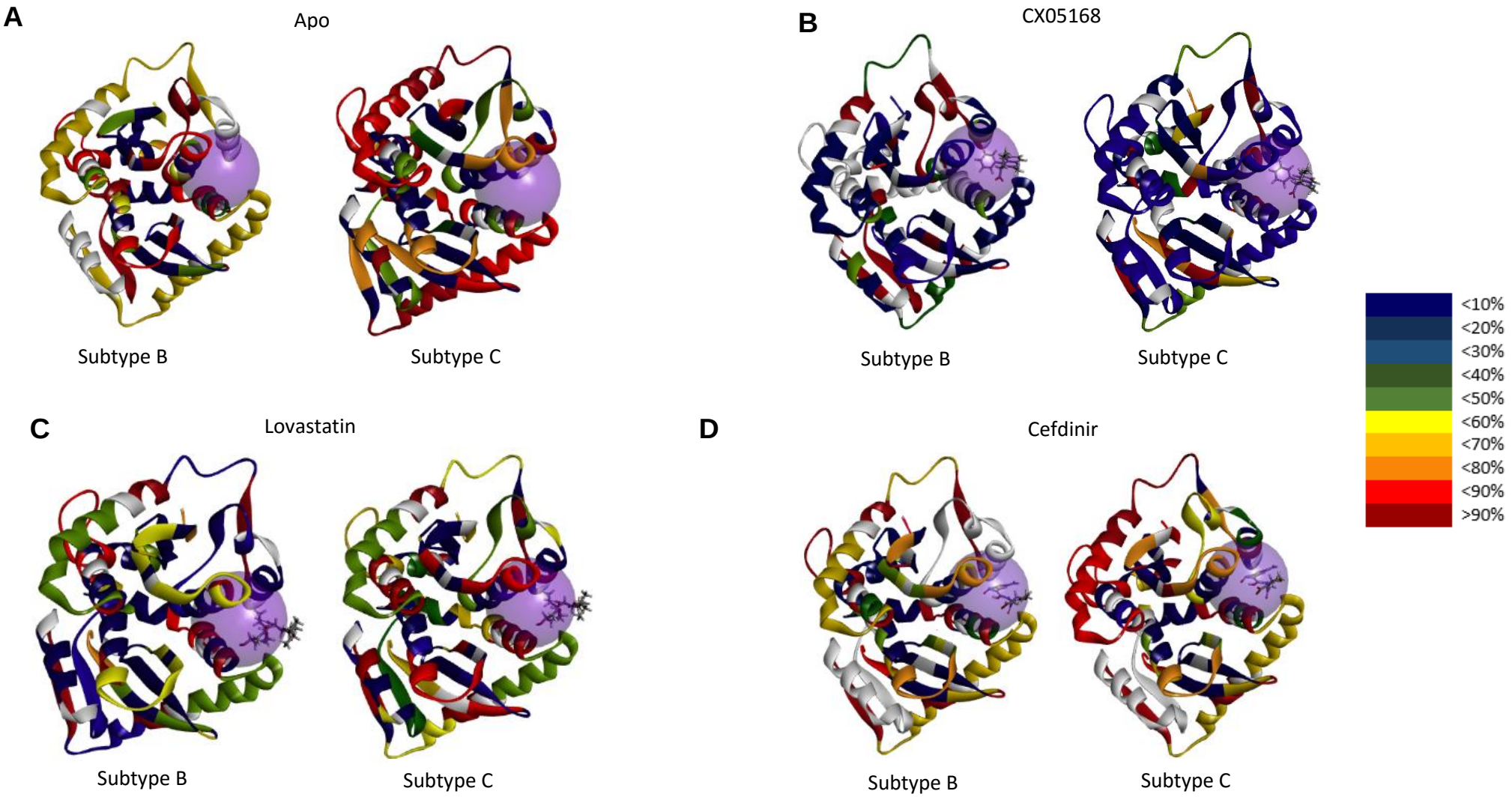


Figure 3. 18: HIV IN ribbon structure displaying the comparison of subtype B and C with the colours related to the deuterium exchange. The purple globe highlights the binding site. The ribbon structure was compiled with the use of Maestro 11.2, Schrodinger, 2017. (**A**) Subtype B and C HIV-1 IN with no compound bound. (**B**) Subtype B and C HIV-1 IN treated with CX05168. (**C**) Subtype B and C HIV-1 IN treated with lovastatin and Figure **(D)** is subtype B and C HIV-1 IN treated with cefdinir.

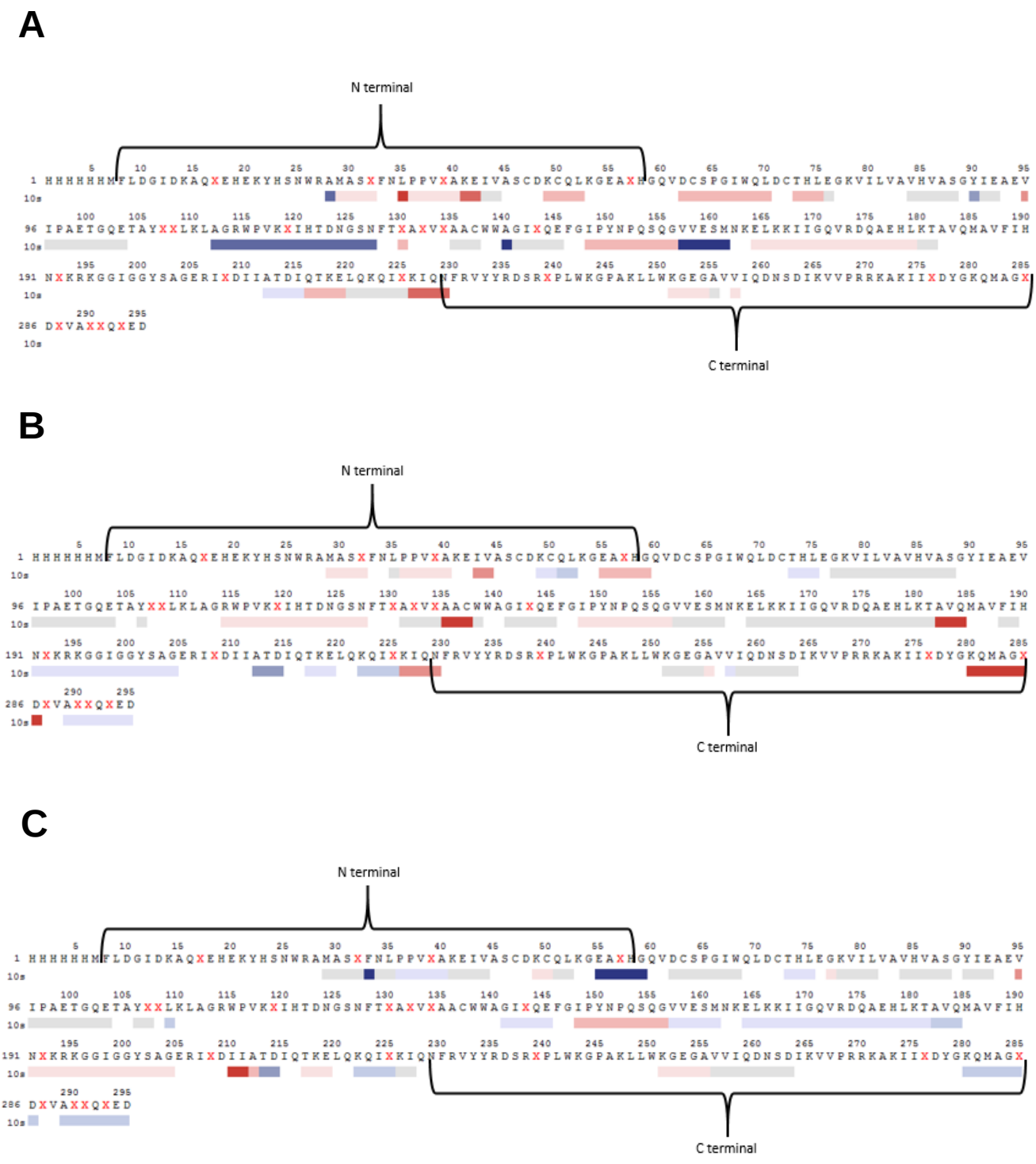


Figure 3. 19: Hydrogen exchange comparison heat map showing the deuterium exchange differences between subtype B and C HIV-1 IN with CX05168 (**A**), lovastatin (**B**) and cefdinir (**C**) treatment. The amino acid changes between subtypes labelled with a red X. Areas where an increase in exchange was seen in subtypes C relative to subtype B are shown in red, areas where a decrease in exchange in subtypes C relative to subtype B are shown in blue, and areas where little to no exchange between subtypes B and C are shown in grey

3.2.6 Surface Plasmon Resonance (SPR)

HIV-1 subtype B and C IN were bound to a GLH sensor chip in duplicate and CX05168 at various concentrations was allowed to flow over the cell for a short contact time. The chip was then regenerated and subsequently lovastatin and cefdinir were tested. When testing CX05168, the duplicate results were comparable with one another and the chi squares for subtype C were within the 10% range of the RU max whilst for the subtype B the chi squares were just outside the 10% range. However, for both lovastatin and cefdinir, binding can be seen but even at high concentrations the level of binding to noise ratio are unacceptable for good readings. The resonance graphs for both subtype B and C can be seen in Figure 3.18A and 3.18B respectively.

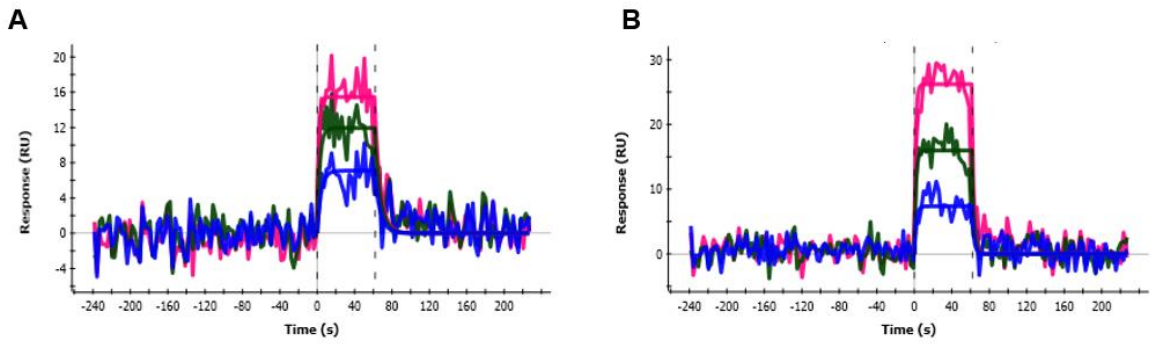


Figure 3. 20: Surface Plasmon resonance graphs for CX05168 for concentrations 10µM, 5µM and 2µM for subtype B (**A**) and C (**B**) HIV-1 IN. The blue line represents 2µM, the green line represents 5µM and the pink line represents 10µM.

The RU max, K_D values and Chi squares for each replicate and subtype can be seen in Table 3.2. The subtype C IN was a better fit and the chi square falls within 10% of the RU max for each run. The subtype B chi squares fall outside the desired 10% of the RU max range, however results are still considered to be acceptable.

Table 3. 2: The maximum response units (RU max), Chi square, association constant (K_a), dissociation constant (K_d) and the equilibrium constant (K_D) of CX05168 for subtype B and C IN.

	RU max	Chi square	$^{a}k_a\ Ms^{-1}$	$^{b}k_d\ s^{-1}$	K_D µM
Subtype B1*	23.08 ±0.89	3.83 ± 0.25	$4.32 \times 10^{4} \pm 0.41$	$2.08 \times 10^{-1} \pm 0.34$	$4.79 \times 10^{-6} \pm 0.42$
Subtype C1*	66.63 ± 4.64	4.75 ± 0.42	$3.27 \times 10^{4} \pm 0.58$	$4.98 \times 10^{-1} \pm 0.19$	$1.57 \times 10^{-5} \pm 0.23$

*Subtype B is representative of 3 biological replicates and subtype C is representative of 3 biological replicates.
[a]K_a is a measure of the speed at which the CX05168 associates with HIV-1 IN.
[b]K_d is a measure of the speed at which CX05168 dissociates from HIV-1 IN.

3.2.7 Cellular screening

3.2.7.1 Cytotoxicity and Antiviral screening

The MT-4 cell line was used to obtain cytotoxicity and antiviral data for both subtype B and C IN (Table 3.3). Lovastatin was found to have a CC_{50} value of 6.59 ± 0.12 µM and antiviral effects of 5.96 ± 1.12 µM for subtype B and 5.65 ± 0.22 µM for subtype C. CX05168 was found to have a CC_{50} of 69.56 ± 1.39 µM with EC_{50}s of 1.85 ± 0.69 µM and 3.65 ± 0.39 µM for subtype B and C respectively. Cefdinir was found to be nontoxic at levels up to 200 µM and has antiviral effects with EC_{50}s of 45.29 ± 10.30 µM and 52.62 ± 7.62 µM for subtype B and C, respectively. The basis of the MTS assay is a living cell will produce formazan from the active ingredient in MTS and this is measurable at 490 nm.

Table 3. 3: Comparison of cytotoxicity and antiviral biological activity of CX05168, lovastatin and cefdinir in MT-4 cells infected with HIV-1 NL4-3 subtype B and HIV-1 93IN905 subtype C isolates.

Compound	**Cytotoxicity CC_{50} (µM)**	**Antiviral EC_{50} (µM)**	
		Subtype B	**Subtype C**
CX015168	69.56 ± 1.39	1.85 ± 0.69	3.65 ± 0.39
Lovastatin	6.59 ± 0.12	5.96 ± 1.12	5.64 ± 0.22
Cefdinir	≥ 200	45.29 ± 10.30	52.62 ± 7.62
Auranofin	1.15 ± 0.1	ND	ND
Raltegravir	≥ 200	0.01 ± 0.00	0.02 ± 0.01

3.2.7.2 Time of Addition screening

A TOA assay was then run. Lovastatin was considered too toxic to be tested in this assay. In Figure 3.19A and 3.19B the results can be seen against HIV-1 subtype B and C, respectively. CX05168 inhibited the virus up until time point 10 and then the viral p24 increased. Interestingly, the addition of cefdinir after 5 hours was not able to stop viral production. This trend was seen against both subtypes.

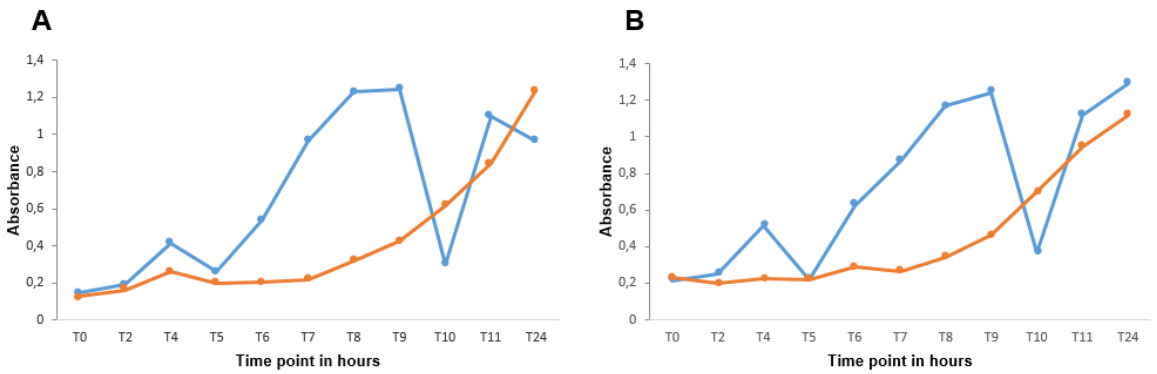


Figure 3. 21: TOA results for the antiviral effects of cefdinir and CX05168 compounds at specified time points for subtype B (**A**) and C (**B**) integrase. The blue line represents cefdinir at 100 µM and the orange trend line represent CX05168 treatment at 30 µM. The experiment for CX05168 was conducted in duplicate per experiment and 3 separate experiments were conducted. Cefdinir was tested in duplicate per experiment and 12 separate experiments were conducted.

Chapter 4

4. Discussion

The inevitable emergence of resistance to current anti HIV-1 drugs is a matter of huge concern. Development of antiretroviral drug resistance has come to the forefront in research and is contributed to by the error prone reverse transcription during viral replication, a consequence of the failure to fully suppress HIV-1 replication, as well as poor patient adherence to treatment regimens. With the surge in antiretroviral drug resistance, novel targets for HIV-1 drug research have been investigated. One of these targets is the interaction of HIV-1 IN with the host co-factor LEDGF/p75 (Christ et al., 2010a; Christ et al., 2012; Kessl et al., 2012; Jurado and Engelman, 2013; Jurado et al., 2013; Le Rouzic et al., 2013; Fader et al., 2014a; Fenwick et al., 2014).

LEDGF/p75 contains the IBD on the CTD (Llano et al., 2006; Turlure et al., 2006; Tsutsui et al., 2011). The importance of LEDGF/p75 to the HIV-1 replication cycle has been found to be protection of the PIC from proteasomal degradation as well as acting as a bifunctional tether where LEDGF/p75 connects HIV-1 IN to host DNA at the correct point for successful integration of viral cDNA into host DNA (Cherepanov et al., 2003; Busschots et al., 2005; Llano et al., 2006).

Previously in our laboratory lovastatin (Harrison et al., 2014), a cholesterol lowering medication and cefdinir, a cephalosporin antibiotic, were identified as HIV-1 IN-LEDGF/p75 inhibitors (Harrison et al., 2014). Cefdinir was of particular interest as cefixime, another cephalosporin antibiotic, was found to have strand transfer inhibitory properties (Abrahams et al., 2018). This study elucidated the modes of action of lovastatin and cefdinir, as compared to the known ALLINI CX05168.

Prior to ligand binding and biophysical characterization studies, the recombinant HIS tagged LEDGF/p75 and HIS tagged HIV-1 IN subtype B and C were expressed and purified to sufficient levels for experimental use. The purification protocols for IN (Jenkins et al., 1996) and LEDGF/p75 (Bartholomeeusen et al., 2009) had to be optimized further to ensure greater purity, to prevent interference with subsequent assays. Following the original protocols, several contaminating proteins were noted on SDS-PAGE and Western blot analyses (results not shown). However, following several modifications of an additional column and purification using an amicon with a cut off close to the protein of interest, fewer contaminants were detected. The strand transfer ELISA (Figure 3.4) confirmed that both purified recombinant subtype B and C HIV-1 INs were catalytically active and conformationally intact since addition of RAL to the assay reduced activity.

4.1 Allosteric inhibition of HIV-1 IN in the presence of DNA

The HIV-1 IN-LEDGF/p75 AlphaScreen assay showed a dose response to increasing concentrations of CX05168, lovastatin and cefdinir, with some differences (Figure 3.5 A and B). The CX05168 findings correlate to those of Christ *et al* , 2010 (Christ et al., 2010), who showed an IC_{50} value of 1.37 ± 0.36 µM in their Alphascreen assay in comparrison with the IC_{50} from our assay of 1.33 ± 0.55µM, confirming the validity of our assay. However, it must be noted that in our assay we used nickel chelating donor and acceptor bead which is slightly unorthodox. This also opens the possibility to cross competition as HIV-1 IN is known to multimerise and could therefore compete with LEDGF/p75 for the other bead. Controls were in place to avoid this cross competition and as the result for CX01568 was similar to the published findings we continued with the assay in the current form. When viewing the slopes and inhibitory profiles, as seen in Figure 3.5 A and B, differences can be seen between all three compounds. The use of the slope to determine clinical outcomes is very important, for instance, if two drugs have similar IC_{50} values but differ greatly in slope, the steeper the slope in protein-protein assays indicates aggregation or promiscuous binding (Shen et al., 2008). By contrast, if a steep slope is achieved in inhibitory cell based assays, it indicates the compound has a better chance at inhibiting the interaction at drug concentrations that are clinically relevant (Rosenbloom et al., 2012). The steepness of the curve is indicative of the cooperativity of the ligand binding the enzyme. The quantification of this relationship is achieved by the Hill coefficient. The steeper the slope, the higher the impact a small change in dose becomes (Shen *et al*., 2008; Rosenbloom *et* al., 2012). With each drug class the slopes differ, for example NRTIs and INSTIs have Hill coefficient values of 1. However, NNRTIs have a Hill coefficient of more than 1.7. It should be noted that PIs can have slopes reaching 4.5, which is significant since PIs can be used as monotherapy (with a high genetic barrier to resistance) unlike the other antiretroviral drugs (Shen *et al*., 2008). ALLINIs have been shown to have slopes greater than 1 (Jurado *et al.*, 2013; Kessl *et al*., 2011).

CX05168 shows almost full inhibition of HIV-1 IN activity, with a steep slope with the Hill coefficient determined with use of Origin 8.1 to be 3.63 ± 1.67 for both subtypes B and 3.76 ± 1.72 for subtype C IN (Figures 3.5A and 3.5B). With reference to a steep slope being indicative of aggregation (Shen et al., 2008) this rings true for CX05168 as based on previous research HIV-1 IN in the presence of ALLINIs initially have ordered aberrant multimerisation that later becomes unordered aggregation. This Hills slope indicates a potent inhibitor and full agonist. The lovastatin slope is vastly different - full inhibition was never reached and the slope was less steep. The Hill coefficient for lovastatin was

calculated to be 1.81 ± 0.34 for subtype B and 1.98 ± 0.37 for subtype C IN. A Hill co-efficient of more than 1 indicates positive cooperativity, however the failure to reach full inhibition is indicative of a weak inhibitor and partial agonist. Cefdinir like lovastatin failed to reach full inhibition of HIV-1 IN activity, however, when the Hill coefficient was calculated it was found to be 4.48 ± 1.12 for subtype B IN and 4.67 ± 1.53 for subtype C IN, which is closer to the profile of CX05168 indicating possible aggregation or promiscuous binding. Thus, the cefdinir profile indicates a potent inhibitor and partial agonist.

It was then decided to determine how the presence of donor DNA would affect the potency of the compounds in the AlphaScreen assay. The recombinant subtype B and C HIV-1 IN had to be cleaved of their HIS tags so that a streptavidin bead could be used for binding to the biotinylated donor DNA ensuring that the HIV-1 IN would then bind solely to the DNA and not an interfering nickel bead. Overall, a significant difference in IC_{50} values was seen in comparison with the AlphaScreen assay in the absence of DNA, with the exception of lovastatin as seen in Figures 3.6 A and B. There is currently no published data for IC_{50} values of CX05168 in the presence of donor DNA in the inhibition of the IN-LEDGF/p75 complex. Christ et al, 2010, showed that the presence of donor DNA prior to the addition of ALLINIs negatively affected the strand transfer inhibitory ability of compounds. This decrease in potency can be explained by the discovery that ALLINIs cause the aberrant multimerisation of HIV-1 IN in the absence of viral DNA (Christ et al., 2012; Sharma et al., 2014; Shkriabai et al., 2014). Thus, results indicate that cefdinir and CX05168 potentially cause multimerisation of HIV-1 IN.

With this stark contrast in HIV-1 IN activity between CX05168, cefdinir and lovastatin, we wanted to ensure these compounds were interacting with HIV-1 IN and not LEDGF/p75. For this we used an HIV-1 IN analogue known to bind to LEDGF/p75, POGz (Bartholomeeusen et al., 2007; Tesina et al., 2015). This AlphaScreen assay showed no inhibition for any of the compounds, confirming that the compounds tested were binding to HIV-1 IN and not LEDGF/p75.

With data being published that ALLINIs also affect the catalytic activity of HIV-1 IN, we then tested the compounds through the strand transfer ELISA assay (Christ *et al*., 2012; Tsiang *et al*., 2012; Kessl *et a*l., 2012; Jurado and Engelman, 2013; Le Rouzic *et al*., 2013). Low levels of inhibition were found with all the compounds, however CX05168 was found to have 34.29 ± 3.12 % inhibition at a single dose of 100 µM for subtype B and 32.96 ± 1.29% for subtype C. The levels of strand transfer inhibition for CX05168 have been published as much higher with IC_{50} values of 4.2 ± 0.6 µM (Christ *et al*., 2012; Kessl *et al*., 2012). This is

possibly attributed to the finding that full potency of ALLINIs against strand transfer is only achieved if the compounds are added to HIV-1 IN before the donor DNA is present (Frauke Christ et al., 2012; Jurado and Engelman, 2013). In the current strand transfer ELISA, the compounds were added after the addition of donor DNA. This too could explain the LEDGF/p75-HIV-1 IN- DNA AlphaScreen results as the DNA was pre-incubated with HIV-1 IN prior to compound addition. However, through the use of the current method we were able to see a clear distinction that the mode of inhibition of LEDGF/p75-HIV-1 IN by lovastatin is different.

4.2 The allosteric inhibition effects of CX05168, cefdinir and lovastatin on HIV-1 IN multimerisation and protein stability

In early 2012, Kessl *et al.,* published findings that illustrated the ALLINIs abilities to cause aberrant multimerisation of HIV-1 IN (Kessl *et al*., 2012). In their study, they developed a homogenous time resolved fluorescence (HTRF) assay to observe the HIV-1 IN-IN interactions. The basis of this assay is that if a compound inhibits the HIV-1 IN-IN interaction the HTRF signal would decrease. If the addition of a compound then stabilises the protein subunits of HIV-1 IN, the HTRF signal would increase. They tested CX05168 and BI1001, and found a dose dependent response, as indicated by the increase in HTRF signal, whereas the RAL signal remained unchanged even with increasing doses. They also evaluated the thermal stability of the interaction by monitoring the protein melting temperature at increasing concentrations. Both CX05168 and BI1001 showed increases in temperature with increasing doses of compound but the melting temperature remained the same with RAL treatment. They deduced that ALLINIs increase the HIV-1 IN multimerisation by stabilising the HIV-1 IN-IN subunit interactions. These findings were confirmed with similar studies by Tsiang *et al.,* and Christ *et al.,* that displayed that although these compounds bind allosterically they still have a profound effect on the catalytic activity of the IN enzyme (Christ *et al*., 2012; Tsiang *et al*., 2012).

CX05168, cefdinir and lovastatin were tested in two separate HIV-1 IN multimerisation assays. Using a cross-linking assay, it was evident that addition of lovastatin did not result in the formation of HIV-1 IN dimers or higher order tetramers and there was no decrease in the intensity of the HIV-1 IN band at 32kDa (both subtype B and C) as seen in Figure 3.8 A and B. Interestingly, when HIV- 1 IN subtype B was treated with cefdinir a light or faint band was seen between 150 and 250kDa, however, there does not appear to be any decrease in intensity of the band at 32kDa; if there are multimerisation effects they are minimal at best. When looking at the results for subtype C HIV-1 IN, no higher order bands

were visible nor any reduction in the intensity of the band at 32kDa. The difference between subtype B and C IN-LEDGF/p75 was also seen in the IC_{50} values for cefdinir, however at this point we cannot differentiate if there was multimerisation with subtype B HIV-1 IN. By contrast, CX05168 displayed vastly different results, with both subtype B and C HIV-1 IN displaying higher order bands seen between 50 and 75kDa as well as 100-250kDa, with almost no monomers of HIV-1 IN seen at 32kDa. The intensity of the bands could also indicate many higher order multimers that could perhaps not migrate through the SDS-PAGE gel due to aggregation.

Because the cross-linking assay had not been used previously for HIV-1 IN multimerisation assays, we performed a recently published assay to study the multimerisation effects using a Malvern Nano series zetasizer (Kessl et al., 2016b). Each compound was also run in the absence of protein to ensure that the increased size is not due to interference of the compound and is correctly attributed to the multimerisation of HIV-1 IN. It must be noted that when in the presence of an inhibitor that causes abberant multimerisation, the multimerisation is initially ordered and then cascades into unordered aggregation. These results confirm our findings from the cross-linking study that lovastatin and cefdinir have no effect on multimerisation of HIV-1 IN whereas CX05168 causes HIV-1 IN to aberrantly multimerise as seen in Figure 3.9. Christ *et al* utilised an AlphaScreen assay to determine the multimerisation effects of ALLINIs on HIV-1 IN subtype B (Christ *et al*., 2012). In their study they determined IC_{50} values for each of their compounds showing improvement in each change in structure. The IC_{50} values were found to be 1,134 ± 63 nM, 309 ± 118 nM and 123 ± 1 nM for CX05168, CX05045 and CX14442, respectively.

To determine the stabilisation effects of the compounds on HIV-1 IN we used a differential scanning fluorometry (DSF) assay similar to Christ *et al* (Christ *et al*., 2012). We were able to monitor the melting temperature of the protein in the absence and presence of the compounds and determine if the compounds have any stabilising effects. If the compounds stabilised the HIV-1 IN-IN subunit interactions the melting temperature would increase as described by Christ *et al*. If the compound had no effect or destabilised the protein either no change in melting temperature or decrease in melting temperature would be seen. When the recombinant HIV-1 IN was incubated with DMSO in the absence of compound the melting temperature was approximately 45°C and 42°C for subtype B and C HIV-1 IN, respectively. As expected from our previous experiments, when lovastatin and cefdinir were added no change in melting temperature was seen, even when we increased the compound concentration to 30 µM. This was the case for both subtype B and C HIV-1 IN (Figures 3.10A and 3.10B). The results for lovastatin and cefdinir are similar to those of Kessl et al

where RAL shows no effect on the melting temperature of the complex but it is known to bind to HIV-1 IN By contrast, an increase in meting temperature was noted with CX05168 incubated with HIV-1 IN subtype B and C, with a 9.9°C increase from 45°C to 54.9°C, and an increase of 8.1°C from 42°C to 50.1°C, respectively. This confirms the stabilising effects that CX05168 has on the HIV-1 IN-IN interaction. This is also the first experiment where we see a slight difference in the effects of CX05168 between these two subtypes where it appears to have a slightly more stabilising effect on subtype B than C HIV-1 IN.

4.3 Allosteric integrase inhibitors induce distinct effects on the HIV-1 IN CCD

In 2005, Cherepanov and co-workers published the crystallographic data for the interaction of the HIV-1 IN CCD dimer and LEDGF/p75 (Cherepanov et al., 2005). This data was invaluable in determining the exact interaction points between the proteins and has enabled researchers to develop small molecules to inhibit or abolish the interaction.

The crystal structure shows a CCD dimer interface and a pair of LEDGF/p75 proteins that bind at the CCD-CCD interface (Figure 1.9). When determining which amino acids are important for the interaction, the crystal structure shows that the Ile 360 from LEDGF/p75 projects into a hydrophobic pocket made up of Leu102, Ala128, Ala129 and Trp132 of HIV-1 IN chain B and Thr174 and Met178 of HIV-1 IN chain A. Amino acids Phe406 and Val408 obstruct the solvent from accessing the Trp131 of the HIV-1 IN chain B. It was found that the amino acid Asp366 of LEDGF/p75, which creates a hydrogen bond with the main chain amide of Glu170 and His171 in IN chain A, is crucial for the binding of HIV-1 IN and LEDGF/p75 (Cherepanov et al., 2005). If a mutation takes place here, the HIV-1 IN-LEDGF/p75 interaction is completely abolished. The backbone amide group of Ile365 forms a hydrogen bond with the backbone carbonyl group of Gln168 in chain A and Thr125 in chain B of HIV-1 IN. Several publications of mutational studies have identified crucial amino acids to the functioning of ALLINIs, and these are discussed below, where relevant.

Molecular modelling was conducted on all three compounds with the use of BIOVIA Discovery Studio 4.0 package. The CCD dimer-dimer interaction with LEDGF/p75 protein data bank code 2B4J was prepared and enabled us to predict the interacting amino acids for each compound. It also enabled us to gauge the tightness of the fit with use of the CDOCKER energy scores. The modelling findings for CX01568 (Figure 3.11A) found that the carboxylic acid group formed hydrogen bonds with His171 and Thr174, correlating with the crystallographic data for CX05168 (Christ *et al*., 2010), confirming the accuracy of the

model. The phenyl ring showed hydrophobic interactions with Gln95, Ala128 and Ala129. The chlorine atom was predicted to occupy the hydrophobic pocket formed by Trp131 and Trp132. CX05168 was found to have a CDOCKER energy of -18.55 kcal/mol (Table 3.1). The more negative a CDOCKER energy is found to be, the tighter the bind is. The correlation of the molecular modelling findings and the crystallographic data for CX05168 gave us confidence in our model. During the molecular modelling studies common amino acid linkages across all 3 inhibitors were found to be Ala128, Ala129, His171 and Thr174. Overall, the model predicted that CX05168 is the best binder to integrase, followed by cefdinir and lovastatin with the lowest binding affinity.

Amide hydrogen exchange with deuterated water has been found to be a practical tool in determining protein structure (Tadeo *et al*., 2007). Nuclear Magnetic Resonance (NMR) has been used coupled with hydrogen exchange for short protein chains to measure the proton exchange (Tadeo *et al*., 2007). Hydrogen exchange coupled with mass spectroscopy allows for the study of larger proteins. Hydrogen exchange requires relatively low amounts of proteins, it is also well suited to those proteins that are difficult to crystalize (Mondal *et al.*, 2016). When analysing the data obtained from hydrogen exchange careful consideration is needed due to the fact that the exchange rate can be altered not only by steric shielding but also by allosteric conformational changes (Konermann *et al*., 2014). Another point to be considered is the possibility of increases in exchange in some areas due to binding (Sowole and Konermann, 2014). Hydrogen exchange is well suited for the discovery and analysis of allosteric inhibitors. Hydrogen exchange was previously used to determine the long range conformational changed of the Hep C viral RNA dependent RNA polymerase when inhibitors were introduced (Deredge *et al*., 2016). It was also used to determine the ligand binding on estrogen receptor alpha that allowed for mechanistic insights and further confirmed results obtained from crystallography (Srinivasan *et al*., 2017). Hydrogen exchange was also used to determine the binding sites of ligands to IL-17A 2 which showed a destabilization of the α-helical region which further explained why the authors could not co-crystallise IL-17A with the ligand (Espada *et al*., 2016).

When comparing the molecular modelling findings with our hydrogen exchange data, as seen in Figure 3.13A, Gln95 exchange is drastically reduced in contrast to high exchanges without CX05168. Ala128, Ala129 show moderate exchange, and these amino acids do not directly bind with CX05168, as CX05168 sits against these amino acids, however this area was not available for exchange in the Apo protein thereby indicating a structural change that allows this area to open for exchange upon CX05168 binding. Glu170 and His171 showed drastic reduction in exchange to almost no exchange when treated with CX05168 whereas in the ligand-free protein there was moderate to high exchange, which correlates

with the molecular modelling data. Gln168 has low exchange in contrast to moderate to high exchange in non-treated protein. These findings correlated with the crystallographic data previously reported by Christ *et al* and therefore gave us confidence in our methodology and research findings (Christ *et al.,* 2010). The DDE triad is only affected by a slight structural change from the Apo protetin whereby D64 is unavailable for exchange whereas in the Apo protein there was low exchange and E152 increases to high exchange. Other areas of interest that have reduced exchange in comparison to the Apo protein are Glu29 - Asp41, Asp55 – Leu102. This area contains the first aspartic acid of the DDE triad active site motif showing binding or structural change to part of the catalytic site. Overall, with all the changes taken into account it is clear that there are major structural changes to the protein as a whole upon the addition of CX05168 indicating allosterism.

When HIV-1 IN subtype B was treated with lovastatin (Figure 3.13B), the same coverage was seen as with CX05168, with two exceptions; lovastatin had coverage over Phe181 – Phe224, and Lys273 – Asp288, whereas the CX05168 and Apo protein had no coverage across the two areas. When comparing the hydrogen exchange maps looking at the important LEDGF/p75 interacting amino acids, Glu170 and His171 show shows a slight reduction from in exchange seen in the untreated protein which correlates with the molecular modelling findings. These amino acids have been found to be crucial in the published data for ALLINIs (Christ *et al*., 2010; Christ *et al*., 2012; Kessl *et al*., 2012; Le Rouzic *et al*., 2013; Sharma *et al*., 2014). Hydrogen exchange at Ala128 is below 10%, and in addition Tyr99 – Trp131 has low exchange, these two sites appear to be important for lovastatin binding. The area spanning Ala104 – Asn120 in CX05168 shows high exchange as well as in the Apo protein which is in contrast to lovastatin indicating that for lovastatin this is direct binding or a structural change. Other areas of interest are single amino acid interactions with very low exchange seen at Ala21, Asn27, Asp41 indicating these are direct binding sites. The biggest area of interest is Tyr99 – Trp131 which includes the Asp116 amino acid that forms part of the DDE triad, Tyr99 – Trp131 is completely reduced for exchange indicating a possible structural change preventing deuterium exchange at this point. Based on the hydrogen exchange heat maps it appears that the binding of lovastatin differs from that of CX05168. Overall less reduction in hydrogen exchange was seen for lovastatin, however a large amount of reduction was seen in comparison to the control protein.

Cefdinir binding did not correlate with molecular modelling nor our other findings thus far. The results were markedly different from both CX05168 and lovastatin (Figure 3.13C). Overall, the level of hydrogen exchange reduction was very low, showing little to no binding and the cefdinir heat map appears to mimic the Apo protein, and however there are some

differences. This is possibly due to insufficient inhibitor addition or possibly needed longer deuteration time than the 10 seconds that was used. Interestingly, the amino acids Phe121 – Ala133 have no coverage which is also seen with Ala105-Phe121, which is in contrast to the Apo protein, CX05168 and lovastatin bound HIV-1 IN. Lys103 – Leu104, Phe181 – His183, Ile208 and Phe223 show drastic reduction in exchange when compared to the Apo protein indicating binding sites. None of the key amino acids seem to be affected with cefdinir. The DDE triad is completely unchanged when cefdinir is bound or present according to our HDX data

The unbound (Apo) HIV-1 subtype C IN showed similar deuteration as subtype B. All the important amino acids for LEDGF/p75 interaction were available for analysis with the exception of Trp132. Currently, there is no crystal structure of the HIV-1 subtype C CCD with CX05168, and as such the results are compared with the findings for subtype B. However, so far there have been indications of differences in the stabilising effect of ALLINIs on subtype B and C HIV-1 IN.

When the subtype C HIV-1 IN is treated with CX05168, as seen in Figure 3.16A, there are numerous differences between the Apo protein and the treated protein. Cys40 shows a 30% reduction in exchange as opposed to the Apo protein. This amino acid is in the NTD and is part of the HHCC motif that coordinates the zinc atom for DNA binding. Asp65, the first aspartic acid of the DDE triad active site motif has high exchange in contrast to the low exchange in the Apo protein, indicating this region is then opened up. Arg107-Ala133 shows complete reduction in the hydrogen exchange, which is in contrast to the control protein with the important amino acids of Ala 128 and Ala129 found within this region as well as Asp116 of the DDE triad. Val150 - Gln177 exchange shows a vast reduction in exchange where amino acids at Glu170, His171, Lys173 and Thr174 all show binding by CX05168 in accordance to crystallographic data of subtype B HIV-1 IN. Asn181 – Gly197 and Ala205 - Glu212 both show high exchange in the control protein but very low exchange in treated protein, this indicates that these areas have possibly undergone a structural change causing an isolating of these areas. Overall the binding sites shown by the crystallographic data of HIV-1 subtype B IN with CX05168 also correlate with HIV-1 subtype C IN. Where structural changes in the protein are seen in correlation with allosterism.

Very few changes between subtype B and C were seen when treated with lovastatin, as seen in Figure 16B, with the exception of Ala128 and Ala129 where in subtype B there was little exchange in this area, in subtype C this area has high exchange and may be due to a structural change with the amino acid change of Arg127 to Lys127 in subtype C. This

correlates with the other finding where there was no statistical difference between the subtypes under the influence of lovastatin.

When looking at the cefdinir data, as seen in Figure 16C, the region of Ala124 – Val126 has 50% exchange where the untreated protein has high exchange. This is of interest as amino acid Thr125 is changed to Ala125 in subtype C, this amino acid has been shown to have an effect of the effectiveness of certain ALLINIs where some ALLINIs are unaffected, some have increased potency and others have a reduced potency (Bonnard et al., 2018). When comparing these results with the Alphascreen results containing DNA there was a statistically significant increase in potency of cefdinir against the subtype C assay. It was also seen that Ala38 – Asp41 showed a vast reduction in exchange in comparison to the apo protein and subtype B treated protein with Asp64 lying in this region. The combination of these two changes and the Alphascreen DNA data shows cefdinir has differences in potency against the HIV-1 IN/LEDGF/p75 interaction between subtype B and C specifically when DNA is present.
Looking at the comparison heat exchange map for CX05168 (Figure 3.20A), there are four areas of vast reduction in exchange. These differences in sequence could be the cause of the difference in binding or structure between the two subtypes. Overall, there are quite a number of exchange differences between the two subtypes when treated with CX05168 which backs up the difference seen in the DSF assay where the stabilization of the protein by CX05168 was reduced in the subtype C protein. When comparing lovastatin and cefdinir heat maps little variance is seen between the subtype with exception to cefdinir that has been explained above.

Overall, when comparing subtype B and C HIV-1 IN data the largest variance is found with binding to CX05168, and this variance appears to be due to some of the amino acid sequence differences found between the subtypes.

4.4 The enzyme kinetics of HIV-1 IN when treated with CX05168

SPR has been used to determine binding kinetics of ligand and protein for many years. SPR allows us to monitor the rate at which a compound/ligand associates with the protein as well as the rate at which it dissociates from the protein. These values allow us to then calculate a K_D value for the interaction of protein with compound/ligand. Currently, there is no published kinetic data available for IN binding to CX05168. We were only able to obtain binding curves for CX05168 (Figure 3.21A and Figure 3.21B for subtype B and C HIV-1 IN, respectively), since when testing lovastatin and cefdinir the noise to binding response was too high for accurate readings - an indication of the low binding affinity for these compounds.

This is backed up by the molecular modelling for lovastatin as well as the hydrogen exchange for cefdinir, once again a much higher concentration is possibly needed to determine accurate binding. For fitting purposes we used the Langmuir method. For CX05168 -subtype B HIV-1 IN, the chi square values were outside of the desired 10% range of the RU MAX, however we still considered these fittings to be acceptable. For subtype B HIV-1 IN, the CX05168 K_D was then determined by dividing the association reaction by the dissociation reaction and was found to be between 4.19 x 10^{-6} M and 5.12 x 10^{-6} M (Table 3.2), which is within the range of the determined IC_{50} values for our subtype B AlphaScreen assay. The chi squared for subtype C IN- CX05168 were all within the desired 10% range of the RU max indicating a good fit. The rate at which CX05168 bound to HIV-1 IN subtype C was found to be between 2.66 x 10^4 Ms^{-1} and 4.05 x 10^4 Ms^{-1}. The rate at which CX05168 dissociates from HIV-1 IN subtype C was determined to be between 4.73 x 10^{-5} s^{-1} and 5.19 x 10^{-5} s^{-1}. This allowed for the K_D to be determined and was found to be between 1.25 x 10^{-5} and 1.78 x 10^{-5} M which is quite different from the IC_{50} values determined in our AlphaScreen assay, however they correlate with the HXD data that showed reduced binding for subtype C IN. Overall, when looking at the HXD data and the SPR data there appears to be a reduction in the binding of CX05168 to HIV-1 subtype C IN in accordance to our findings in the DSF assay. Our inability to obtain SPR data for lovastatin and cefdinir is perhaps an indication that the compounds bind with less affinity to HIV-1 IN which is also in accordance with findings made in the molecular modelling and HDX.

4. 5 Cytotoxic and antiviral effects of CX05168, lovastatin and cefdinir

Cellular studies of ALLINIs have shown the inhibition of HIV-1 replication through the integration step and that the most potent effects are found in the later phases of the HIV-1 replication cycle (Christ *et al*., 2012; Le Rouzic *et al*., 2013). The ALLINI compounds cause HIV-1 IN to multimerize internally which results in defective particle maturation (Christ *et al*., 2012; Le Rouzic *et al.*, 2013). The resultant progeny virus is then immature and is defective for second round infection (Christ *et al.*, 2012; Le Rouzic *et al*., 2013).

Cytotoxic testing is important to see how the test compounds affect mammalian cell lines but is also very important to determine that any antiviral effects of the compound are wholly due to the compounds effect on the virus and not due to cell death. All compounds were tested in a dose response manner ranging from 200 µM to 0.3 µM.

In a previous study, lovastatin was found to be extremely toxic during *in vitro* studies - we confirmed these results, as well as conducting antiviral testing against both subtype B and

C viruses (Harrison *et al*., 2014). In agreement with previous findings, the CC_{50} values for lovastatin was found to be highly toxic in MT-4 cells (Table 3.3). Thus, the cellular toxicity of lovastatin prevented us from pursuing further cellular studies.

CX05168 is well documented for cytotoxicity and viral inhibition data (Christ *et al.*, 2010; Christ *et al*., 2012). In our experiment the CC_{50} data was found to be 69.56 ± 1.39 µM and the EC_{50} for subtype B to be 1.85 ±0.69 µM in agreement with previously published data (Harrison *et al.*, 2014). By contrast, the EC_{50} for HIV-1 subtype C IN was 3.65 ± 0.39 µM, which correlates with our other findings where CX05168 does not appear to be as effective against HIV-1 subtype C.

For cefdinir we have no previous data for comparison. In the current study, we found cefdinir to be non-toxic at levels up to 200 µM. In the antiviral assay, cefdinir had an EC_{50} of 45.29 ± 10.30 µM against HIV-1 subtype B and 52.62 ± 7.62 µM against HIV-1 subtype C which is the opposite of the Alphascreen assay with DNA as cefdinir was more potent with the subtype C assay, however this finding is backed up by the hydrogen exchange data. However, cefdinir proved to be problematic in the antiviral assays, as seen by the large standard error values, the effects of cefdinir varied extensively, where some assay showed no inhibition. The results reported here are from 12 independent experiments and two statistical duplicates. Results correlate with the SPR data, which showed that cefdinir is a poor binder, and this is likely attributed to a lack of specificity or the compound has solubility issues.

Following the results of the antiviral assays, we decided to perform a TOA assay to see where CX05168 and cefdinir elicit their antiviral effect. There is no TOA data available for CX05168 but there is TOA data for the structurally improved compound CX14442 (Christ *et al*., 2012). Mohammadi *et al.* (2013) did a time study for each phase of the viral lifecycle to determine what steps in the replication process were occurring at what time point post entry. It was found that early reverse transcription occurred from 3 hours until 22 hours, and late reverse transcription occurred from 5 hours until approximately 14 hours. The LTRs formed from a 7 hour point until the end of the 24 hours cycle with integration starting from hour 8 and was estimated to go up to hour 34. Finally, new virion release was evident from 18 hours post infection (Mohammadi et al., 2013). During our tests CX05168 displayed a similar pattern (Figure 3.22A and 3.22B) as the published data for the improved compound CX14442 (Christ *et al*., 2012). The compound exhibited an inhibitory effect on the virus until approximately 10 hours post infection, and then viral replication was evident when compound was added after 10 hours of infection, in line with what is expected with an

integrase inhibitor. Once again with cefdinir we did not obtain consistent results (6 independent experiments with two statistical duplicates) likely due to poor binding or solubility problems. Nonetheless results show inhibition at two hours post infection, relating to early inhibition of the reverse transcription step. A slight increase in viral replication is seen when compound is added at four hours post infection, and then an increase in viral replication is noted between 4-9 hours, relating to the end of the reverse transcription step. This is followed by no/low viral replication when compound was added at 10 hours post infection, correlating to the beginning phases of integration. The virus is then fully replicative when compound was added at 11 hours post infection. This trend was consistent for both subtypes and is indicative of a reverse transcriptase inhibitor. Overall, from the data we can conclude that CX05168 behaves as a traditional ALLINI whereas cefdinir appears to behave as a reverse transcriptase inhibitor. Lovastatin could not be studied further.

4.6 Conclusion

The known ALLINI CX05168 showed inhibition of the HIV-1 IN/LEDGF/p75 interaction in both the assay including cDNA and the one without, however a marked difference in inhibitory effect was seen in the presence of cDNA. The slope of the curve indicates aggregation or promiscuous binding but us a potent inhibitor and full agonist. CX05168 shows moderate strand transfer activity inhibition in contrast to published literature. This is due to the order of addition of components in the assay used. Where if DNA is present prior to the addition of inhibitor the effects of the inhibitor are vastly reduced. It was clear that CX05168 cause aberrant multimerization as seen in the cross linking studies as well as the DLS data and was further confirmed when the DSF data showed the stabilising effects the inhibitor has on the subunit interaction by an increase in melting temperature of the protein. This finding was also backed up by the steepness of the slope in the protein-protein assay which indicated aggregation of protein. It was clear at this point that CX05168 had a reduced effect on the subtype C virus where the increase in melt temperature was not as strong for the subtype C protein. HDX data obtained showed there was a difference in binding between the 2 subtypes confirming the DSF results. SPR results correlated with our AlphaScreen findings and once again corroborated the difference in binding between subtype B and C with CX05168 showing a decrease in binding with the subtype C protein. During the cellular studies it was found that CX05168 does have a decreased inhibitory effect on the subtype C virus and with the TOA data this clearly indicates that CX05168 behaves as a traditional ALLINI in both subtypes.

Lovastatin was unaffected by the presence of cDNA in the AlphaScreen assay and showed good inhibition in both assays. The slope of the curve indicates cooperative binding but a weak inhibitor and partial agonist. No evidence of multimerization effects were seen in both assay and this was confirmed in the DSF assay where no increase in melting temperature was seen in either subtype. Some differences were seen in the HDX data between the subtype B and C but overall the binding was similar. However the binding areas were different between lovastatin and CX05168 where definite binding can be seen by lovastatin but there are less structural changes in the protein. SPR data was non-conclusive as the noise ratio was too high to differentiate the protein inhibitor complex this confirms the findings of the molecular modelling indicating that lovastatin was a weak binder. Cellular data could not be obtained due to the high toxicity of lovastatin and therefore the conclusions we can draw are based on few experiments. Lovastatin acts as a cooperative binder to HIV-1 IN disrupting the HIV-1 IN-LEGDF/p75 interaction with no effects on multimerization. No large differences are seen between the 2 subtypes studied.

Cefdinir showed a decrease in inhibitory effect in the Alphascreen with DNA present the same as CX05168. This slope indicates aggregation or promiscuous binding but is seen as a potent inhibitor but partial agonist. A difference in subtype B and C was seen where cefdinir was more potent against the subtype C protein. However in contrast to CX05168 no effects on multimerisation or stabilisation could be seen in either subtypes. Hydrogen exchange data showed very few spots of contact between cefdinir and the protein however binding areas were seen but no structural changes were evident. Of interest was the reduction in exchange where Thr125 lies specifically with the subtype C protein. This area has been indicated in potency effects of various ALLINIs. In the subtype C protein position 125 is alanine, this change in amino acid appears to make cefdinir more potent in the subtype C virus where more binding areas can be seen in the HDX data between subtype B and C. The SPR data confirms the poor binding seen in the HXD data where it was not possible to obtain SPR data for cefdinir. Cellular experiments highlighted a possible solubility problem with cefdinir which may explain the poor binding found in HDX and SPR experiments. Several rounds of viral assays were conducted to conclude that cefdinir has antiviral effects but less potent with the subtype C virus than with the subtype B virus which is in contract to the protein studies. The TOA data indicates that cefdinir is a reverse transcriptase inhibitor. Overall, it can be concluded that cefdinir inhibits the HIV-1 IN-LEDGF/p75 interaction with no effects on stability or multimerization and behaves as a reverse transcriptase inhibitor in the TOA experiments opening the possibility of a dual inhibitor, effecting both integrase and reverse transcriptase.

Future work could focus on the development of second and third generation compounds from lovastatin and cefdinir as they show promise in their respective results. Investigation into the reverse transcriptase activity of cefdinir as well as TEM experiments to determine if the compounds show any effects on virion maturation as is seen with ALLINI compounds that exact a potent antiviral effect (Le Rouzic *et al*., 2013; Sharma *et al.*, 2014; Kessl *et al*., 2016a).

Overall, results from this study confirm that all three compounds (CX01568, lovastatin and cefdinir), affect HIV-1 IN activity differently. CX05168 by typical ALLINI function, lovastatin by direct inhibition of the HIV-1 IN-LEDGF/p75 interaction and cefdinir by disrupting the HIV-1 IN-LEDGF/p75 interaction and possible reverse transcriptase activity. The difference seen in this study between the subtype indicate that CX05168 and cefdinir have slightly varied effects on the subtype C virus possibly due to specific amino acid changes.

Chapter 5

5. References

Abrahams, S., Mosebi, S., Fish, M.Q., Papathanasopoulos, M.A., Hewer, R., 2018. Screening of the NIH Clinical Collection for inhibitors of HIV-1 integrase activity. South Afr. J. Sci. 114. https://doi.org/10.17159/sajs.2018/20170324

Agrawal, A., DeSoto, J., Fullagar, J.L., Maddali, K., Rostami, S., Richman, D.D., Pommier, Y., Cohen, S.M., 2012. Probing chelation motifs in HIV integrase inhibitors. Proc. Natl. Acad. Sci. 109, 2251–2256. https://doi.org/10.1073/pnas.1112389109

Al-Mawsawi, L.Q., Al-Safi, R.I., Neamati, N., 2008. Anti-infectives: clinical progress of HIV-1 integrase inhibitors. Expert Opin. Emerg. Drugs 13, 213–225. https://doi.org/10.1517/14728214.13.2.213

Amet, T., Nonaka, M., Dewan, M.Z., Saitoh, Y., Qi, X., Ichinose, S., Yamamoto, N., Yamaoka, S., 2008. Statin-induced inhibition of HIV-1 release from latently infected U1 cells reveals a critical role for protein prenylation in HIV-1 replication. Microbes Infect. 10, 471–480. https://doi.org/10.1016/j.micinf.2008.01.009

Balakrishnan, M., Yant, S.R., Tsai, L., O'Sullivan, C., Bam, R.A., Tsai, A., Niedziela-Majka, A., Stray, K.M., Sakowicz, R., Cihlar, T., 2013. Non-Catalytic Site HIV-1 Integrase Inhibitors Disrupt Core Maturation and Induce a Reverse Transcription Block in Target Cells. PLoS ONE 8, e74163. https://doi.org/10.1371/journal.pone.0074163

Bartholomeeusen, K., Christ, F., Hendrix, J., Rain, J.-C., Emiliani, S., Benarous, R., Debyser, Z., Gijsbers, R., De Rijck, J., 2009. Lens epithelium-derived growth factor/p75 interacts with the transposase-derived DDE domain of PogZ. J. Biol. Chem. 284, 11467–11477. https://doi.org/10.1074/jbc.M807781200

Bartholomeeusen, K., De Rijck, J., Busschots, K., Desender, L., Gijsbers, R., Emiliani, S., Benarous, R., Debyser, Z., Christ, F., 2007. Differential Interaction of HIV-1 Integrase and JPO2 with the C Terminus of LEDGF/p75. J. Mol. Biol. 372, 407–421. https://doi.org/10.1016/j.jmb.2007.06.090

Beese, L.S., Steitz, T.A., 1991. Structural basis for the 3'-5' exonuclease activity of Escherichia coli DNA polymerase I: a two metal ion mechanism. EMBO J. 10, 25–33.

Berg, J.M., Tymoczko, J.L., Stryer, L., 2002. Enzymes Can Be Inhibited by Specific Molecules. Biochem. 5th Ed.

Blanco, J.-L., Varghese, V., Rhee, S.-Y., Gatell, J.M., Shafer, R.W., 2011. HIV-1 integrase inhibitor resistance and its clinical implications. J. Infect. Dis. 203, 1204–1214. https://doi.org/10.1093/infdis/jir025

Bowerman, B., Brown, P.O., Bishop, J.M., Varmus, H.E., 1989. A nucleoprotein complex mediates the integration of retroviral DNA. Genes Dev. 3, 469–478.

Brown, P.O., Bowerman, B., Varmus, H.E., Bishop, J.M., 1987. Correct integration of retroviral DNA in vitro. Cell 49, 347–356.

Bukrinsky, M.I., Sharova, N., McDonald, T.L., Pushkarskaya, T., Tarpley, W.G., Stevenson, M., 1993. Association of integrase, matrix, and reverse transcriptase antigens of human immunodeficiency virus type 1 with viral nucleic acids following acute infection. Proc. Natl. Acad. Sci. U. S. A. 90, 6125–6129.

Buonaguro, L., Tornesello, M.L., Buonaguro, F.M., 2007. Human Immunodeficiency Virus Type 1 Subtype Distribution in the Worldwide Epidemic: Pathogenetic and Therapeutic Implications. J. Virol. 81, 10209–10219. https://doi.org/10.1128/JVI.00872-07

Burlein, C., Wang, C., Xu, M., Bhatt, T., Stahlhut, M., Ou, Y., Adam, G.C., Heath, J., Klein, D.J., Sanders, J., Narayan, K., Abeywickrema, P., Heo, M.R., Carroll, S.S., Grobler, J.A., Sharma, S., Diamond, T.L., Converso, A., Krosky, D.J., 2017. Discovery of a Distinct Chemical and Mechanistic Class of Allosteric HIV-1 Integrase Inhibitors with Antiretroviral Activity. ACS Chem. Biol. 12, 2858–2865. https://doi.org/10.1021/acschembio.7b00550

Bushman, F.D., Engelman, A., Palmer, I., Wingfield, P., Craigie, R., 1993. Domains of the integrase protein of human immunodeficiency virus type 1 responsible for polynucleotidyl transfer and zinc binding. Proc. Natl. Acad. Sci. U. S. A. 90, 3428–3432.

Bushman, F.D., Fujiwara, T., Craigie, R., 1990. Retroviral DNA integration directed by HIV integration protein in vitro. Science 249, 1555–1558.

Busschots, K., Vercammen, J., Emiliani, S., Benarous, R., Engelborghs, Y., Christ, F., Debyser, Z., 2005. The interaction of LEDGF/p75 with integrase is lentivirus-specific and promotes DNA binding. J. Biol. Chem. 280, 17841–17847. https://doi.org/10.1074/jbc.M411681200

Busschots, K., Voet, A., De Maeyer, M., Rain, J.-C., Emiliani, S., Benarous, R., Desender, L., Debyser, Z., Christ, F., 2007. Identification of the LEDGF/p75 Binding Site in HIV-1 Integrase. J. Mol. Biol. 365, 1480–1492. https://doi.org/10.1016/j.jmb.2006.10.094

Cai, M., Zheng, R., Caffrey, M., Craigie, R., Clore, G.M., Gronenborn, A.M., 1997. Solution structure of the N-terminal zinc binding domain of HIV-1 integrase. Nat. Struct. Biol. 4, 567–577.

Chen, J.C., Krucinski, J., Miercke, L.J., Finer-Moore, J.S., Tang, A.H., Leavitt, A.D., Stroud, R.M., 2000. Crystal structure of the HIV-1 integrase catalytic core and C-terminal domains: a model for viral DNA binding. Proc. Natl. Acad. Sci. U. S. A. 97, 8233–8238. https://doi.org/10.1073/pnas.150220297

Cherepanov, P., Ambrosio, A.L.B., Rahman, S., Ellenberger, T., Engelman, A., 2005a. Structural basis for the recognition between HIV-1 integrase and transcriptional coactivator p75. Proc. Natl. Acad. Sci. U. S. A. 102, 17308–17313. https://doi.org/10.1073/pnas.0506924102

Cherepanov, P., Devroe, E., Silver, P.A., Engelman, A., 2004. Identification of an evolutionarily conserved domain in human lens epithelium-derived growth factor/transcriptional co-activator p75 (LEDGF/p75) that binds HIV-1 integrase. J. Biol. Chem. 279, 48883–48892. https://doi.org/10.1074/jbc.M406307200

Cherepanov, P., Maertens, G., Proost, P., Devreese, B., Van Beeumen, J., Engelborghs, Y., De Clercq, E., Debyser, Z., 2003. HIV-1 integrase forms stable tetramers and associates with LEDGF/p75 protein in human cells. J. Biol. Chem. 278, 372–381. https://doi.org/10.1074/jbc.M209278200

Cherepanov, P., Sun, Z.-Y.J., Rahman, S., Maertens, G., Wagner, G., Engelman, A., 2005b. Solution structure of the HIV-1 integrase-binding domain in LEDGF/p75. Nat. Struct. 38 Mol. Biol. 12, 526–532. https://doi.org/10.1038/nsmb937

Choe, H., Farzan, M., Sun, Y., Sullivan, N., Rollins, B., Ponath, P.D., Wu, L., Mackay, C.R., LaRosa, G., Newman, W., Gerard, N., Gerard, C., Sodroski, J., 1996. The beta-chemokine receptors CCR3 and CCR5 facilitate infection by primary HIV-1 isolates. Cell 85, 1135–1148.

Christ, F., Shaw, S., Demeulemeester, J., Desimmie, B.A., Marchand, A., Butler, S., Smets, W., Chaltin, P., Westby, M., Debyser, Z., Pickford, C., 2012. Small-Molecule Inhibitors of the LEDGF/p75 Binding Site of Integrase Block HIV Replication and Modulate Integrase Multimerization. Antimicrob. Agents Chemother. 56, 4365–4374. https://doi.org/10.1128/AAC.00717-12

Christ, Frauke, Shaw, S., Demeulemeester, J., Desimmie, B.A., Marchand, A., Butler, S., Smets, W., Chaltin, P., Westby, M., Debyser, Z., Pickford, C., 2012. Small-molecule inhibitors of the LEDGF/p75 binding site of integrase block HIV replication and modulate integrase multimerization. Antimicrob. Agents Chemother. 56, 4365–4374. https://doi.org/10.1128/AAC.00717-12

Christ, F., Voet, A., Marchand, A., Nicolet, S., Desimmie, B.A., Marchand, D., Bardiot, D., Van der Veken, N.J., Van Remoortel, B., Strelkov, S.V., De Maeyer, M., Chaltin, P., Debyser, Z., 2010a. Rational design of small-molecule inhibitors of the LEDGF/p75-integrase interaction and HIV replication. Nat. Chem. Biol. 6, 442–448. https://doi.org/10.1038/nchembio.370

Christ, F., Voet, A., Marchand, A., Nicolet, S., Desimmie, B.A., Marchand, D., Bardiot, D., Van der Veken, N.J., Van Remoortel, B., Strelkov, S.V., De Maeyer, M., Chaltin, P., Debyser, Z., 2010b. Rational design of small-molecule inhibitors of the LEDGF/p75-

integrase interaction and HIV replication. Nat. Chem. Biol. 6, 442–448. https://doi.org/10.1038/nchembio.370

Cocohoba, J., Dong, B.J., 2008. Raltegravir: The first HIV integrase inhibitor. Clin. Ther. 30, 1747–1765. https://doi.org/10.1016/j.clinthera.2008.10.012

Craigie, R., 2001. HIV integrase, a brief overview from chemistry to therapeutics. J. Biol. Chem. 276, 23213–23216. https://doi.org/10.1074/jbc.R100027200

del Real, G., Jiménez-Baranda, S., Mira, E., Lacalle, R.A., Lucas, P., Gómez-Moutón, C., Alegret, M., Peña, J.M., Rodríguez-Zapata, M., Alvarez-Mon, M., Martínez-A., C., Mañes, S., 2004. Statins Inhibit HIV-1 Infection by Down-regulating Rho Activity. J. Exp. Med. 200, 541–547. https://doi.org/10.1084/jem.20040061

Delelis, O., Carayon, K., Saïb, A., Deprez, E., Mouscadet, J.-F., 2008. Integrase and integration: biochemical activities of HIV-1 integrase. Retrovirology 5, 114. https://doi.org/10.1186/1742-4690-5-114

Deng, H., Liu, R., Ellmeier, W., Choe, S., Unutmaz, D., Burkhart, M., Di Marzio, P., Marmon, S., Sutton, R.E., Hill, C.M., Davis, C.B., Peiper, S.C., Schall, T.J., Littman, D.R., Landau, N.R., 1996. Identification of a major co-receptor for primary isolates of HIV-1. Nature 381, 661–666. https://doi.org/10.1038/381661a0

Deng, N., Hoyte, A., Mansour, Y.E., Mohamed, M.S., Fuchs, J.R., Engelman, A.N., Kvaratskhelia, M., Levy, R., 2016. Allosteric HIV-1 integrase inhibitors promote aberrant protein multimerization by directly mediating inter-subunit interactions: Structural and thermodynamic modeling studies. Protein Sci. n/a-n/a. https://doi.org/10.1002/pro.2997

Deprez, E., Barbe, S., Kolaski, M., Leh, H., Zouhiri, F., Auclair, C., Brochon, J.-C., Le Bret, M., Mouscadet, J.-F., 2004. Mechanism of HIV-1 integrase inhibition by styrylquinoline derivatives in vitro. Mol. Pharmacol. 65, 85–98. https://doi.org/10.1124/mol.65.1.85

Deredge, D., Li, J., Johnson, K.A., Wintrode, P.L., 2016. Hydrogen/Deuterium Exchange Kinetics Demonstrate Long Range Allosteric Effects of Thumb Site 2 Inhibitors of Hepatitis C Viral RNA-dependent RNA Polymerase. J. Biol. Chem. 291, 10078–10088. https://doi.org/10.1074/jbc.M115.708370

Devroe, E., 2003. Intracellular transport of human immunodeficiency virus type 1 integrase. J. Cell Sci. 116, 4401–4408. https://doi.org/10.1242/jcs.00747

Dragic, T., Litwin, V., Allaway, G.P., Martin, S.R., Huang, Y., Nagashima, K.A., Cayanan, C., Maddon, P.J., Koup, R.A., Moore, J.P., Paxton, W.A., 1996. HIV-1 entry into CD4+ cells is mediated by the chemokine receptor CC-CKR-5. Nature 381, 667–673. https://doi.org/10.1038/381667a0

Dyda, F., Hickman, A.B., Jenkins, T.M., Engelman, A., Craigie, R., Davies, D.R., 1994. Crystal structure of the catalytic domain of HIV-1 integrase: similarity to other polynucleotidyl transferases. Science 266, 1981–1986.

Eijkelenboom, A.P., Lutzke, R.A., Boelens, R., Plasterk, R.H., Kaptein, R., Hård, K., 1995. The DNA-binding domain of HIV-1 integrase has an SH3-like fold. Nat. Struct. Biol. 2, 807–810.

Eijkelenboom, A.P., van den Ent, F.M., Vos, A., Doreleijers, J.F., Hård, K., Tullius, T.D., Plasterk, R.H., Kaptein, R., Boelens, R., 1997. The solution structure of the amino-terminal HHCC domain of HIV-2 integrase: a three-helix bundle stabilized by zinc. Curr. Biol. CB 7, 739–746.

Engelman, A., Mizuuchi, K., Craigie, R., 1991. HIV-1 DNA integration: mechanism of viral DNA cleavage and DNA strand transfer. Cell 67, 1211–1221.

Espada, A., Broughton, H., Jones, S., Chalmers, M.J., Dodge, J.A., 2016. A Binding Site on IL-17A for Inhibitory Macrocycles Revealed by Hydrogen/Deuterium Exchange Mass Spectrometry. J. Med. Chem. 59, 2255–2260. https://doi.org/10.1021/acs.jmedchem.5b01693

Esposito, D., Craigie, R., 1998. Sequence specificity of viral end DNA binding by HIV-1 integrase reveals critical regions for protein–DNA interaction. EMBO J. 17, 5832–5843.

Fader, L.D., Carson, R., Morin, S., Bilodeau, F., Chabot, C., Halmos, T., Bailey, M.D., Kawai, S.H., Coulombe, R., Laplante, S., Mekhssian, K., Jakalian, A., Garneau, M., Duan, J., Mason, S.W., Simoneau, B., Fenwick, C., Tsantrizos, Y., Yoakim, C., 2014a. Minimizing the Contribution of Enterohepatic Recirculation to Clearance in Rat for the NCINI Class of Inhibitors of HIV. ACS Med. Chem. Lett. 5, 711–716. https://doi.org/10.1021/ml500110j

Fader, L.D., Malenfant, E., Parisien, M., Carson, R., Bilodeau, F., Landry, S., Pesant, M., Brochu, C., Morin, S., Chabot, C., Halmos, T., Bousquet, Y., Bailey, M.D., Kawai, S.H., Coulombe, R., LaPlante, S., Jakalian, A., Bhardwaj, P.K., Wernic, D., Schroeder, P., Amad, M., Edwards, P., Garneau, M., Duan, J., Cordingley, M., Bethell, R., Mason, S.W., Bös, M., Bonneau, P., Poupart, M.-A., Faucher, A.-M., Simoneau, B., Fenwick, C., Yoakim, C., Tsantrizos, Y., 2014b. Discovery of BI 224436, a Noncatalytic Site Integrase Inhibitor (NCINI) of HIV-1. ACS Med. Chem. Lett. 5, 422–427. https://doi.org/10.1021/ml500002n

Fenwick, C., Amad, M., Bailey, M.D., Bethell, R., Bos, M., Bonneau, P., Cordingley, M., Coulombe, R., Duan, J., Edwards, P., Fader, L.D., Faucher, A.-M., Garneau, M., Jakalian, A., Kawai, S., Lamorte, L., LaPlante, S., Luo, L., Mason, S., Poupart, M.-A., Rioux, N., Schroeder, P., Simoneau, B., Tremblay, S., Tsantrizos, Y., Witvrouw,

M., Yoakim, C., 2014. Preclinical Profile of BI 224436, a Novel HIV-1 Non-Catalytic-Site Integrase Inhibitor. Antimicrob. Agents Chemother. 58, 3233–3244. https://doi.org/10.1128/AAC.02719-13

Fitzkee, N.C., Torchia, D.A., Bax, A., 2011. Measuring rapid hydrogen exchange in the homodimeric 36 kDa HIV-1 integrase catalytic core domain. Protein Sci. Publ. Protein Soc. 20, 500–512. https://doi.org/10.1002/pro.582

Fouchier, R.A., Malim, M.H., 1999. Nuclear import of human immunodeficiency virus type-1 preintegration complexes. Adv. Virus Res. 52, 275–299.

Fujiwara, T., Mizuuchi, K., 1988. Retroviral DNA integration: structure of an integration intermediate. Cell 54, 497–504.

Gallay, P., Hope, T., Chin, D., Trono, D., 1997. HIV-1 infection of nondividing cells through the recognition of integrase by the importin/karyopherin pathway. Proc. Natl. Acad. Sci. U. S. A. 94, 9825–9830.

Ganesan, A., Crum-Cianflone, N., Higgins, J., Qin, J., Rehm, C., Metcalf, J., Brandt, C., Vita, J., Decker, C.F., Sklar, P., Bavaro, M., Tasker, S., Follmann, D., Maldarelli, F., 2011. High Dose Atorvastatin Decreases Cellular Markers of Immune Activation Without Affecting HIV-1 RNA Levels: Results of a Double-blind Randomized Placebo Controlled Clinical Trial. J. Infect. Dis. 203, 756–764. https://doi.org/10.1093/infdis/jiq115

Gao, K., Butler, S.L., Bushman, F., 2001. Human immunodeficiency virus type 1 integrase: arrangement of protein domains in active cDNA complexes. EMBO J. 20, 3565–3576. https://doi.org/10.1093/emboj/20.13.3565

Ge, Hui, Si, Y., Roeder, R.G., 1998. Isolation of cDNAs encoding novel transcription coactivators p52 and p75 reveals an alternate regulatory mechanism of transcriptional activation. EMBO J. 17, 6723–6729. https://doi.org/10.1093/emboj/17.22.6723

Ge, H., Si, Y., Roeder, R.G., 1998. Isolation of cDNAs encoding novel transcription coactivators p52 and p75 reveals an alternate regulatory mechanism of transcriptional activation. EMBO J. 17, 6723–6729. https://doi.org/10.1093/emboj/17.22.6723

Gérard, A., Ségéral, E., Naughtin, M., Abdouni, A., Charmeteau, B., Cheynier, R., Rain, J.-C., Emiliani, S., 2015. The integrase cofactor LEDGF/p75 associates with Iws1 and Spt6 for postintegration silencing of HIV-1 gene expression in latently infected cells. Cell Host Microbe 17, 107–117. https://doi.org/10.1016/j.chom.2014.12.002

Giguère, J.-F., Tremblay, M.J., 2004. Statin Compounds Reduce Human Immunodeficiency Virus Type 1 Replication by Preventing the Interaction between Virion-Associated

Host Intercellular Adhesion Molecule 1 and Its Natural Cell Surface Ligand LFA-1. J. Virol. 78, 12062–12065. https://doi.org/10.1128/JVI.78.21.12062-12065.2004

Goldgur, Y., Dyda, F., Hickman, A.B., Jenkins, T.M., Craigie, R., Davies, D.R., 1998. Three new structures of the core domain of HIV-1 integrase: an active site that binds magnesium. Proc. Natl. Acad. Sci. U. S. A. 95, 9150–9154.

Gu, S.-X., Xue, P., Ju, X.-L., Zhu, Y.-Y., 2016. Advances in rationally designed dual inhibitors of HIV-1 reverse transcriptase and integrase. Bioorg. Med. Chem. 24, 5007–5016. https://doi.org/10.1016/j.bmc.2016.09.025

Gulizia, J., Dempsey, M.P., Sharova, N., Bukrinsky, M.I., Spitz, L., Goldfarb, D., Stevenson, M., 1994. Reduced nuclear import of human immunodeficiency virus type 1 preintegration complexes in the presence of a prototypic nuclear targeting signal. J. Virol. 68, 2021–2025.

Gupta, Kushol, Brady, T., Dyer, B.M., Malani, N., Hwang, Y., Male, F., Nolte, R.T., Wang, L., Velthuisen, E., Jeffrey, J., Van Duyne, G.D., Bushman, F.D., 2014. Allosteric inhibition of human immunodeficiency virus integrase: late block during viral replication and abnormal multimerization involving specific protein domains. J. Biol. Chem. 289, 20477–20488. https://doi.org/10.1074/jbc.M114.551119

Gupta, K., Brady, T., Dyer, B.M., Malani, N., Hwang, Y., Male, F., Nolte, R.T., Wang, L., Velthuisen, E., Jeffrey, J., Van Duyne, G.D., Bushman, F.D., 2014. Allosteric Inhibition of Human Immunodeficiency Virus Integrase: LATE BLOCK DURING VIRAL REPLICATION AND ABNORMAL MULTIMERIZATION INVOLVING SPECIFIC PROTEIN DOMAINS. J. Biol. Chem. 289, 20477–20488. https://doi.org/10.1074/jbc.M114.551119

Gupta, K., Turkki, V., Sherrill-Mix, S., Hwang, Y., Eilers, G., Taylor, L., McDanal, C., Wang, P., Temelkoff, D., Nolte, R.T., Velthuisen, E., Jeffrey, J., Van Duyne, G.D., Bushman, F.D., 2016. Structural Basis for Inhibitor-Induced Aggregation of HIV Integrase. PLoS Biol. 14. https://doi.org/10.1371/journal.pbio.1002584

Hare, S., Cherepanov, P., 2009. The Interaction Between Lentiviral Integrase and LEDGF: Structural and Functional Insights. Viruses 1, 780–801. https://doi.org/10.3390/v1030780

Hare, S., Gupta, S.S., Valkov, E., Engelman, A., Cherepanov, P., 2010a. Retroviral intasome assembly and inhibition of DNA strand transfer. Nature 464, 232–236. https://doi.org/10.1038/nature08784

Hare, S., Nunzio, F.D., Labeja, A., Wang, J., Engelman, A., Cherepanov, P., 2009a. Structural Basis for Functional Tetramerization of Lentiviral Integrase. PLOS Pathog. 5, e1000515. https://doi.org/10.1371/journal.ppat.1000515

Hare, S., Shun, M.-C., Gupta, S.S., Valkov, E., Engelman, A., Cherepanov, P., 2009b. A novel co-crystal structure affords the design of gain-of-function lentiviral integrase mutants in the presence of modified PSIP1/LEDGF/p75. PLoS Pathog. 5, e1000259. https://doi.org/10.1371/journal.ppat.1000259

Hare, S., Vos, A.M., Clayton, R.F., Thuring, J.W., Cummings, M.D., Cherepanov, P., 2010b. Molecular mechanisms of retroviral integrase inhibition and the evolution of viral resistance. Proc. Natl. Acad. Sci. U. S. A. 107, 20057–20062. https://doi.org/10.1073/pnas.1010246107

Harrison, A.T., Kriel, F.H., Papathanasopoulos, M.A., Mosebi, S., Abrahams, S., Hewer, R., 2014. The Evaluation of Statins as Potential Inhibitors of the LEDGF/p75-HIV-1 Integrase interaction. Chem. Biol. Drug Des. https://doi.org/10.1111/cbdd.12384

Hazuda, D.J., 2012. HIV integrase as a target for antiretroviral therapy. Curr. Opin. HIV AIDS 7, 383–389. https://doi.org/10.1097/COH.0b013e3283567309

Hazuda, D.J., Felock, P., Witmer, M., Wolfe, A., Stillmock, K., Grobler, J.A., Espeseth, A., Gabryelski, L., Schleif, W., Blau, C., Miller, M.D., 2000. Inhibitors of Strand Transfer That Prevent Integration and Inhibit HIV-1 Replication in Cells. Science 287, 646–650. https://doi.org/10.1126/science.287.5453.646

Hemelaar, J., 2012. The origin and diversity of the HIV-1 pandemic. Trends Mol. Med. 18, 182–192. https://doi.org/10.1016/j.molmed.2011.12.001

Henrich, T.J., Kuritzkes, D.R., 2013. HIV-1 entry inhibitors: recent development and clinical use. Curr. Opin. Virol. 3, 51–57. https://doi.org/10.1016/j.coviro.2012.12.002

Henriquez, D.R., Zhao, C., Zheng, H., Arbildua, J.J., Acevedo, M.L., Roth, M.J., Leon, O., 2013. Crosslinking and mass spectrometry suggest that the isolated NTD domain dimer of Moloney murine leukemia virus integrase adopts a parallel arrangement in solution. BMC Struct. Biol. 13, 14. https://doi.org/10.1186/1472-6807-13-14

Heuer, T.S., Brown, P.O., 1998. Photo-cross-linking studies suggest a model for the architecture of an active human immunodeficiency virus type 1 integrase-DNA complex. Biochemistry 37, 6667–6678. https://doi.org/10.1021/bi972949c

Heuer, T.S., Brown, P.O., 1997. Mapping features of HIV-1 integrase near selected sites on viral and target DNA molecules in an active enzyme-DNA complex by photo-cross-linking. Biochemistry 36, 10655–10665. https://doi.org/10.1021/bi970782h

Hindmarsh, P., Leis, J., 1999. Retroviral DNA Integration. Microbiol. Mol. Biol. Rev. 63, 836–843.

Ho, D.D., Neumann, A.U., Perelson, A.S., Chen, W., Leonard, J.M., Markowitz, M., 1995. Rapid turnover of plasma virions and CD4 lymphocytes in HIV-1 infection. Nature 373, 123–126. https://doi.org/10.1038/373123a0

Hosseini, I., Mac Gabhann, F., 2012. Multi-Scale Modeling of HIV Infection in vitro and APOBEC3G-Based Anti-Retroviral Therapy. PLoS Comput. Biol. 8. https://doi.org/10.1371/journal.pcbi.1002371

Huang, A., Ho, C.S.W., Ponzielli, R., Barsyte-Lovejoy, D., Bouffet, E., Picard, D., Hawkins, C.E., Penn, L.Z., 2005. Identification of a novel c-Myc protein interactor, JPO2, with transforming activity in medulloblastoma cells. Cancer Res. 65, 5607–5619. https://doi.org/10.1158/0008-5472.CAN-05-0500

Hughes, S., Jenkins, V., Dar, M.J., Engelman, A., Cherepanov, P., 2010. Transcriptional Co-activator LEDGF Interacts with Cdc7-Activator of S-phase Kinase (ASK) and Stimulates Its Enzymatic Activity. J. Biol. Chem. 285, 541–554. https://doi.org/10.1074/jbc.M109.036491

Iyengar, S., Hildreth, J.E., Schwartz, D.H., 1998. Actin-dependent receptor colocalization required for human immunodeficiency virus entry into host cells. J. Virol. 72, 5251–5255.

Jain, M.K., Ridker, P.M., 2005. Anti-inflammatory effects of statins: clinical evidence and basic mechanisms. Nat. Rev. Drug Discov. 4, 977–987. https://doi.org/10.1038/nrd1901

Jenkins, T.M., Engelman, A., Ghirlando, R., Craigie, R., 1996. A soluble active mutant of HIV-1 integrase: involvement of both the core and carboxyl-terminal domains in multimerization. J. Biol. Chem. 271, 7712–7718.

Jenkins, T.M., Esposito, D., Engelman, A., Craigie, R., 1997. Critical contacts between HIV-1 integrase and viral DNA identified by structure-based analysis and photo-crosslinking. EMBO J. 16, 6849–6859. https://doi.org/10.1093/emboj/16.22.6849

Johns, B.A., Kawasuji, T., Weatherhead, J.G., Taishi, T., Temelkoff, D.P., Yoshida, H., Akiyama, T., Taoda, Y., Murai, H., Kiyama, R., Fuji, M., Tanimoto, N., Jeffrey, J., Foster, S.A., Yoshinaga, T., Seki, T., Kobayashi, M., Sato, A., Johnson, M.N., Garvey, E.P., Fujiwara, T., 2013. Carbamoyl pyridone HIV-1 integrase inhibitors 3. A diastereomeric approach to chiral nonracemic tricyclic ring systems and the discovery of dolutegravir (S/GSK1349572) and (S/GSK1265744). J. Med. Chem. 56, 5901–5916. https://doi.org/10.1021/jm400645w

Jurado, K.A., Engelman, A., 2013. Multimodal mechanism of action of allosteric HIV-1 integrase inhibitors. Expert Rev. Mol. Med. 15, e14. https://doi.org/10.1017/erm.2013.15

Jurado, K.A., Wang, H., Slaughter, A., Feng, L., Kessl, J.J., Koh, Y., Wang, W., Ballandras-Colas, A., Patel, P.A., Fuchs, J.R., Kvaratskhelia, M., Engelman, A., 2013. Allosteric integrase inhibitor potency is determined through the inhibition of HIV-1 particle

maturation. Proc. Natl. Acad. Sci. 110, 8690–8695. https://doi.org/10.1073/pnas.1300703110

Kessl, J.J., Jena, N., Koh, Y., Taskent-Sezgin, H., Slaughter, A., Feng, L., de Silva, S., Wu, L., Le Grice, S.F.J., Engelman, A., Fuchs, J.R., Kvaratskhelia, M., 2012. Multimode, Cooperative Mechanism of Action of Allosteric HIV-1 Integrase Inhibitors. J. Biol. Chem. 287, 16801–16811. https://doi.org/10.1074/jbc.M112.354373

Kessl, J.J., Kutluay, S.B., Townsend, D., Rebensburg, S., Slaughter, A., Larue, R.C., Shkriabai, N., Bakouche, N., Fuchs, J.R., Bieniasz, P.D., Kvaratskhelia, M., 2016a. HIV-1 Integrase Binds the Viral RNA Genome and Is Essential during Virion Morphogenesis. Cell 166, 1257-1268.e12. https://doi.org/10.1016/j.cell.2016.07.044

Kessl, J.J., Li, M., Ignatov, M., Shkriabai, N., Eidahl, J.O., Feng, L., Musier-Forsyth, K., Craigie, R., Kvaratskhelia, M., 2011. FRET analysis reveals distinct conformations of IN tetramers in the presence of viral DNA or LEDGF/p75. Nucleic Acids Res. 39, 9009–9022. https://doi.org/10.1093/nar/gkr581

Kessl, J.J., Sharma, A., Kvaratskhelia, M., 2016b. Methods for the Analyses of Inhibitor-Induced Aberrant Multimerization of HIV-1 Integrase. Methods Mol. Biol. Clifton NJ 1354, 149–164. https://doi.org/10.1007/978-1-4939-3046-3_10

Konermann, L., Pan, J., Liu, Y.-H., 2011. Hydrogen exchange mass spectrometry for studying protein structure and dynamics. Chem. Soc. Rev. 40, 1224–1234. https://doi.org/10.1039/c0cs00113a

Konermann, L., Rodriguez, A.D., Sowole, M.A., 2014. Type 1 and Type 2 scenarios in hydrogen exchange mass spectrometry studies on protein-ligand complexes. The Analyst 139, 6078–6087. https://doi.org/10.1039/c4an01307g

Krishnan, L., Engelman, A., 2012. Retroviral integrase proteins and HIV-1 DNA integration. J. Biol. Chem. 287, 40858–40866. https://doi.org/10.1074/jbc.R112.397760

la Porte, C.J.L., 2009. Saquinavir, the pioneer antiretroviral protease inhibitor. Expert Opin. Drug Metab. Toxicol. 5, 1313–1322. https://doi.org/10.1517/17425250903273160

Laskey, S.B., Siliciano, R.F., 2014. A mechanistic theory to explain the efficacy of antiretroviral therapy. Nat. Rev. Microbiol. 12, 772–780. https://doi.org/10.1038/nrmicro3351

Lataillade, M., Kozal, M.J., 2006. The hunt for HIV-1 integrase inhibitors. AIDS Patient Care STDs 20, 489–501. https://doi.org/10.1089/apc.2006.20.489

Le Rouzic, E., Bonnard, D., Chasset, S., Bruneau, J.-M., Chevreuil, F., Le Strat, F., Nguyen, J., Beauvoir, R., Amadori, C., Brias, J., Vomscheid, S., Eiler, S., Lévy, N., Delelis, O., Deprez, E., Saïb, A., Zamborlini, A., Emiliani, S., Ruff, M., Ledoussal, B., Moreau, F., Benarous, R., 2013. Dual inhibition of HIV-1 replication by integrase-

LEDGF allosteric inhibitors is predominant at the post-integration stage. Retrovirology 10, 144. https://doi.org/10.1186/1742-4690-10-144

Li, M., Mizuuchi, M., Burke, T.R., Craigie, R., 2006. Retroviral DNA integration: reaction pathway and critical intermediates. EMBO J. 25, 1295–1304. https://doi.org/10.1038/sj.emboj.7601005

Lins, R.D., Straatsma, T.P., Briggs, J.M., 2000. Similarities in the HIV-1 and ASV integrase active sites upon metal cofactor binding. Biopolymers 53, 308–315. https://doi.org/10.1002/(SICI)1097-0282(20000405)53:4<308::AID-BIP3>3.0.CO;2-H

Llano, M., Vanegas, M., Hutchins, N., Thompson, D., Delgado, S., Poeschla, E.M., 2006. Identification and Characterization of the Chromatin-binding Domains of the HIV-1 Integrase Interactor LEDGF/p75. J. Mol. Biol. 360, 760–773. https://doi.org/10.1016/j.jmb.2006.04.073

Lodi, P.J., Ernst, J.A., Kuszewski, J., Hickman, A.B., Engelman, A., Craigie, R., Clore, G.M., Gronenborn, A.M., 1995. Solution Structure of the DNA Binding Domain of HIV-1 Integrase. Biochemistry 34, 9826–9833. https://doi.org/10.1021/bi00031a002

Lutzke, R.A., Plasterk, R.H., 1998. Structure-based mutational analysis of the C-terminal DNA-binding domain of human immunodeficiency virus type 1 integrase: critical residues for protein oligomerization and DNA binding. J. Virol. 72, 4841–4848.

Maertens, G., Cherepanov, P., Debyser, Z., Engelborghs, Y., Engelman, A., 2004. Identification and characterization of a functional nuclear localization signal in the HIV-1 integrase interactor LEDGF/p75. J. Biol. Chem. 279, 33421–33429. https://doi.org/10.1074/jbc.M404700200

Maertens, G.N., Cherepanov, P., Engelman, A., 2006. Transcriptional co-activator p75 binds and tethers the Myc-interacting protein JPO2 to chromatin. J. Cell Sci. 119, 2563–2571. https://doi.org/10.1242/jcs.02995

McKee, C.J., Kessl, J.J., Shkriabai, N., Dar, M.J., Engelman, A., Kvaratskhelia, M., 2008. Dynamic Modulation of HIV-1 Integrase Structure and Function by Cellular Lens Epithelium-derived Growth Factor (LEDGF) Protein. J. Biol. Chem. 283, 31802–31812. https://doi.org/10.1074/jbc.M805843200

Meleddu, R., Distinto, S., Corona, A., Tramontano, E., Bianco, G., Melis, C., Cottiglia, F., Maccioni, E., 2017. Isatin thiazoline hybrids as dual inhibitors of HIV-1 reverse transcriptase. J. Enzyme Inhib. Med. Chem. 32, 130–136. https://doi.org/10.1080/14756366.2016.1238366

Michael, N.L., 1999. Host genetic influences on HIV-1 pathogenesis. Curr. Opin. Immunol. 11, 466–474. https://doi.org/10.1016/S0952-7915(99)80078-8

Mocroft, A., Ledergerber, B., Katlama, C., Kirk, O., Reiss, P., d'Arminio Monforte, A., Knysz, B., Dietrich, M., Phillips, A.N., Lundgren, J.D., EuroSIDA study group, 2003. Decline in the AIDS and death rates in the EuroSIDA study: an observational study. Lancet Lond. Engl. 362, 22–29.

Mohammadi, P., Desfarges, S., Bartha, I., Joos, B., Zangger, N., Muñoz, M., Günthard, H.F., Beerenwinkel, N., Telenti, A., Ciuffi, A., 2013. 24 Hours in the Life of HIV-1 in a T Cell Line. PLOS Pathog. 9, e1003161. https://doi.org/10.1371/journal.ppat.1003161

Mondal, T., Wang, H., DeKoster, G.T., Baban, B., Gross, M.L., Frieden, C., 2016. ApoE: In Vitro Studies of a Small Molecule Effector. Biochemistry 55, 2613–2621. https://doi.org/10.1021/acs.biochem.6b00324

Mondor, I., Ugolini, S., Sattentau, Q.J., 1998. Human immunodeficiency virus type 1 attachment to HeLa CD4 cells is CD4 independent and gp120 dependent and requires cell surface heparans. J. Virol. 72, 3623–3634.

Moulard, M., Lortat-Jacob, H., Mondor, I., Roca, G., Wyatt, R., Sodroski, J., Zhao, L., Olson, W., Kwong, P.D., Sattentau, Q.J., 2000. Selective interactions of polyanions with basic surfaces on human immunodeficiency virus type 1 gp120. J. Virol. 74, 1948–1960.

Murai, M.J., Pollock, J., He, S., Miao, H., Purohit, T., Yokom, A., Hess, J.L., Muntean, A.G., Grembecka, J., Cierpicki, T., 2014. The same site on the integrase-binding domain of lens epithelium-derived growth factor is a therapeutic target for MLL leukemia and HIV. Blood 124, 3730–3737. https://doi.org/10.1182/blood-2014-01-550079

Nabatov, A.A., Pollakis, G., Linnemann, T., Paxton, W.A., de Baar, M.P., 2007. Statins Disrupt CCR5 and RANTES Expression Levels in CD4+ T Lymphocytes In Vitro and Preferentially Decrease Infection of R5 Versus X4 HIV-1. PLoS ONE 2. https://doi.org/10.1371/journal.pone.0000470

Niesen, F.H., Berglund, H., Vedadi, M., 2007. The use of differential scanning fluorimetry to detect ligand interactions that promote protein stability. Nat. Protoc. 2, 2212–2221. https://doi.org/10.1038/nprot.2007.321

Op de Coul, E.L., Prins, M., Cornelissen, M., van der Schoot, A., Boufassa, F., Brettle, R.P., Hernández-Aguado, L., Schiffer, V., McMenamin, J., Rezza, G., Robertson, R., Zangerle, R., Goudsmit, J., Coutinho, R.A., Lukashov, V.V., European and Italian Seroconverter Studies, 2001. Using phylogenetic analysis to trace HIV-1 migration among western European injecting drug users seroconverting from 1984 to 1997. AIDS Lond. Engl. 15, 257–266.

Paneth, A., Frączek, T., Grzegorczyk, A., Janowska, D., Malm, A., Paneth, P., 2017. A Search for Dual Action HIV-1 Reverse Transcriptase, Bacterial RNA Polymerase Inhibitors. Molecules 22, 1808. https://doi.org/10.3390/molecules22111808

Rambaut, A., Posada, D., Crandall, K.A., Holmes, E.C., 2004. The causes and consequences of HIV evolution. Nat. Rev. Genet. 5, 52–61. https://doi.org/10.1038/nrg1246

Roberts, J.D., Bebenek, K., Kunkel, T.A., 1988. The accuracy of reverse transcriptase from HIV-1. Science 242, 1171–1173.

Rosenbloom, D.I.S., Hill, A.L., Rabi, S.A., Siliciano, R.F., Nowak, M.A., 2012. Antiretroviral dynamics determines HIV evolution and predicts therapy outcome. Nat. Med. 18, 1378–1385. https://doi.org/10.1038/nm.2892

Sato, M., Motomura, T., Aramaki, H., Matsuda, T., Yamashita, M., Ito, Y., Kawakami, H., Matsuzaki, Y., Watanabe, W., Yamataka, K., Ikeda, S., Kodama, E., Matsuoka, M., Shinkai, H., 2006. Novel HIV-1 integrase inhibitors derived from quinolone antibiotics. J. Med. Chem. 49, 1506–1508. https://doi.org/10.1021/jm0600139

Sharma, A., Slaughter, A., Jena, N., Feng, L., Kessl, J.J., Fadel, H.J., Malani, N., Male, F., Wu, L., Poeschla, E., Bushman, F.D., Fuchs, J.R., Kvaratskhelia, M., 2014. A New Class of Multimerization Selective Inhibitors of HIV-1 Integrase. PLoS Pathog. 10, e1004171. https://doi.org/10.1371/journal.ppat.1004171

Sharp, P.M., Hahn, B.H., 2011. Origins of HIV and the AIDS pandemic. Cold Spring Harb. Perspect. Med. 1, a006841. https://doi.org/10.1101/cshperspect.a006841

Shen, L., Peterson, S., Sedaghat, A.R., McMahon, M.A., Callender, M., Zhang, H., Zhou, Y., Pitt, E., Anderson, K.S., Acosta, E.P., Siliciano, R.F., 2008. Dose-response curve slope sets class-specific limits on inhibitory potential of anti-HIV drugs. Nat. Med. 14, 762–766. https://doi.org/10.1038/nm1777

Shkriabai, N., Dharmarajan, V., Slaughter, A., Kessl, J.J., Larue, R.C., Feng, L., Fuchs, J.R., Griffin, P.R., Kvaratskhelia, M., 2014. A critical role of the C-terminal segment for allosteric inhibitor-induced aberrant multimerization of HIV-1 integrase. J. Biol. Chem. 289, 26430–26440. https://doi.org/10.1074/jbc.M114.589572

Simon, V., Ho, D.D., Karim, Q.A., 2006. HIV/AIDS epidemiology, pathogenesis, prevention, and treatment. Lancet 368, 489–504. https://doi.org/10.1016/S0140-6736(06)69157-5

Simoneau, B., Amad, M., Bailey, M.D., Bethell, R., Bhardwaj, P., Bilodeau, F., Bonneau, P., Bos, M., Bousquet, Y., Brochu, C., Carson, R., Chabot, C., Cordingley, M., Edwards, P., Duan, J., Fader, L.D., Faucher, A., Fenwick, C., Garneau, M., Halmos, T., Jakalian, A., Kawai, S., Landry, S., LaPlante, S., Malenfant, E., Mason, S., Morin, S., Parisien, M., Pesant, M., Poupart, M.-A., Tsantrizos, Y., Wernic, D., Yoakim, C.,

Coulombe, R., 2011. Identification of novel non-catalytic site integrase inhibitors (NCINIs)of LTR DNA 3' processing. Presented at the International The 24th International Conference on Antiviral Research (ICAR).

Singh, D.P., Ohguro, N., Chylack, L.T., Shinohara, T., 1999. Lens epithelium-derived growth factor: increased resistance to thermal and oxidative stresses. Invest. Ophthalmol. Vis. Sci. 40, 1444–1451.

Sluis-Cremer, N., Temiz, N.A., Bahar, I., 2004. Conformational Changes in HIV-1 Reverse Transcriptase Induced by Nonnucleoside Reverse Transcriptase Inhibitor Binding. Curr. HIV Res. 2, 323–332.

Sowole, M.A., Konermann, L., 2014. Effects of protein-ligand interactions on hydrogen/deuterium exchange kinetics: canonical and noncanonical scenarios. Anal. Chem. 86, 6715–6722. https://doi.org/10.1021/ac501849n

Srinivasan, S., Nwachukwu, J.C., Bruno, N.E., Dharmarajan, V., Goswami, D., Kastrati, I., Novick, S., Nowak, J., Cavett, V., Zhou, H.-B., Boonmuen, N., Zhao, Y., Min, J., Frasor, J., Katzenellenbogen, B.S., Griffin, P.R., Katzenellenbogen, J.A., Nettles, K.W., 2017. Full antagonism of the estrogen receptor without a prototypical ligand side chain. Nat. Chem. Biol. 13, 111–118. https://doi.org/10.1038/nchembio.2236

Stetefeld, J., McKenna, S.A., Patel, T.R., 2016. Dynamic light scattering: a practical guide and applications in biomedical sciences. Biophys. Rev. 8, 409–427. https://doi.org/10.1007/s12551-016-0218-6

Summa, V., Petrocchi, A., Bonelli, F., Crescenzi, B., Donghi, M., Ferrara, M., Fiore, F., Gardelli, C., Gonzalez Paz, O., Hazuda, D.J., Jones, P., Kinzel, O., Laufer, R., Monteagudo, E., Muraglia, E., Nizi, E., Orvieto, F., Pace, P., Pescatore, G., Scarpelli, R., Stillmock, K., Witmer, M.V., Rowley, M., 2008. Discovery of raltegravir, a potent, selective orally bioavailable HIV-integrase inhibitor for the treatment of HIV-AIDS infection. J. Med. Chem. 51, 5843–5855. https://doi.org/10.1021/jm800245z

Sundquist, W.I., Kräusslich, H.-G., 2012. HIV-1 assembly, budding, and maturation. Cold Spring Harb. Perspect. Med. 2, a006924. https://doi.org/10.1101/cshperspect.a006924

Tadeo, X., Castaño, D., Millet, O., 2007. Anion modulation of the 1H/2H exchange rates in backbone amide protons monitored by NMR spectroscopy. Protein Sci. 16, 2733–2740. https://doi.org/10.1110/ps.073027007

Temin, H.M., 1993. Retrovirus variation and reverse transcription: abnormal strand transfers result in retrovirus genetic variation. Proc. Natl. Acad. Sci. U. S. A. 90, 6900–6903.

Tesina, P., Čermáková, K., Hořejší, M., Procházková, K., Fábry, M., Sharma, S., Christ, F., Demeulemeester, J., Debyser, Z., De Rijck, J., Veverka, V., Řezáčová, P., 2015. Multiple cellular proteins interact with LEDGF/p75 through a conserved unstructured consensus motif. Nat. Commun. 6, 7968. https://doi.org/10.1038/ncomms8968

Tsiang, M., Jones, G.S., Niedziela-Majka, A., Kan, E., Lansdon, E.B., Huang, W., Hung, M., Samuel, D., Novikov, N., Xu, Y., Mitchell, M., Guo, H., Babaoglu, K., Liu, X., Geleziunas, R., Sakowicz, R., 2012. New class of HIV-1 integrase (IN) inhibitors with a dual mode of action. J. Biol. Chem. 287, 21189–21203. https://doi.org/10.1074/jbc.M112.347534

Tsutsui, K.M., Sano, K., Hosoya, O., Miyamoto, T., Tsutsui, K., 2011. Nuclear protein LEDGF/p75 recognizes supercoiled DNA by a novel DNA-binding domain. Nucleic Acids Res. 39, 5067–5081. https://doi.org/10.1093/nar/gkr088

Turlure, F., Maertens, G., Rahman, S., Cherepanov, P., Engelman, A., 2006. A tripartite DNA-binding element, comprised of the nuclear localization signal and two AT-hook motifs, mediates the association of LEDGF/p75 with chromatin in vivo. Nucleic Acids Res. 34, 1653–1665. https://doi.org/10.1093/nar/gkl052

UNAIDS fact sheet - Latest statistics on the status of the AIDS epidemic - UNAIDS_FactSheet_en.pdf [WWW Document], n.d. URL http://www.unaids.org/sites/default/files/media_asset/UNAIDS_FactSheet_en.pdf (accessed 11.13.17).

Vaisocherová, H., Snásel, J., Springer, T., Sípová, H., Rosenberg, I., Stepánek, J., Homola, J., 2009. Surface plasmon resonance study on HIV-1 integrase strand transfer activity. Anal. Bioanal. Chem. 393, 1165–1172. https://doi.org/10.1007/s00216-008-2485-y

van Gent, D.C., Elgersma, Y., Bolk, M.W., Vink, C., Plasterk, R.H., 1991. DNA binding properties of the integrase proteins of human immunodeficiency viruses types 1 and 2. Nucleic Acids Res. 19, 3821–3827.

van Nuland, R., Smits, A.H., Pallaki, P., Jansen, P.W.T.C., Vermeulen, M., Timmers, H.T.M., 2013. Quantitative Dissection and Stoichiometry Determination of the Human SET1/MLL Histone Methyltransferase Complexes. Mol. Cell. Biol. 33, 2067–2077. https://doi.org/10.1128/MCB.01742-12

Vandekerckhove, L., Christ, F., Maele, B.V., Rijck, J.D., Gijsbers, R., Haute, C.V. den, Witvrouw, M., Debyser, Z., 2006. Transient and Stable Knockdown of the Integrase Cofactor LEDGF/p75 Reveals Its Role in the Replication Cycle of Human Immunodeficiency Virus. J. Virol. 80, 1886–1896. https://doi.org/10.1128/JVI.80.4.1886-1896.2006

Venner, C.M., Nankya, I., Kyeyune, F., Demers, K., Kwok, C., Chen, P.-L., Rwambuya, S., Munjoma, M., Chipato, T., Byamugisha, J., Van Der Pol, B., Mugyenyi, P., Salata, R.A., Morrison, C.S., Arts, E.J., 2016. Infecting HIV-1 Subtype Predicts Disease Progression in Women of Sub-Saharan Africa. EBioMedicine 13, 305–314. https://doi.org/10.1016/j.ebiom.2016.10.014

Vincent, K.A., Ellison, V., Chow, S.A., Brown, P.O., 1993. Characterization of human immunodeficiency virus type 1 integrase expressed in Escherichia coli and analysis of variants with amino-terminal mutations. J. Virol. 67, 425–437.

Wang, J.-Y., Ling, H., Yang, W., Craigie, R., 2001. Structure of a two-domain fragment of HIV-1 integrase: implications for domain organization in the intact protein. EMBO J. 20, 7333–7343. https://doi.org/10.1093/emboj/20.24.7333

Yang, W., Lee, J.Y., Nowotny, M., 2006. Making and breaking nucleic acids: two-Mg2+-ion catalysis and substrate specificity. Mol. Cell 22, 5–13. https://doi.org/10.1016/j.molcel.2006.03.013

Yokoyama, A., Cleary, M.L., 2008. Menin critically links MLL proteins with LEDGF on cancer-associated target genes. Cancer Cell 14, 36–46. https://doi.org/10.1016/j.ccr.2008.05.003

Zhang, F.-H., Debnath, B., Xu, Z.-L., Yang, L.-M., Song, L.-R., Zheng, Y.-T., Neamati, N., Long, Y.-Q., 2017. Discovery of novel 3-hydroxypicolinamides as selective inhibitors of HIV-1 integrase-LEDGF/p75 interaction. Eur. J. Med. Chem. 125, 1051–1063. https://doi.org/10.1016/j.ejmech.2016.10.045

Zhao, Z., McKee, C.J., Kessl, J.J., Santos, W.L., Daigle, J.E., Engelman, A., Verdine, G., Kvaratskhelia, M., 2008. Subunit-specific protein footprinting reveals significant structural rearrangements and a role for N-terminal Lys-14 of HIV-1 Integrase during viral DNA binding. J. Biol. Chem. 283, 5632–5641. https://doi.org/10.1074/jbc.M705241200

Zheng, R., Jenkins, T.M., Craigie, R., 1996. Zinc folds the N-terminal domain of HIV-1 integrase, promotes multimerization, and enhances catalytic activity. Proc. Natl. Acad. Sci. U. S. A. 93, 13659–13664.

6. Appendix

Human Research Ethics Committee (Medical) 50 years 1966 – 2016

Rsearch Office Secretariat: Faculty of Health Sciences, Phillip Tobias Building, 3rd Floor, Office 301, 29 Princess of Wales Terrace, Parktown, 2193 Tel +27 (0)11-717-1252 /1234/2656/2700
Private Bag 3, Wits 2050, email: zanele.ndlovu@wits.ac.za
Office email: hrec-medical.researchoffice@wits.ac.za
Website: www.wits.ac.za/research/about-our-research/ethics-and-research-integrity/

Ref: W-CJ-170606-5 06/06/2017

TO WHOM IT MAY CONCERN:

Waiver: This certifies that the following research does not require clearance from the Human Research Ethics Committee (Medical).

Investigator: Ms Angela Harrison (student no. 690739).

Project title: Characterisation of inhibitor binding to the LEDGF/p75-binding domain of HIV-1 integrase.

Reason: This laboratory study entails the expression and purification of recombinant HIV-1 proteins that will be used to biochemically characterise the interaction of HIV-1 integrase and LEDGF/p75 in the presence/absence of inhibitors. There are no human participants.

Professor Peter Cleaton-Jones

Chair: Human Research Ethics Committee (Medical)

UNIVERSITY OF THE WITWATERSRAND
PROF PB CLEATON-JONES
HREC (MEDICAL)
2017 -06- 06
JOHANNESBURG

Copy – HREC (Medical) Secretariat: Zanele Ndlovu, Rhulani Mkansi, Lebo Moeng.

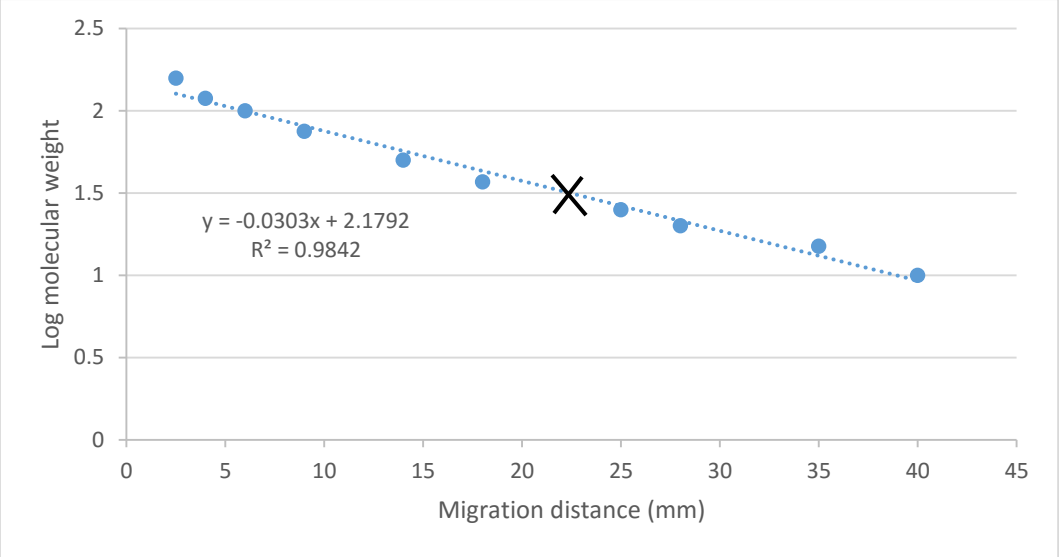


Figure 6. 1 Standard curve for SDS PAGE gel in Figure 3.1 A for the purification and expression of HIV-1 subtype B integrase. The X indicates the migration of the band to calculate the molecular weight

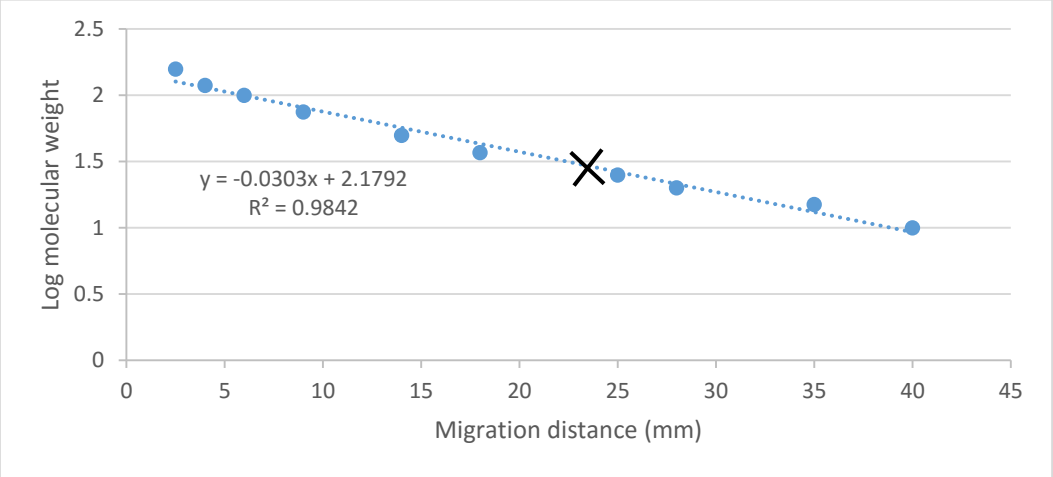


Figure 6. 2 Standard curve for SDS PAGE gel in figure 3.1 B for the purification and expression of subtype C integrase. The X indicates the migration of the band to calculate the molecular weight

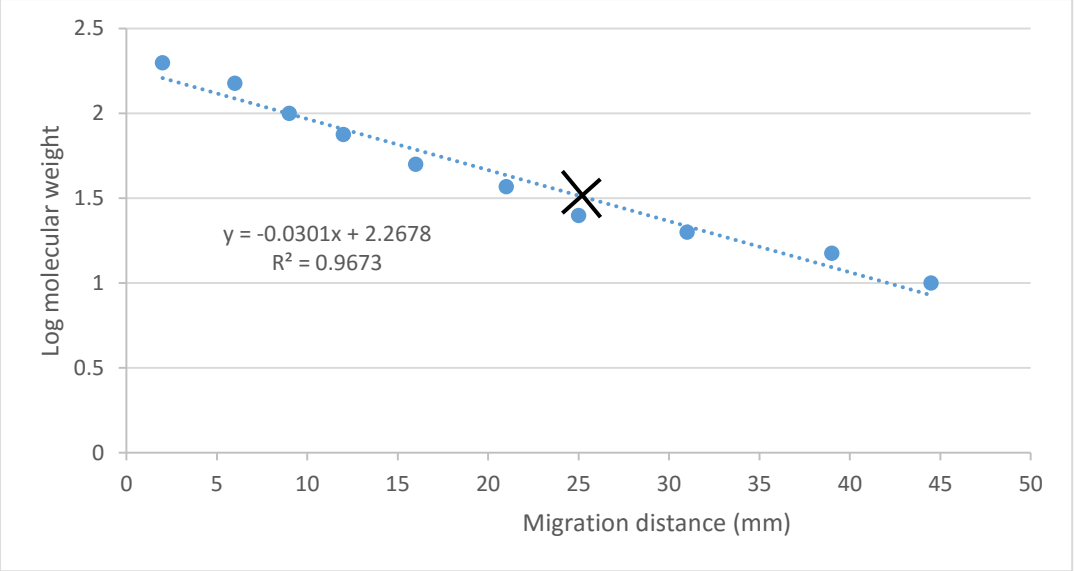


Figure 6. 3 Standard curve for western blot in Figure 3.1 C confirming the expression of subtype B and C integrase. The X indicates the migration of the band to calculate the molecular weight

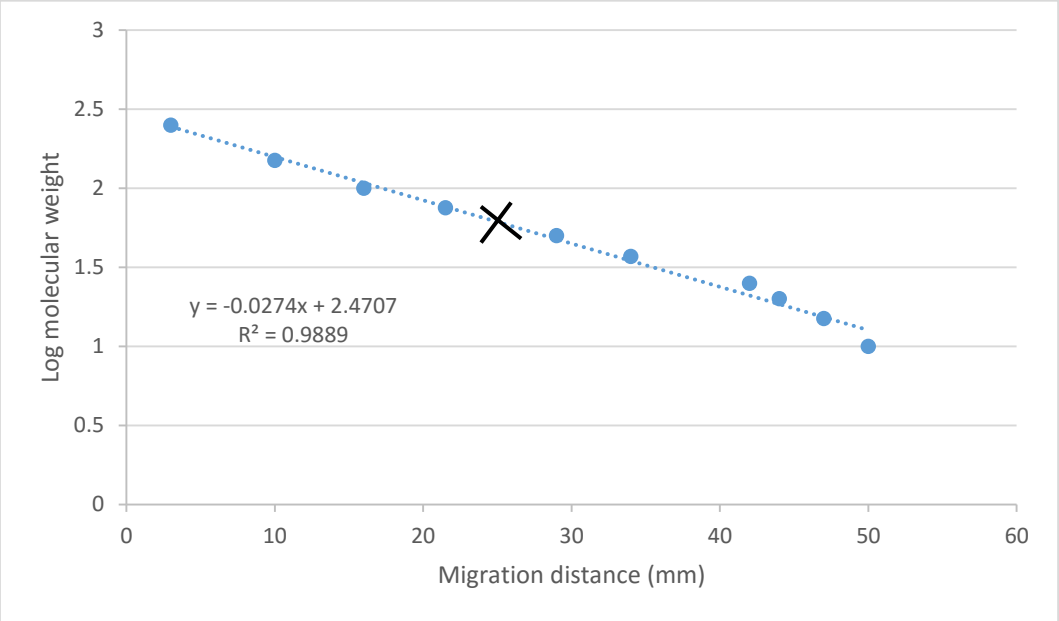


Figure 6. 4 Standard curve for SDS PAGE gel in Figure 3.2A of the purification and expression of LEDGF/p75. The X indicates the migration of the band to calculate the molecular weight

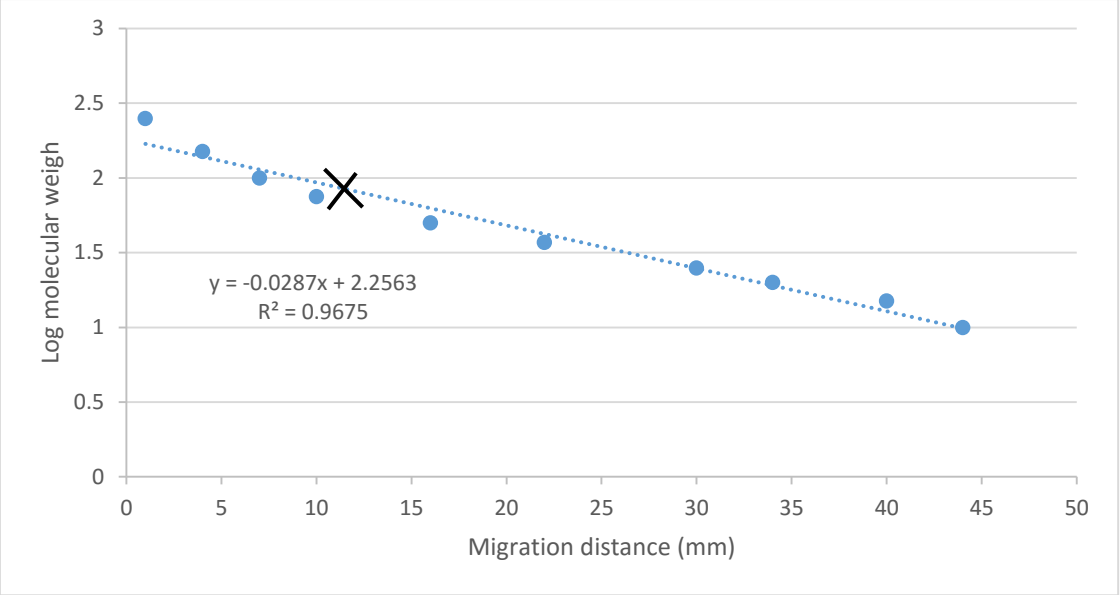


Figure 6. 5 Standard curve for the western blot in Figure 3.2 confirming the successful expression of LEDGF/p75. The X indicates the migration of the band to calculate the molecular weight

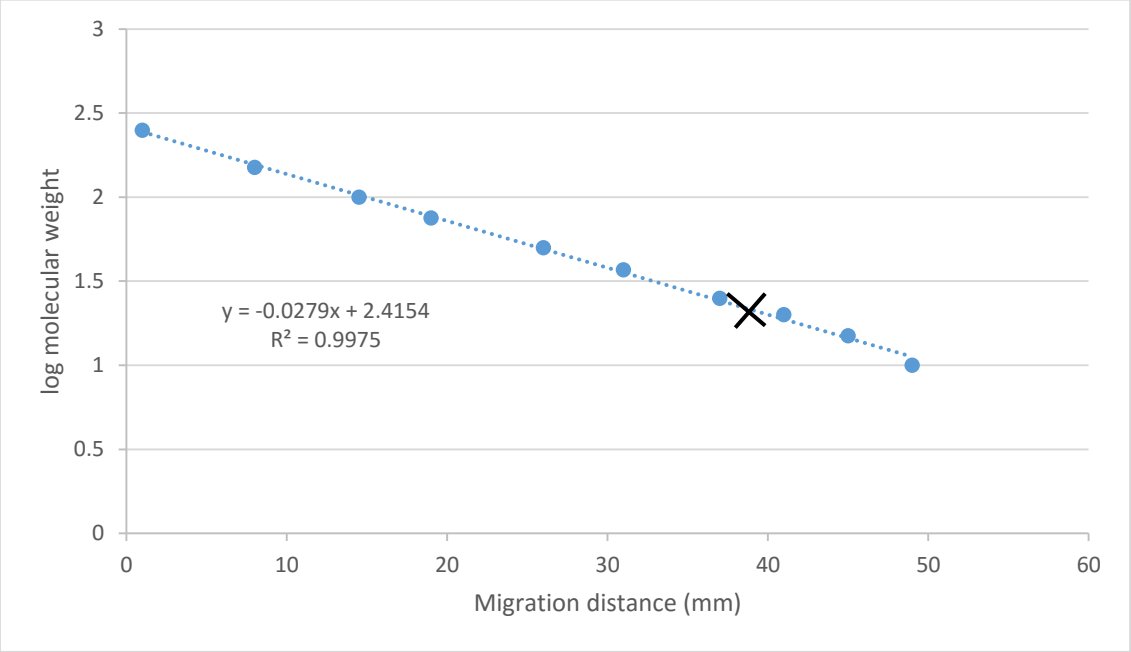


Figure 6. 6 Standard curve for the SDS PAGE gel in Figure 3.3 A of HIV-1 subtype B and C integrase before and after thrombin cleavage of the HIS tag. The X indicates the migration of the band to calculate the molecular weight

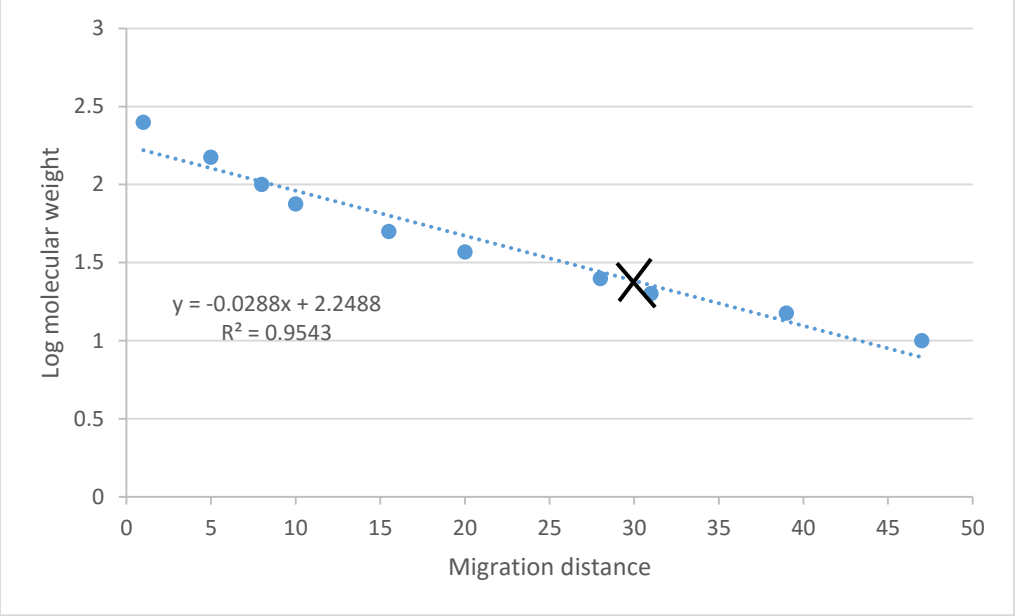


Figure 6. 7 Standard curve of the western blot in Figure 3.3 B showing the successful cleavage of the HIS tag from HIV-1 subtype B and C integrase. The X indicates the migration of the band to calculate the molecular weight.

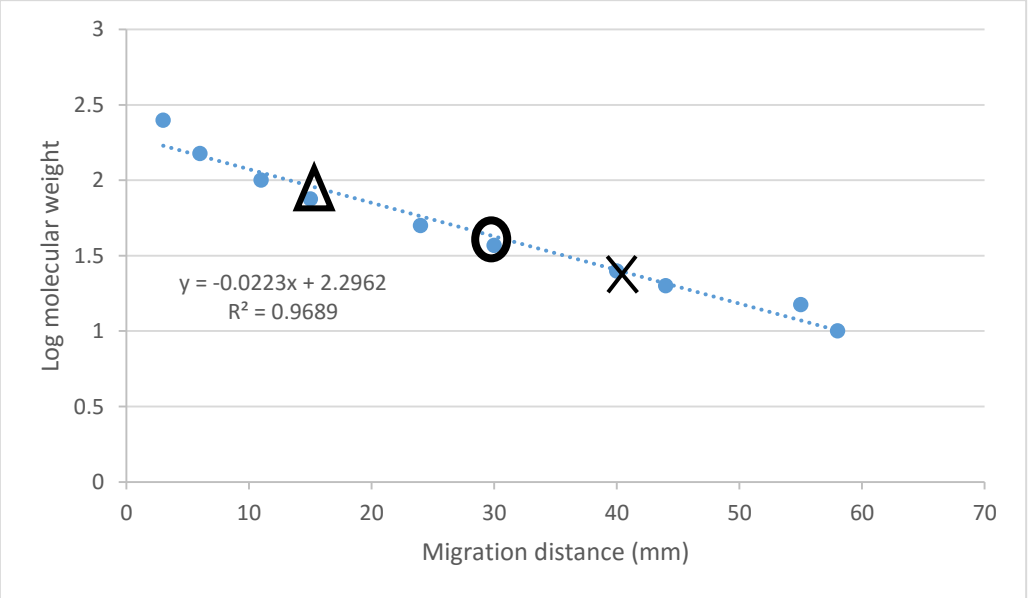


Figure 6. 8 Standard curve of the western blot in Figure 3.7A showing the dimerization studies of HIV-1 subtype B integrase and inhibitors. The X, circle and triangle indicates the migration of the bands to calculate the molecular weight

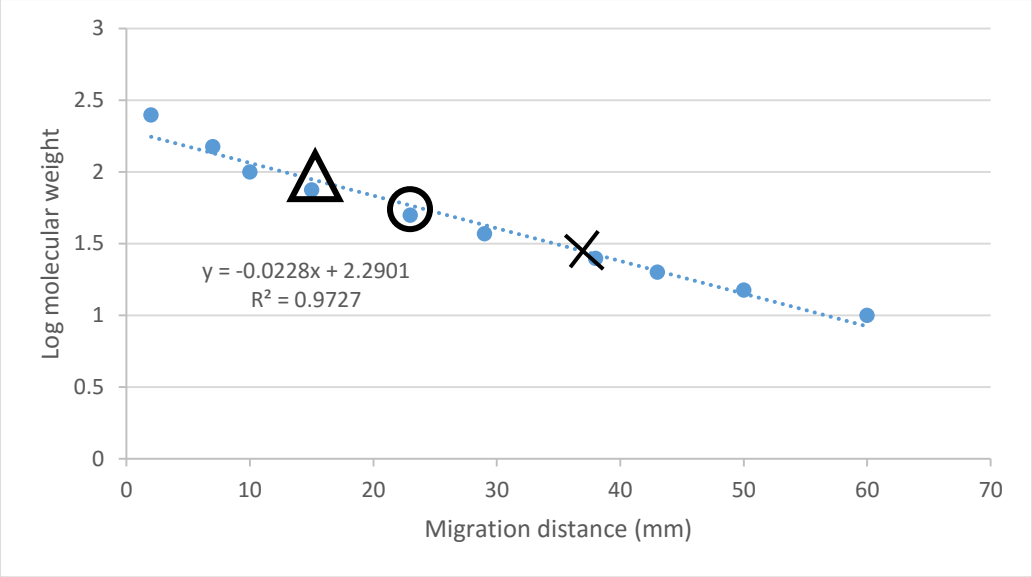


Figure 6. 9 Standard curve of the western blot in Figure 3.7B showing the dimerization studies of HIV-1 subtype C integrase and inhibitors. The X, circle and triangle indicates the migration of the bands to calculate the molecular weight

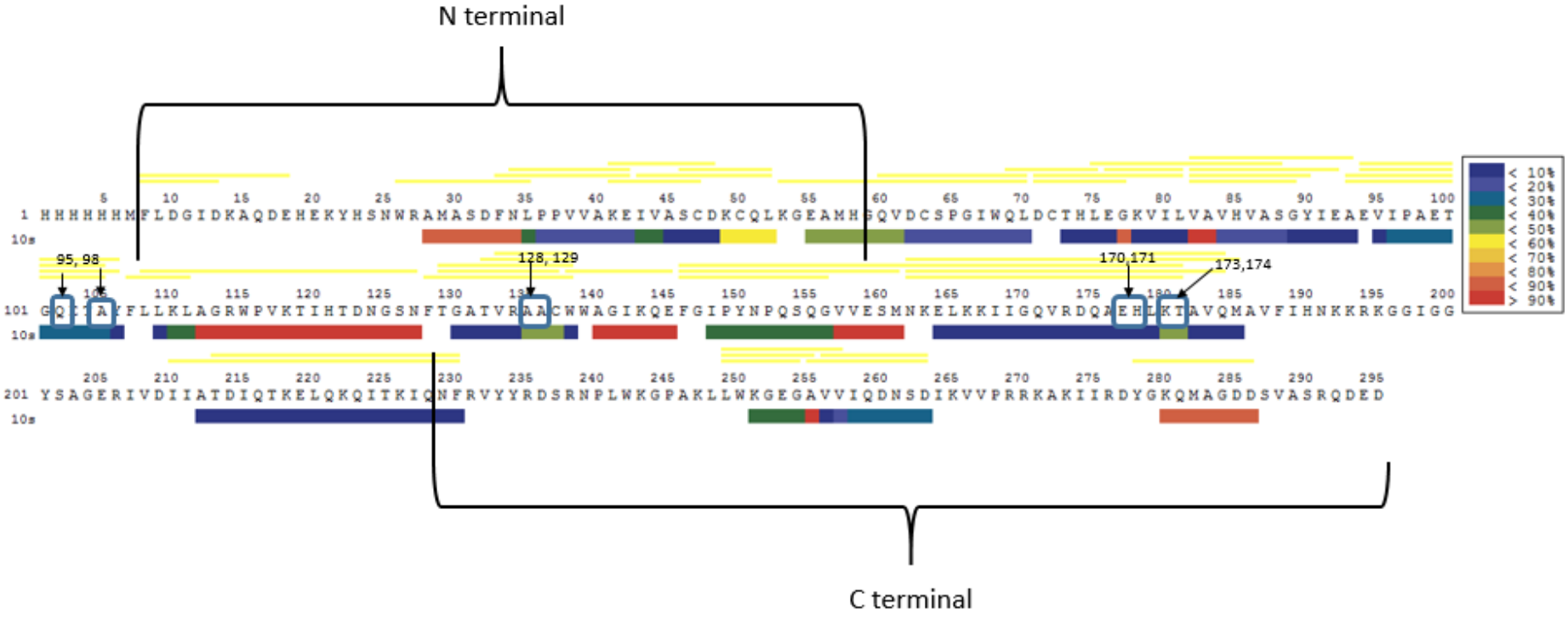


Figure 6. 10: Hydrogen exchange heat map of subtype B integrase with deuteration for 10s treated with CX05168. The N terminal domain and C terminal domain are labelled with important amino acids of 128, 129, 170, 171, 173 and 174 highlighted for ease of analysis.

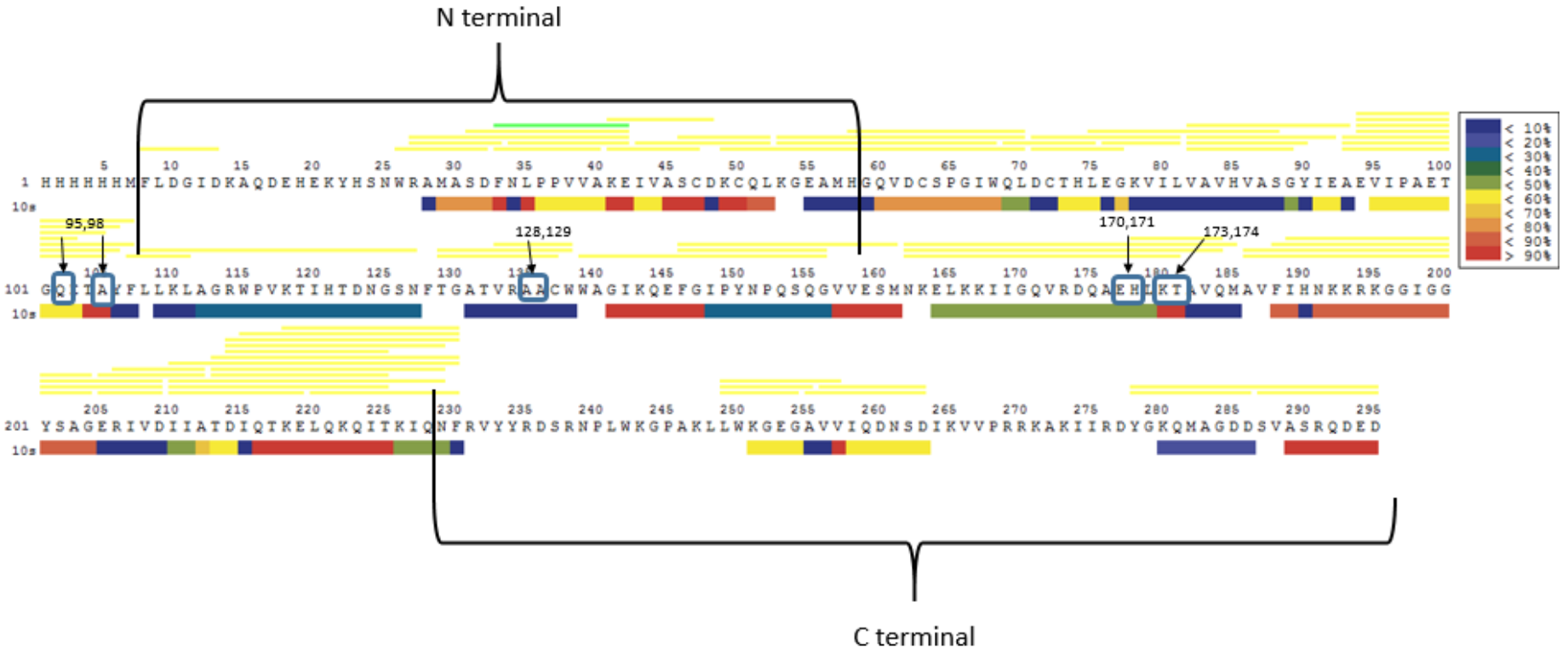


Figure 6. 11: Hydrogen exchange heat map of subtype B integrase with deuteration for 10s treated with lovastatin. The N terminal domain and C terminal domain are labelled with important amino acids of 128, 129, 170, 171, 173 and 174 highlighted for ease of analysis**.**

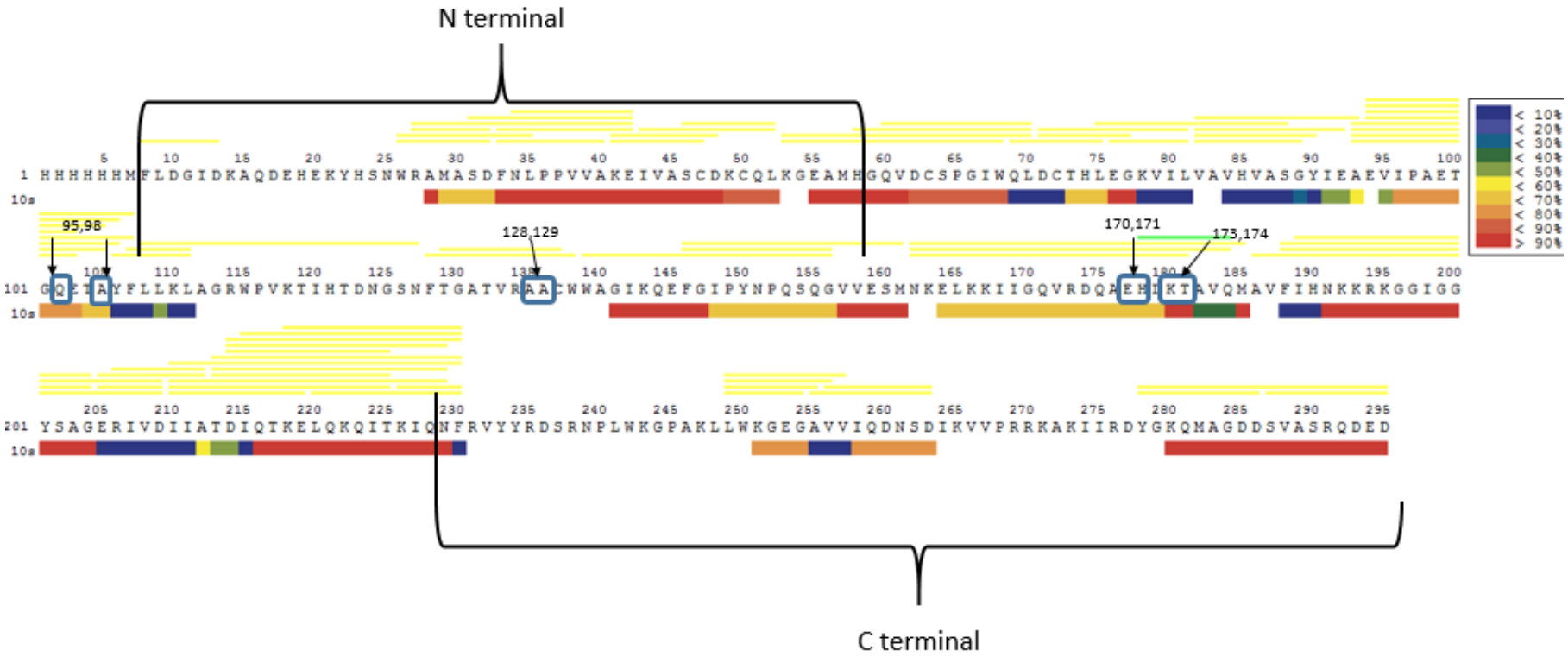


Figure 6. 12: Hydrogen exchange heat map of subtype B integrase with deuteration for 10s treated with cefdinir. The N terminal domain and C terminal domain are labelled with important amino acids of 128, 129, 170, 171, 173 and 174 highlighted for ease of analysis**.**

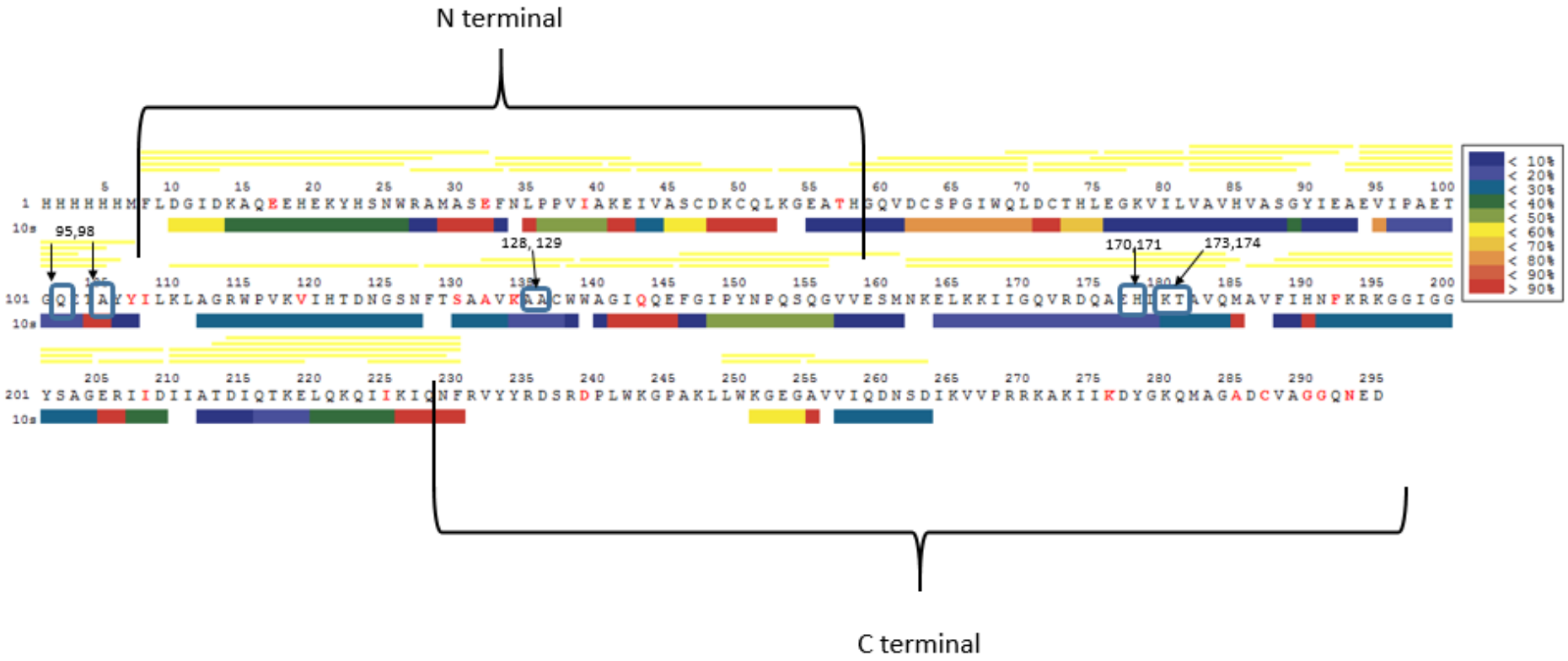


Figure 6. 13: Hydrogen exchange heat map of subtype c integrase with deuteration for 10s treated with CX05168. The N terminal domain and C terminal domain are labelled with important amino acids of 128, 129, 170, 171, 173 and 174 highlighted for ease of analysis**.** Amino acids that have changed from subtype B are in red.

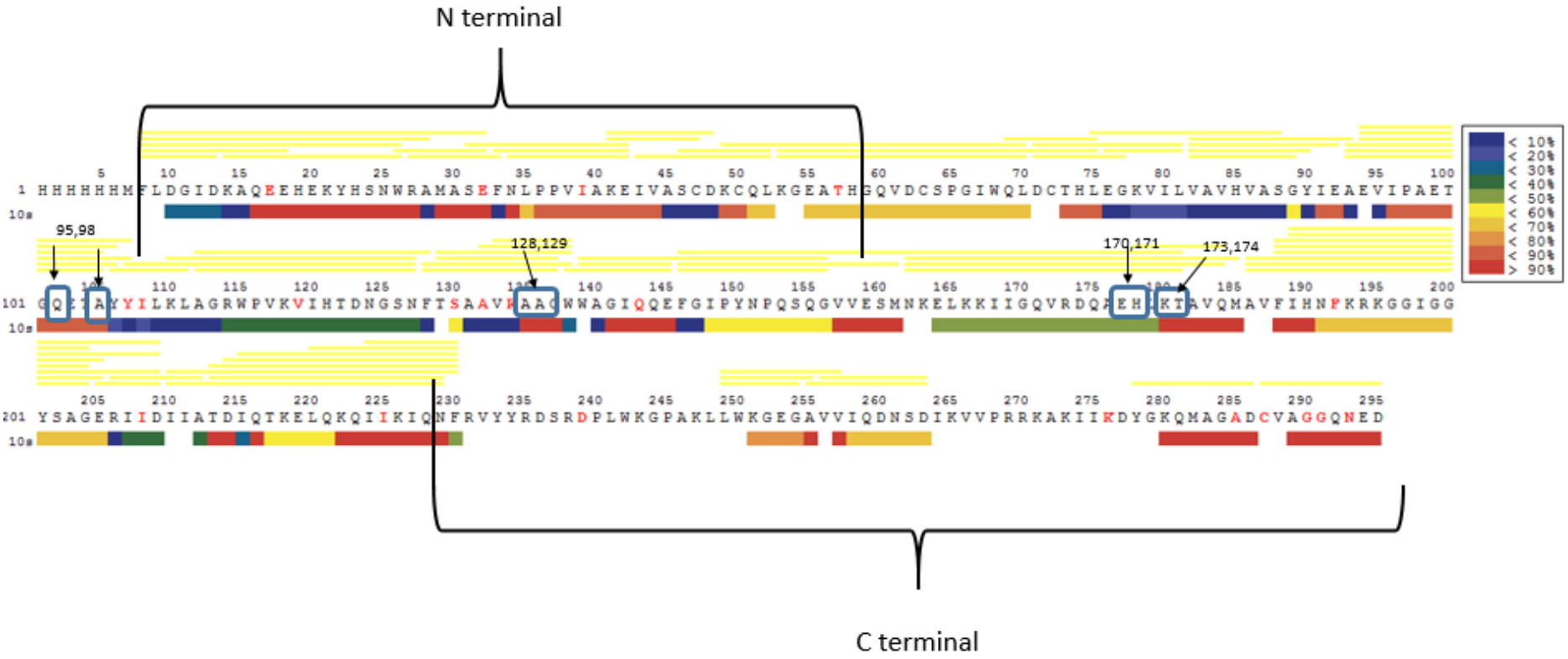


Figure 6. 14: Hydrogen exchange heat map of subtype C integrase with deuteration for 10s treated with lovastatin. The N terminal domain and C terminal domain are labelled with important amino acids of 128, 129, 170, 171, 173 and 174 highlighted for ease of analysis**.** Amino acids that have changed from subtype B are in red.

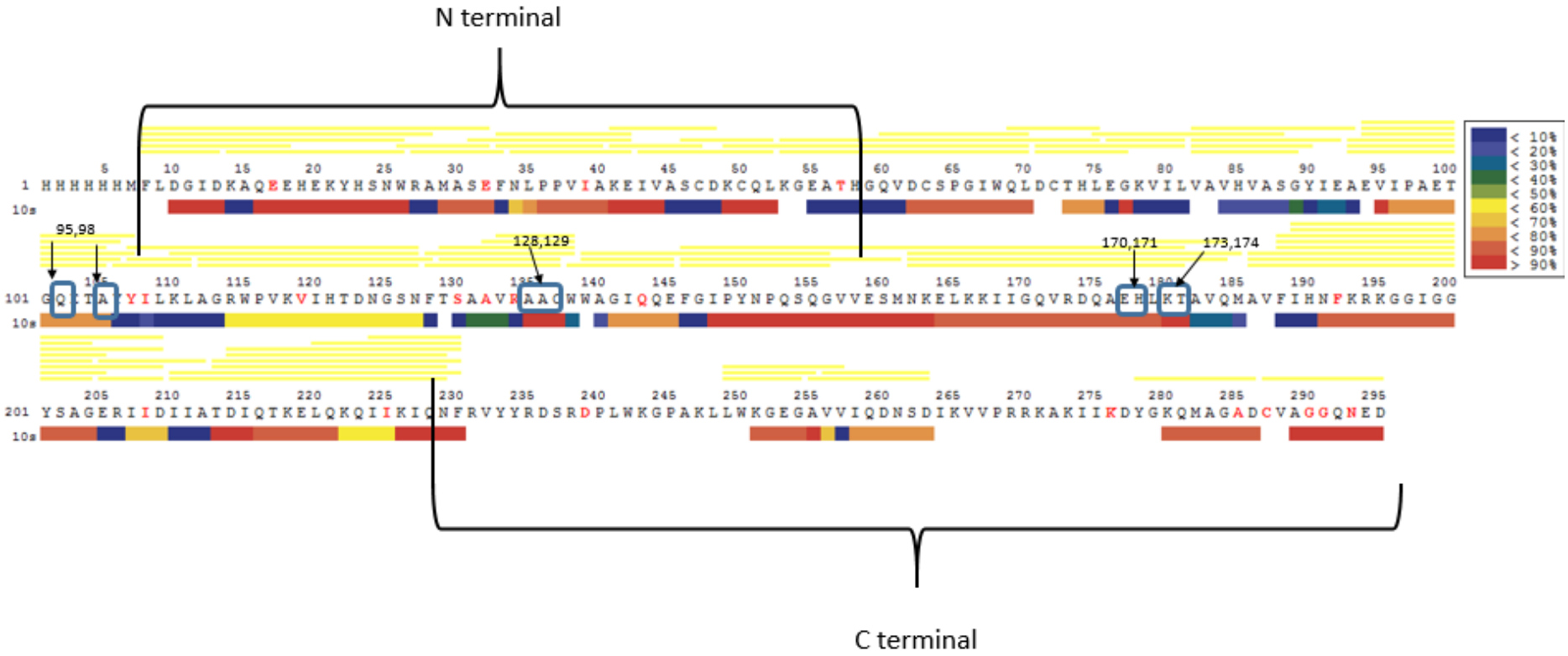


Figure 6. 15: Hydrogen exchange heat map of subtype C integrase with deuteration for 10s treated with cefdinir. The N terminal domain and C terminal domain are labelled with important amino acids of 95, 98, 128, 129, 170, 171, 173 and 174 highlighted for ease of analysis**.** Amino acids that have changed from subtype B are in red.

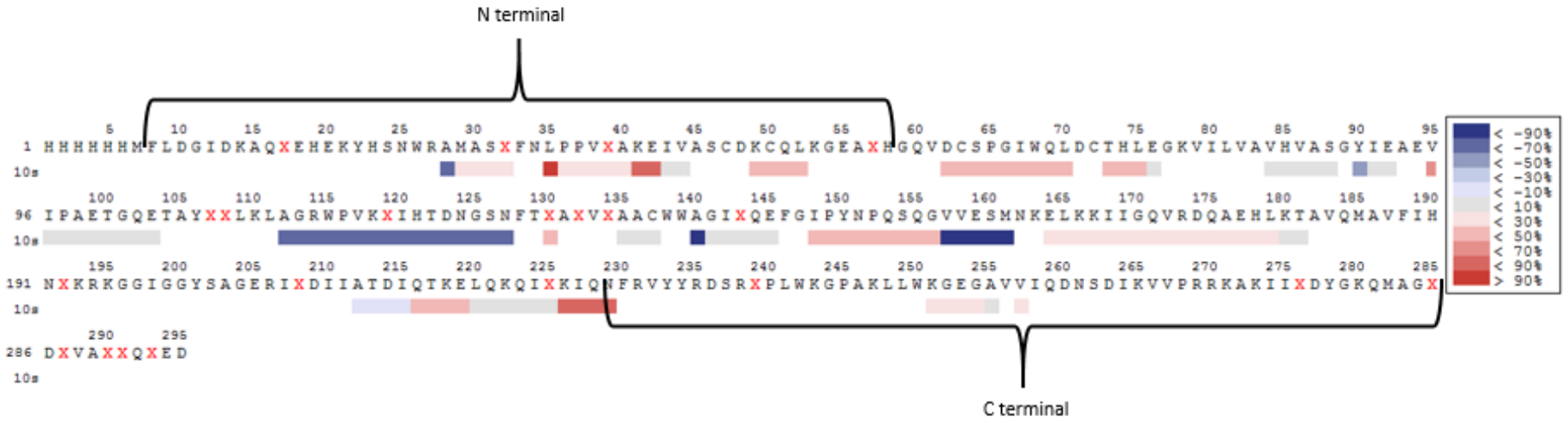


Figure 6. 16: Hydrogen exchange comparison heat map showing the deuterium exchange differences between subtype B and C HIV-1 IN with CX05168 treatment. The N terminal domain and C terminal domain are labelled with the amino acid changes between subtypes labelled with a red X.

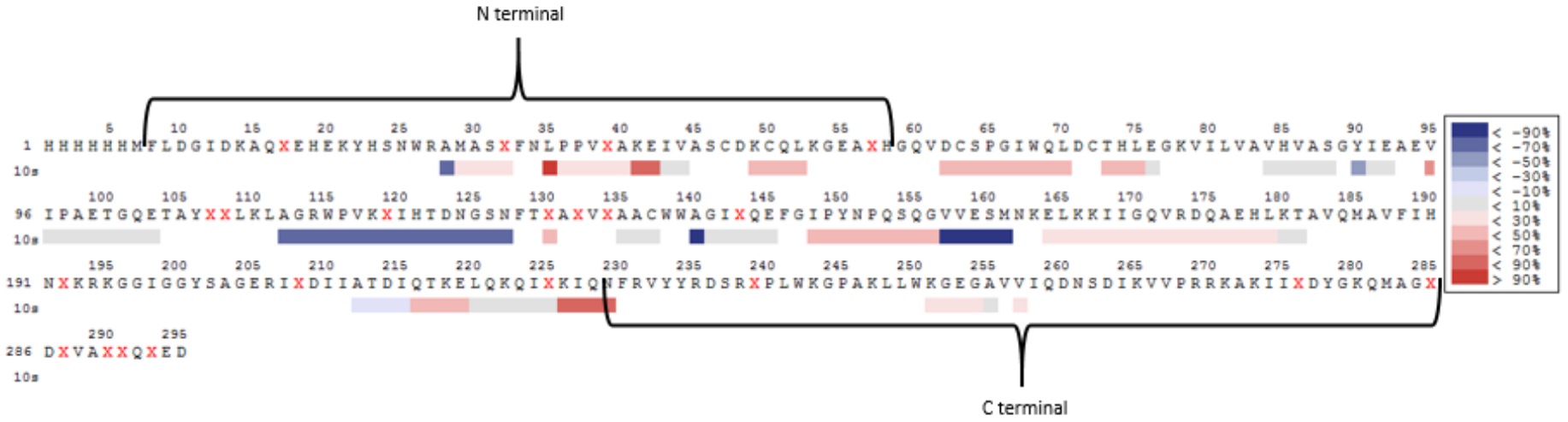


Figure 6. 17: Hydrogen exchange comparison heat map showing the deuterium exchange differences between subtype B and C HIV-1 IN with lovastatin treatment. The N terminal domain and C terminal domain are labelled with the amino acid changes between subtypes labelled with a red X.

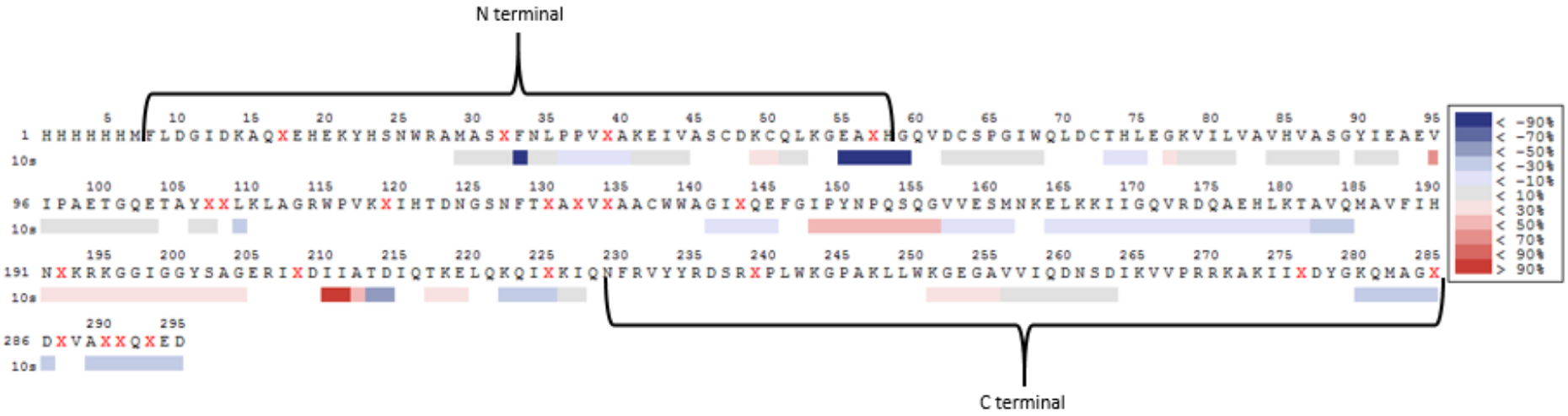


Figure 6. 18: Hydrogen exchange comparison heat map showing the deuterium exchange differences between subtype B and C HIV-1 IN with cefdinir treatment. The N terminal domain and C terminal domain are labelled with the amino acid changes between subtypes labelled with a red X.